2018

The Role Of Insulin-Like Growth Factor-2 Mrna Binding Protein 1 (imp1) In Intestinal Epithelial Homeostasis

Priya Chatterji
University of Pennsylvania, priyac@pennmedicine.upenn.edu

The Role Of Insulin-Like Growth Factor-2 Mrna Binding Protein 1 (imp1) In Intestinal Epithelial Homeostasis

Abstract

The intestinal epithelium spans proliferating crypts at its base to differentiated villi at the luminal surface and renews itself every 3-5 days. It maintains a dynamic equilibrium between proliferation, differentiation and apoptosis. The regulation of homeostasis, response to injury, regeneration and transformation is a complex set of dynamic processes. mRNA binding proteins (RBPs) are newly recognized regulators of intestinal homeostasis. The RBP:mRNA complexes act as rheostats of key signaling processes by regulating expression of already transcribed RNAs. Their functional effects are tissue and context dependent. The manner in which RBPs operate and their interactions with other pivotal pathways in colorectal cancer provide a framework for new insights and potential therapeutic applications. This thesis focuses upon the interplay between LIN28B and IGF2 mRNA binding protein (IMP1) in the regulation of intestinal epithelial regeneration and malignant transformation, unraveling a new perspective on these processes.

LIN28B, an mRNA binding protein, plays a critical role in regulating growth and proliferation in the intestinal epithelium. Previous work in our lab revealed that LIN28B promotes growth and tumorigenesis of the intestinal epithelium via suppression of mature let-7 miRNAs. LIN28B suppression of let-7 promotes upregulation of let-7 targets, including IMP1 (Insulin-like growth factor II mRNA-binding protein 1). Our lab has shown that transgenic mice expressing LIN28B from the mouse Vil1 promoter (Vil-Lin28b mice) have increased proliferation and tumor formation in the small intestine. IMP1 protein levels are upregulated in these mice epithelia and tumors but specific role of IMP1 in Lin28b-mediated tumorigenesis remains unknown. The current study tested the hypothesis that IMP1 may be required for LIN28B-mediated tumorigenesis and that LIN28B and IMP1 may cooperatively promote a tumor-initiating phenotype.

Additionally, IMP1 hypomorphic mice exhibit severe intestinal growth defects, yet it's role in adult epithelium is unclear. We investigated the mechanistic contribution of epithelial IMP1 to intestinal homeostasis and repair. We evaluated IMP1 expression in Crohn's disease patients followed by unbiased ribosome profiling in IMP1 knockout cells. We used irradiation and dextran sodium sulphate (DSS) induced colitis as injury models to evaluate regeneration in intestinal epithelium lacking IMP1.

These studies show that in the context of LIN28B overexpression, IMP1 loss led to increased tumor initiation and progression. Ribosome profiling and RNA sequencing revealed a potential role for IMP1 in negatively regulating the Wnt pathway, stem cell signature and other pathways associated with proliferation. This pro-proliferative effect with the loss of IMP1 has been previously observed in breast cancer and intestinal stroma. Additionally, IMP1 acts as a post-transcriptional regulator of gut epithelial repair post-colitis and irradiation, in part through modulation of autophagy. This study provides a new perspective on post-transcriptional regulation of autophagy as a contributing factor to the pathogenesis of inflammatory bowel disease.

In total, these studies provide new insights into the role of IMP1 in regulating homeostasis, response to injury, and tumorigenesis in the intestine. It provides evidence that IMP1 regulates the expression of its targets at both the transcriptional and translational levels.

Degree Type
Dissertation

Degree Name
Doctor of Philosophy (PhD)

Graduate Group
Cell & Molecular Biology

First Advisor
Anil K. Rustgi

Keywords
Colon Cancer, IMP1, Inflammatory Bowel disorders, LIN28B, Ribosome profiling, RNA binding proteins

Subject Categories
Genetics | Molecular Biology

THE ROLE OF INSULIN-LIKE GROWTH FACTOR-2 mRNA BINDING PROTEIN 1 (IMP1) IN INTESTINAL EPITHELIAL HOMEOSTASIS

Priya Chatterji

A DISSERTATION

in

Cell and Molecular Biology

Presented to the Faculties of the University of Pennsylvania

in

Partial Fulfillment of the Requirements for the

Degree of Doctor of Philosophy

2018

_____

Supervisor of Dissertation

Anil K. Rustgi, M.D.

T. Grier Miller Professor of Medicine; Chief of Division of Gastroenterology,
Perelman School of Medicine

_____

Graduate Group Chairperson

Daniel S. Kessler, Ph.D.

Associate Professor of Cell and Developmental Biology

Dissertation Committee

Christopher J. Lengner, Ph.D. (Committee Chair)
Associate Professor, Department of Biomedical Sciences

Eileen M. Shore, Ph.D.
Cali and Weldon Research Professor in FOP

John P. Lynch, Ph.D
Director, Immunology Clinical Development (Janssen Research and Development)

Xianxin Hua, MD, Ph.D. Professor
Investigator, Abramson Family Cancer Research Institute

DEDICATION

To my grandfather, the Late Shri Hari Prasad Chatterjee, who believed in me before I believed in myself. You're my guardian angel.

And to my grandmother, thank you for the values you've instilled in us. They make us who we are.

Jai Sai Ram.

TABLE OF CONTENTS

ACKNOWLEDGEMENTS

"It is the long history of humankind that those who learned to collaborate and improvise most effectively have prevailed."

– Charles Darwin

First and foremost, I would like to thank my thesis advisor and mentor Dr. Anil Rustgi for his constant support and encouragement throughout my doctoral work. For the past 4+ years Dr. Rustgi has helped me grow, both as a researcher and as a person. He is a champion for women in science and I am grateful for his guidance and unwavering support in all my endeavors. I owe a special thanks to my committee Drs. Chris Lengner, Eileen Shore, John Lynch and Xianxin Hua for their immense support, constructive comments, and encouragement throughout my dissertation work. I am grateful to Dr. Hiroshi Nakagawa for always being encouraging and helpful.

I am grateful to all my colleagues in the Rustgi and the Nakagawa labs for their continuous support. To Dr. Kathryn Hamilton, you've been a mentor and a friend, and I owe you a lot of gratitude. You've helped me through hurdles, both experimental and personal. Your advice, support and friendship mean a great deal to me and I hope we maintain this relationship throughout our lives. To Dr. Sarah Andres, thank you for being an amazing friend and benchmate to me and helping me on a daily basis. I wish I were half as organized and structured in my life as you are in yours. To Dr. Veronique Giroux, you've been the best of friends to me. Your hugs just make everything easier and your scientific insight has been extremely helpful to me at each step. To Dr. Emma Lundsmith, thank you for being kind and making me comfortable right from the day I joined the lab. To Dr. Catrina King and Dr. Blair Madison, thank you for laying the foundation of the work that formed my dissertation. To Philip Hicks and Lauren Simon, thanks for taking care of all aspects of the animal husbandry without which my thesis would not have been possible. To Ben Rhoades, thank you for all you do for the lab and

for helping me with radiation experiments and making my grad life easier. To Prasanna, thank you for being the best of friends and helping me every single day with experiments and scientific thoughts and listening to my incessant chatting with incredible patience.

I am grateful to all our collaborators who've helped with my project and made this dissertation possible. Thank you to Drs. Premal Shah, Chris Lengner, Amanda Mah, Laurienne Van Landeghem, Brian Gregory, Gary Wu and Shun Liang. Special thanks to Premal who started by being an amazing friend and practically family and then became an indispensable collaborator. You and Samhita are amazing. Thank you for making me feel so loved.

I would also like to thank other members of my lab Drs. Rei Mizuno, Tatiana Karakasheva, Jason Pitaressi, Kelly Whelan, Amanda Muir, Benoit Marchand, Ashley Lento, Basil Bakhir, Leticia Moreira, Ken Suzuki and Qiaosi Tang for making the lab feel like a second family to me. I owe a special gratitude to the Molecular Biology Core and Molecular Pathology and Imaging Core, especially to Adam Bedenbaugh and Daniela Budo who helped me with experiments and taught be so much.

I have been blessed with the best family anyone can hope for. They anchor me and give me stability in a way that makes my life wonderful. Their unconditional love is the reason for who I am and what I do. To my parents, Maitri and Harish Chatterjee, you're my life. Thank you will never suffice. I'm forever indebted to you, I pray you're my family in every life. To my brother, Himanshu, you've the light in my life and the best person I know. I love you. To my amazing extended family, thank you for having my back and making me strong. Thanks to my sisters Pallavi, Preetisha, Purabi and Promiti, you're the brightness and color in my life.

I've made the most amazing friends at Penn and I would be remiss if I failed to thank them. To Christin Herrmann and Annie Chen, thank you for being the most amazing friends and being by my side through thick and thin. I love you both. To Shawn

Foley, in you I've found a friend for life, someone I respect and appreciate. Thank you for helping me with my project, you're a Rockstar. To Arwa Abbas and Jonathan Rumley, I have immensely enjoyed our discussions on everything from religion to politics and from Pokémon to Star Wars (or was it Star Trek? I still don't know the difference). To Poitr Kopinski, thank you for being my confidant and my partner in food adventures, you're amazing. To Michael Peel, your sarcastic humor lightens up my days and your friendship makes me happy. To Akriti Kharbanda, you're like a sister to me and your kindness and love has enriched my life in more ways than one. Thank you to Frances, Anna, Seth, Stephen, Chris, Peiwei, Dan and all my friends in CAMB for being fabulous. Thanks to everyone in the Biomedical Graduate Student Association executive board for a lovely year of helping grad students.

Thank you to the administrative staff at the Department of Gastroenterology, especially Michelle, Kim and Marielle for helping me promptly with all official work and just being lovely. To the CAMB coordinators, especially Meagan Schofer and Christina Strathearn, for helping and guiding me through all official paperwork throughout my time at Penn.

I am thankful to my friends Neha Bibireddy, Meitreyi Panchmia, Vijetha Kumar, Pranitha Reddy, Divya Kali Ranga, Jayant Charthad, Amogh Halgeri, Prenitha Mercy, Manali Chugh, Siddhartha Naha and Harshit Shah for supporting me and loving me for who I am. Thanks to Piyush and Jitesh for shaping who I am. And finally, thanks to One Direction and its members for providing me with a distraction.

LIST OF FIGURES

LIST OF SUPPLEMENTAL DATA

ABSTRACT

THE ROLE OF INSULIN-LIKE GROWTH FACTOR-2 mRNA BINDING PROTEIN 1 (IMP1) IN INTESTINAL EPITHELIAL HOMEOSTASIS

Priya Chatterji

Anil K. Rustgi

The intestinal epithelium spans proliferating crypts at its base to differentiated villi at the luminal surface and renews itself every 3-5 days. It maintains a dynamic equilibrium between proliferation, differentiation and apoptosis. The regulation of homeostasis, response to injury, regeneration and transformation is a complex set of dynamic processes. mRNA binding proteins (RBPs) are newly recognized regulators of intestinal homeostasis. The RBP:mRNA complexes act as rheostats of key signaling processes by regulating expression of already transcribed RNAs. Their functional effects are tissue and context dependent. The manner in which RBPs operate and their interactions with other pivotal pathways in colorectal cancer provide a framework for new insights and potential therapeutic applications. This thesis focuses upon the interplay between LIN28B and IGF2 mRNA binding protein (IMP1) in the regulation of intestinal epithelial regeneration and malignant transformation, unraveling a new perspective on these processes.

LIN28B plays a critical role in regulating growth and proliferation in the intestinal epithelium. LIN28B suppression of let-7 promotes upregulation of let-7 targets, including IMP1 (Insulin-like growth factor II mRNA-binding protein 1). Mice expressing LIN28B from the mouse Vil1 promoter (Vil-Lin28b mice) have increased proliferation and tumor formation in the small intestine. IMP1 protein levels are upregulated in these mice epithelia and tumors but specific role of IMP1 in Lin28b-mediated tumorigenesis remains unknown.

Additionally, IMP1 hypomorphic mice exhibit severe intestinal growth defects, yet it's role in adult epithelium is unclear. We investigated the mechanistic contribution of epithelial IMP1 to intestinal homeostasis and repair. We evaluated IMP1 expression in Crohn's disease patients followed by unbiased ribosome profiling in IMP1 knockout cells. We used irradiation and dextran sodium sulphate (DSS) induced colitis as injury models to evaluate regeneration in intestinal epithelium lacking IMP1.

In total, these studies provide new insights into the role of IMP1 in regulating homeostasis, response to injury, and tumorigenesis in the intestine. It provides evidence that IMP1 regulates the expression of its targets at both the transcriptional and translational levels.

CHAPTER I: INTRODUCTION

(Parts of this section have been published as a review in (Chatterji and Rustgi 2018))

The intestinal epithelium

The intestinal epithelium is a layer of simple columnar cells that line the small and large intestine at the luminal surface. This epithelium forms a barrier against microorganisms and harmful substances while helping absorb nutrients and minerals and also secreting hormones and digestive peptides (all in the small intestine). The intestinal epithelium comprises two major structural components: the crypts that are invaginations in the epithelium and the villi that protrude into the lumen and house the differentiated cells. The crypts and villi help increase the surface area four-fold.

The intestinal epithelium is one of the most proliferative organs and renews itself every 3-5 days. The intestinal epithelium consists of stem cells, absorptive cells and secretory cells. The crypt base is the compartment for two types of stem cells; the actively dividing crypt base columnar stem cells (CBCs), and the quiescent +4 stem cells. All intestinal lineages (absorptive and secretory) arise from the stem cells and migrate upwards towards the luminal surface except for Paneth cells that migrate towards the base. The secretory cells consist of Paneth cells (secreting anti-microbial peptides), goblet cells (secrete mucus), enteroendocrine cells (secreting hormones) and tuft cells (secrete cytokines). The absorptive enterocytes make up the majority of the epithelium and absorb micronutrients, water and electrolytes. The transit amplifying cells are immediate progeny of stem cells. The colon epithelium is similar to the small intestinal epithelium but lacks villi and serves to absorb remaining water and provide a barrier against micro-organisms (FIGURE 1).

The crypt base columnar stem cells are actively dividing cells at the base of the crypts. Over the past decade, several markers of this population have been identified. Leu-rich repeat containing G protein-coupled receptor 5 (Lgr5), has been identified, through lineage tracing experiments, as an important selective marker for CBC cells in the small intestine and the colon (Barker et al. 2007). Other markers include Achaete-

Scute homologue 2 (Ascl2), SPARC-related modular calcium-binding 2 (Smoc2), Prominin 1(Prom1), Musashi homologue 1 (Msi1), Olfactomedin 4 (Olfm4), and EphB2 (Kim et al. 2017a). These cells can give rise to the entire epithelium in 60 days. They are radiosensitive and can be completely eliminated by radiation injury of 12Gy and above. The +4 stem cells on the other hand, are label retaining cells that are radio-resistant and can give rise to all the different cell types, including CBC cells when activated, especially in cases of injury. These cells are marked by Bmi1, Homeodomain-only (Hopx), Leu-rich repeats and immunoglobulin-like domains 1 (Lrig1), and telomerase reverse transcriptase (Tert) and Hopx. All markers of stem cells have been identified using lineage tracing experiments (Kim et al. 2017a).

The Paneth cells are secretory cells that are interspersed between the stem cells in the crypt base. They are characterized by the large eosinophilic refractive granules that occupy most of their cytoplasm. These granules are comprised of anti-microbial compounds and hormones that help maintaining the gastrointestinal barrier as well as secrete some hormones to aid the stem cells (Adolph et al. 2013; Clevers and Bevins 2013). While the ablation of Paneth cells does not have any effect on the intestinal epithelium at homeostasis, loss of these cells impairs the regenerative response following injury (Parry et al. 2013). The other secretory cells include goblet, tuft and enteroendocrine cells. The goblet and tuft cells accumulate and respond to parasites and help restructure the intestinal barrier (Haber et al. 2017). The goblet cells mainly secrete mucus, a viscous fluid composed primarily of highly glycosylated proteins called mucins suspended in a solution of electrolytes. These cells are upregulated to help protect from chemical damage and shear stress as well as microbial infections (Specian and Oliver 1991). The tuft cells have been shown to play an important role in the innate immunity response (Grencis and Worthington 2016). Finally, enteroendocrine cells secrete gastrointestinal hormones or peptides that are diffused as messengers in

response to various stimuli. The secreted hormones include

somatostatin, motilin, cholecystokinin, neurotensin, vasoactive intestinal peptide,

and enteroglucagon, depending on the location of the cells within the gastrointestinal

tract (Krause et al. 1985). The enterocytes constitute the absorptive cell population in the

intestinal epithelium. The cells have a glycocalyx surface coat and contain digestive

enzymes. Their apical surface is lined with microvilli to increase surface area for the

digestion and transport of molecules from the intestinal lumen. These cells help with

uptake of water, sugars, ions, peptides and amino acids, lipids, vitamin B12 and bile

salts among others (Washabau 2013).

Together the different cellular lineages help maintain a dynamic equilibrium and

respond efficiently to stress and injury. This equilibrium is disturbed during inflammation

and injury and can give rise to inflammatory bowel disorders (IBD). IBD is a complex

disease that results from immunological responses and responses of the intestine to

inflammation. Several different factors including genetic factors, diet, environment,

microbiota, intestinal barrier defects and hormonal variability can contribute to the

disease. Crohns and ulcerative colitis are the principal types of IBD. This disease

manifests with several symptoms that may include abdominal pain, diarrhea, vomiting,

rectal bleeding, muscle spasm/cramps, anemia, and weight loss. It is diagnosed and

confirmed with biopsies during colonoscopies. Therapeutic interventions include anti-

inflammatory and immunosuppressive drugs, diet and lifestyle changes, microbiome

changes and surgery .

In certain cases, IBD can be a risk factor for colorectal cancer (CRC). Globally,

CRC affects more than 1 million people every year and remains the fourth most common

cause of cancer related deaths worldwide (Cunningham et al. 2010). It remains among

the top causes of cancer-related deaths in the United States, with greater than 50,000

deaths per year. Despite significant emphasis placed on improving early detection, only

40% of new CRC cases are diagnosed with localized-stage disease. The 5-year survival rate for regional and distal metastases is 68% and 11%, respectively, underscoring the importance of elucidating the underlying mechanisms for these invasive processes. The molecular events underlying colorectal cancer (CRC) progression are predicated upon alterations in oncogenes and tumor suppressor genes, however, new mechanisms for regulating these genes are still being discovered and may hold the promise for better diagnostic and/or therapeutic targets.

RNA binding proteins as regulators of intestinal homeostasis

An emerging node of regulation of intestinal epithelial homeostasis, response to injury, and malignant transformation, is through RNA binding proteins (RBP). Broadly speaking, RNA binding proteins (RBPs) are vital for regulation of several essential cellular processes such as RNA splicing, modifications, transport, localization, stability, degradation and translation (Wang et al. 2018). Several RBPs are expressed ubiquitously and are evolutionarily conserved (Gerstberger et al. 2014) to maintain their roles in basic cellular functions. Any significant change or disturbance in the RBPs regulating these essential cellular functions can lead to different diseases, including cancer (Wang et al. 2018). RBPs function by binding to their target RNA, forming ribonucleoprotein (RNP) complexes (Dreyfuss et al. 2002) and regulating gene expression post-transcriptionally in a plethora of ways. Since RBPs can regulate already transcribed RNAs, they act in a rapid and efficient manner to alter gene expression, especially during changes in the microenvironment. A single RBP can bind to hundreds, if not thousands of targets, and a combination of several RNP interactions contribute to cellular identity and response to stimuli (Smith and Valcarcel 2000). RBPs can help recruit translation machinery to activate translation (Michlewski et al. 2008). By contrast,

RBPs involved in the RNA-induced silencing complex (miRISC) result in decapping, deadenylation and translational repression of the target mRNAs (Fabian et al. 2010). They can also suppress translation and induce degradation (Kim et al. 2009). In some cases, two RBPs can bind to the same RNA target to stabilize it, either enhancing or repressing translation (Sureban et al. 2007). RBPs can also have dichotomous functions where they can both enhance (Hamilton et al. 2013; Gutschner et al. 2014) or repress (Hamilton et al. 2015; Wang et al. 2016a) tumorigenesis depending upon the cellular context. Figure 2 shows a simplistic schematic of the functional consequences of mRBP binding to its targets.

Structure of RNA binding proteins

The functional effects of conventional RNA binding proteins are dependent upon their binding to their target RNAs and forming ribonucleoprotein (RNP) complexes. The RNP complexes help with RNA processing, translation, export and localization. Since RBPs have multiple biological roles, their structures consist of multiple small domains. These consist of several types of RNA recognition and binding domains interspersed between catalytic domains to efficiently recognize a wide range of targets and regulate catalytic activity (Lunde et al. 2007). These catalytic domains include helicases, deaminases and RNAse III domains (Han et al. 2006; Nishikura 2010). Multiple RNA binding domains (RBDs) provide specificity to recognize and bind either long RNA sequences or sequences separated by many nucleotides or two different RNAs(Lunde et al. 2007). These can help form large complexes and regulate major signaling pathways. RBDs may comprise RNA recognition motifs (RRMs), dsRNA binding motifs (dsRBD), K-homology domain (KH), Zinc fingers, S1 domain, Piwi and PAZ (PIWI, AGO, and Zwill) domains amongst others. RRM is by far the most common and well-characterized domain and most RBPs have multiple RRMs to provide specificity. By contrast, RBPs

involved in translation, such as initiation and elongation factors, bind all mRNAs and lack specificity (Lunde et al. 2007). RBPs can regulate subcellular localization of their targets due to nuclear and/or nucleolar localization signals (NLS/NoLS) or nuclear export signals (NES) depending upon their functional requirements(Rosenblum et al. 1998; Cassola et al. 2010). Overall, the structure of these conventional RBPs comprise multiple repeats of different RBDs with varying functional specificities and catalytic domains to regulate their target RNAs.

The target RNAs for RBPs are quite diverse. While RBPs can bind different regions of mRNAs (exonic, intronic, UTRs), there is increasing evidence of interactions with other types of RNAs, including non-coding RNAs, namely microRNAs, t-RNAs, small interfering RNAs (siRNA), telomerase RNA, small nucleolar RNAs (snoRNAs), splicesomal small nuclear RNAs (snRNA), as well as the RNA moiety of the signal recognition particle (SRP RNA or 7SL RNA). These non-coding RNAs form extensive secondary structures to associate with proteins and regulate several processes like splicing, RNA modifications, protein localization and secretion as well as chromosomal maintenance (Hentze et al. 2018).

In recent years, advanced structural-analysis studies have provided evidence of complex protein–RNA interactions that do not require canonical RBDs (Hentze et al. 2018). RNA interactome capture (RIC) (Castello et al. 2013) studies have identified 'non-conventional' RBPs in several organisms that do not have discernible RBDs and have no known relationship to RNA biology(Hentze et al. 2018). Further studies have also shown that disordered protein regions can also facilitate protein-RNA interactions that can be specific or non-specific (Jarvelin et al. 2016). These unorthodox interactions can regulate RNA metabolism and different RNA processes, both co- and post-transcriptionally(Jarvelin et al. 2016). (The role of non-conventional or non-canonical RBPs in cancer has been beautifully reviewed in (Moore et al. 2017)).

LIN28B

  LIN-28 was first discovered in *C.elegans* as a heterochronic gene that plays a vital role in developmental events (Ambros and Horvitz 1984). LIN28 has been studied in multiple species as a promoter of pluripotency. It has been shown to be expressed highly in undifferentiated tissues and its expression is downregulated as differentiation and development progress (Tsialikas and Romer-Seibert 2015). Hence, LIN28 is evolutionarily conserved to promote pluripotency and act as a 'gatekeeper' of differentiation. The most well studied mechanism of LIN28B function is via its interaction with the let-7 miRNAs (Balzeau et al. 2017).

  In mammals, there are two paralogs of LIN28; LIN28A and LIN28B that have mostly overlapping functions (Viswanathan and Daley 2010). LIN28A and LIN28B have a cysteine cysteine histidine cysteine (CCHC) zinc finger domain and a cold shock domain (Hafner et al. 2013). LIN28B also contains an extended C terminal region with a nuclear localization signal (NLS) (Piskounova et al. 2011) (Figure 3). In mice, LIN28 proteins are expressed highly during embryonic development but their expression declines rapidly after E18.5 in the small intestine and colon correlating reciprocally with intestinal differentiation (Gregorieff and Clevers 2005; Madison et al. 2013b). In adult mice, LIN28B expression is limited to the crypt compartment (Madison et al. 2013b). This correlates with the reciprocal increase in the expression of the *Let-7* microRNAs. LIN28B expression is observed in the nucleus of undifferentiated cells whereas low expression of LIN28B can be seen in the cytoplasm of differentiated intestinal cells. The constitutive knockout of either *Lin28a* or *Lin28b* causes dwarfism and a growth retardation phenotype in mice (Shinoda et al. 2013). The double knockout is synthetically lethal, and the mice do not survive past E12.5. This phenotype, however, is not observed when the genes are deleted in neonatal or adult mice (Shinoda et al.

2013). The intestinal epithelium specific single or double knockouts of *Lin28a* and *Lin28b* show no obvious intestinal phenotype (Tu et al. 2015). Furthermore, these mice also do not show any difference in susceptibility to colonic tumorigenesis with dextran sodium sulphate (DSS)/azoxymethane (AOM) when compared to their wild-type littermates (Tu et al. 2015).

Several studies have shown that LIN28B is overexpressed in about 30% of colorectal tumors (King et al. 2011a; King et al. 2011b). LIN28B overexpression correlates with invasive tumor phenotype, worse survival and increased tumor recurrence in colorectal cancer (CRC) (Madison et al. 2013b; Madison et al. 2015; Tu et al. 2015). In mice, intestinal epithelial cell (IEC) specific *Lin28b* overexpression is sufficient to transform the epithelium and give rise to adenomas and adenocarcinomas between 9-12 months of age, which is accelerated by the concurrent knockout of *Let7 b1/c2* with faster and greater formation of adenocarcinomas within 6 months (Madison et al. 2013b; Madison et al. 2015). LIN28B cooperates with Wnt signaling to increase tumor formation in carcinogen-induced mouse model of colitis-associated tumorigenesis (Tu et al. 2015). Furthermore, LIN28 overexpression increases tumor formation and decreases tumor latency in an *Apc*[+/min] model of colon cancer (Tu et al. 2015). LIN28A, which is structurally similar to LIN28B (Wang et al. 2016c), is upregulated in over 70% of CRC patients (Wang et al. 2016b) and overexpression of LIN28A is functionally similar to LIN28B (Tu et al. 2015). While silencing either LIN28 protein leads to increased apoptosis by targeting of anti-apoptotic BCL2L1 protein for degradation (Zhang et al. 2018), LIN28A overexpression however, leads to increased chemosensity in CRC cells lines to 5FU (fluorouracil) treatment through induction of apoptosis (Wang et al. 2016b). In summary, LIN28B is critical in colorectal tumorigenesis and has been established to oncogenic effects in this context. While less studied in colorectal cancers, LIN28A has similar functions.

Insulin-like growth factor 2 mRNA binding protein 1 (IGF2BPs/IMPs)

The insulin-like growth factor-2 mRNA binding proteins (IGF2BPs or IMPs) belong to a conserved subfamily of RBPs. The IMPs have been studied for their roles in regulation of post-transcriptional processes such as mRNA localization, turnover, and translational control (Nielsen et al. 2001; Yaniv and Yisraeli 2002). In mammals, the canonical domain structure of IMPs is similar. IMP1 and IMP3 are more closely related and have 73% sequence similarity whereas IMP2 shares 56% similarity (Bell et al. 2013) (Figure 3). IMPs contain 2 RRMs in their N-terminal region and 4 KH domains in the C-terminal region(Nielsen et al. 1999). The KH domains are the primary RBDs while the RRMs are involved in stabilization of IMP-mRNA complexes (Nielsen et al. 2004; Wachter et al. 2013). The IMPs bind their targets in multiple low affinity higher-order complexes because KH domains allow recognition of only short stretches of RNA with relatively weak binding affinity (Chao et al. 2010).

Imp proteins, especially Imp1, are expressed highly during development but expression is reduced drastically after post-natal day 12 in the small and large intestine. The adult mice retain low expression of IMP1 in the crypts (Hansen et al. 2004). IMP3, an isoform of IMP1, also follows a similar pattern of expression in the intestine (Mori et al. 2001). IMP2, by contrast, has been shown to be expressed postnatally (Dai et al. 2011) and is mainly found in Processing bodies (P bodies) in the cytoplasm (Lui et al. 2014). Similarly, *Imp1* null mice show significant growth retardation at E17.5 and more than 50% of the mice do not survive past post-natal day 3. The mice show impaired intestinal morphology and development (Hansen et al. 2004). By contrast, *Imp2* null mice have no growth retardation but are highly resistant to diet induced obesity (Dai et al. 2015). In

colorectal cancer cell lines and fibroblasts, *Imp2* deletion results in reduced proliferation (Dai et al. 2017).

IMP1 plays a functional role in the RNA stability by binding and shielding several mRNAs that play critical roles in cell growth and proliferation from proteolytic degradation (Noubissi et al. 2006). IMP1 also regulates cell cycle progression and migration in human CRC cells (Boyerinas et al. 2008). *IMP1* is overexpressed in more than 80% of human CRC (Ross et al. 2001) and correlates with invasion, lymph node metastasis, and worse prognosis (Dimitriadis et al. 2007b; Hamilton et al. 2013; Madison et al. 2013b). IMP1 overexpression in CRC cell lines causes a significant increase in tumor volume in xenograft models (Hamilton et al. 2013). By contrast, *Imp1* loss in the stroma is associated with increased tumor number in the AOM-DSS model of colonic carcinogenesis. This dichotomous role of Imp1 is seen in other instances where IMP1 stabilizes *β-catenin* mRNA in breast cancer cells (Gu et al. 2008) and is in turn activated by it in a feedback mechanism (Gu et al. 2009). In other studies, IMP1 was shown to bind and stabilize *beta-TRCP1*, a *β-catenin* antagonist in CRC cell lines (Elcheva et al. 2009). *IMP2* gene is amplified at a higher frequency in several solid tumors. IMP2 depletion inhibits proliferation of mouse embryonic fibroblasts (MEFs) and well as several human cancer cell lines. It is also shown to stabilize oncogenic transcriptional regulator HMGA1 in MEFs (Dai et al. 2017). IMP3 expression has been shown to correlate with worse prognosis and increased recurrence in colon cancer patients(Li et al. 2009). It has also been associated with low progression-free survival in small-intestinal neuroendocrine neoplasms (Massironi et al. 2017) and studied as an immunohistochemical marker in small intestinal adenocarcinomas (Daikuhara et al. 2015).

These studies imply divergent roles for IMP1, depending upon whether one considers the epithelial vs. stromal compartment.

Other RNA binding proteins in the intestine

Several other mRNA binding proteins are increasingly being studied for their roles in intestinal homeostasis and disease. A few of the prominent ones are listed below.

Musashi

In the intestinal epithelium, the MSI family of proteins are expressed in the crypts in mice (Wang et al. 2015a). Their expression is observed in adult mice in both the active and reserve stem cell compartments (Li et al. 2014; Li et al. 2015). The MSI family of proteins consist of the functionally redundant MSI1 and MSI2. Ablation of *Msi* proteins (*Msi1* or 2) in IEC, either individually or together, showed no changes in morphology, proliferation or differentiation (Yousefi et al. 2016). Although, intestinal epithelial specific double knockout of *Msi1* and *Msi2* (*Msi1$^{\Delta IEC}$ Msi2$^{\Delta IEC}$*) in mice does not show any overt phenotype under basal conditions(Yousefi et al. 2016) .However, following 12Gy radiation injury, *Msi1$^{\Delta IEC}$ Msi2$^{\Delta IEC}$* mice show a significant impairment in the regenerative response. MSI proteins are also up-regulated during activation of reserve intestinal stem cells and are required for lineage tracing from these cells under basal conditions by enabling their S-phase entry (Yousefi et al. 2016). MSI1 overexpression has been shown to induce tumorigenesis by activation of Wnt and Notch pathways in primary intestinal cells and xenograft models (Rezza et al. 2010). The overexpression of either MSI is sufficient to transform the intestinal epithelium and form tumors (Li et al. 2015; Wang et al. 2015a; Yousefi et al. 2016) via activation of the mTORC1 complex with inhibition of Pten (Li et al. 2015; Wang et al. 2015a). In patients with small intestinal adenocarcinomas, MSI1 is overexpressed in 71% of the tumors as compared to the normal tissue and correlated with depth of wall invasion (Wang et al. 2015c). In patients with Irritable bowel syndrome (IBS) the density of MSI1+ cells are significantly reduced

and correlates with dysfunctional stem cell potential (El-Salhy and Gilja 2017). MSI1+ cells have been shown to be involved in repair of the intestinal epithelium induced by 5-FU (Luo et al. 2017). Due to their roles in EMT, stem cell identity, and oncogenesis, the MSI proteins have increasingly been linked to therapeutic resistance in cancer treatments (Han et al. 2015; de Araujo et al. 2016; Lee et al. 2016). This has resulted in efforts to develop inhibitors of MSI proteins as potential therapeutic targets (Clingman et al. 2014; Lan et al. 2015).

HuR

HuR , a member of ELAV family of RBPs (reviewed extensively in (Hinman and Lou 2008)) consists of 2 RRM domains, a hinge region and a third RRM (Brennan and Steitz 2001) that helps it bind to adenylate uridylate (AU) rich regions in 3' UTRs of target RNAs involved in cell survival and tumorigenesis(Brody and Gonye 2011). HuR is expressed throughout the intestinal epithelium in mice (Giammanco et al. 2014) (Liu et al. 2014a). Although mice with intestinal epithelial cell (IEC) knockout specific *HuR* show signs of mucosal atrophy, there are no changes in body weight or other abnormalities (Giammanco et al. 2014). These mice show reduction in proliferating cells in the intestine and shorter crypts and villi but are otherwise healthy and reproduce normally (Giammanco et al. 2014) (Liu et al. 2014a).

High HuR protein expression is found in both the nucleus and cytoplasm of human colon cancers (Denkert et al. 2006). While low HuR protein expression is observed in the normal colon (Young et al. 2009), it is increased significantly in the cytoplasm of colorectal tumors (Young et al. 2009). Mice with intestinal specific *HuR* deletion (*HuR$^{\Delta IEC}$*) show increased injury in a doxorubicin induced acute injury model (Giammanco et al. 2014). These mice also show increased regeneration and compensatory proliferation during the peak damage phase. Furthermore *HuR$^{\Delta IEC}$* mice

show more than 60% attenuation in the polyposis phenotype in the $Apc^{min/+}$ mice (Giammanco et al. 2014).By contrast, $HuR^{\Delta IEC}$ mice show increased protection in the AOM-DSS model of tumorigenesis (Giammanco et al. 2014). In intestinal cell lines, HUR inhibition causes a significant decrease in Wnt signaling, thereby suggesting a potential role in the regulation of the Wnt pathway (Liu et al. 2014a). HuR also has tumor suppressive functions via the regulation of tumor suppressors p21 and Wnt family protein Wnt-5a (Leandersson et al. 2006). HuR is known to mediate post-transcriptional regulation of its target mRNAs and is critical for neoplastic transformation and cancer development. Furthermore, HuR is activated in response to various stressors(Brody and Dixon 2018). HuR is being explored as a therapeutic target and small molecule inhibitors are being developed (Brody and Gonye 2011; Blanco et al. 2016; Brody and Dixon 2018).One such molecule , MS-444, has been shown to inhibit HuR that in turn decreases GI tumorigenesis and the proliferation of colon cancer cells (Blanco et al. 2016; Lang et al. 2017).

Mex3A

In humans, MEX3 has 4 homologous isoforms MEX 3A-3D(Buchet-Poyau et al. 2007). In mice, MEX3A is expressed in the crypt base and labels a slowly cycling subpopulation of Lgr5+ intestinal stem cell population that can give rise to all lineages (Barriga et al. 2017). These MEX3A- high cells appear to resist the deleterious effects of chemotherapy or irradiation and play an important role in regeneration of damaged crypts(Barriga et al. 2017). Previous studies have shown that MEX3A regulates CDX2 in human colon cancer and correlates with "stemness" (Pereira et al. 2013). *Mex3a* deletion in IEC does not cause any changes in reproduction and intestinal morphology in mice (Barriga et al. 2017). In Caco2 cells that can spontaneously differentiate into an enterocytic-like phenotype upon reaching confluence (Pinto et al. 1983), inhibition of

endogenous *MEX3A* using siRNA resulted in higher *CDX2* expression (Pereira et al. 2013). MEX3A overexpressing Caco2 cells show increased RNA expression of stem cell markers (Pereira et al. 2013). Mex3a is overexpressed in cancers like bladder urothelial carcinoma (Sakurai et al. 2017) and Wilm's tumor (Jiang et al. 2012) whereas knockdown of MEX3A in human gastric cancer cells has been shown to significantly reduce cell proliferation (Jiang et al. 2012) thus indicating its role in carcinogenesis and potential as a therapeutic target. This indicates the potential to study Mex3a in colorectal cancer.

CELF1

CUG binding protein 1 (CUBP1) or CELF1 is a multifunctional RBP studied primarily for its role in RNA metabolism related processes like decay, translation and splicing. CELF1 is known to bind GU rich elements in 3'UTR of target RNAs to regulate RNA stability (Vlasova-St Louis and Bohjanen 2011). In mice, CELF1 is expressed throughout the small intestinal epithelium (Liu et al. 2015) and can be repressed by mir-503 and recruited to P bodies (Cui et al. 2012). mRNAs are localized to these cytoplasmic RNP foci and sorted for degradation and/or translational repression. CELF1 is also known to recruit certain target mRNAs like occludin to these P bodies and partially repress their translation (Liu et al. 2015). Although CELF1 expression is found to increase proliferation and progression of several cancers (House et al. 2015; Xia et al. 2015; Cifdaloz et al. 2017), increased CELF1 causes G1 phase growth arrest in intestinal epithelial cells. By contrast, CELF1 silencing enhances cell proliferation, with an increase in cells residing in S-phase, and elevated cell number. CELF1 silencing enhances MYC translation by releasing MYC RNA from RNP complexes (Liu et al. 2015). HUR is found to competitively repress this CELF1-MYC interaction (Liu et al. 2015). CELF1 is mainly studied for its role in regulation of splicing in myotonic dystrophy

(Ho et al. 2005; Zhang et al. 2008). In the context of cancer, CELF1 can act as a tumor suppressor (in liver cancer (Lewis et al. 2017)) , increase caspase activity/apoptosis (in hepatocellular carcinoma(Kim et al. 2017b) and esophageal cancer (Chang et al. 2012)) and act as a central node in post-transcriptional regulatory programs underlying EMT (in breast cancer (Chaudhury et al. 2016)) indicating its diverse role in carcinogenesis.

RBM3

RNA-binding motif protein 3 (RBM3) , a glycine rich RBP (Kishore et al. 2010), is an important cold shock protein that is upregulated during environmental stimuli such as hypothermia, ischemia, and hypoxia (Yang et al. 2014). RBM3 deficient mice show no overt phenotype or growth changes and are fertile (Matsuda et al. 2011). RBM3 overexpression in HCT116 and DLD1 colon cancer cells increases proliferation and engenders chemotherapy resistance. These cells also exhibit increased stem cell markers via an increase in B-CATENIN activity. Therefore, the *B-CATENIN* signaling pathway may be regulated through alterations in expression of RBM3 (Venugopal et al. 2016). In colon cancer, RBM3 is upregulated in a stage dependent manner and its overexpression is capable of inducing oncogenic transformation (Sureban et al. 2008). RBM3 is shown to increase the stability and translation of rapidly degraded mRNAs such as cyclooxygenase 2 (*COX-2*), interleukin-8 (*IL-8*), and vascular endothelial growth factor (*VEGF*) (Sureban et al. 2008). Like the other RBPs, the role of RBM3 can be dichotomous in different contexts. In breast cancer, higher RBM3 expression correlates with increased disease-free survival (Jogi et al. 2009). RBM3 expression is upregulated in, and correlates with, good prognosis in several cancers, including ovarian, prostate, bladder, gastric, and colorectal cancer (Grupp et al. 2014; Melling et al. 2016; Jang et al. 2017; Ye et al. 2017). RBM3 causes cellular differentiation and apoptosis in these cancers.

Dichotomous roles of RBPs in gastrointestinal cancer

RBPs are rapid and effective regulators since they bind already transcribed targets. The functional role of RBPs therefore depend on the transcripts present within a specific cell type. Even in the same cell type, changes in the transcriptome, due to environmental changes or injury, can lead to different functional outcomes for RBPs. This is also true for different tissues or organs where transcriptome profiles vary. Furthermore, since RBPs binding to target transcripts can result in a number of functional outcomes, it may be difficult to extrapolate the functional role from one context to another. For example, although IMP1 is recognized as an oncofetal protein due to its over-expression in colorectal cancers and increased tumor burden with IMP1 expression in xenograft models(Hamilton et al. 2013), IMP1 deletion in mesenchymal cells in the intestinal mucosa leads to increased tumor burden in mice(Hamilton et al. 2015). Similar, opposing roles for IMP1 has also been reported in breast cancer (Nwokafor et al. 2016) (Wang et al. 2016a) (Tessier et al. 2004). IMP may therefore can exhibit both tumor-initiating or tumor suppressive functions. Another example of this paradigm is HuR, which has been known to stabilize and increase translation of several key cancer related pathways(Mazan-Mamczarz et al. 2008). In a recent study in pancreatic ductal adenocarcinoma cells, HuR deletion resulted in a decrease in proliferation and an increase in cell death, possibly via regulation of KRAS pathway genes(Lal et al. 2017). In contrast, other studies have shown that *HuR* knockdown in myeloid lineage cells in mice caused an increased susceptibility to colitis associated cancer and increase in inflammatory mRNAs(Yiakouvaki et al. 2012).

Similarly, while CELF1 deletion in several cancer cell lines decreased proliferation and migration(Gao et al. 2015; House et al. 2015), and *Celf1*-deficient mice exhibited growth retardation(Kress et al. 2007), it has also been reported to promote apoptotic resistance in esophageal cancer(Chang et al. 2012). Furthermore, CELF1

exhibits opposing effects on cell proliferation in primary versus malignant T cells due to differences in the transcriptomes (Bohjanen et al. 2015). In yet another example, *Mex3a* is expressed in slow dividing intestinal stem cells(Barriga et al. 2017), but in CRC cell lines, the effect of MEX3A on differentiation depends on cell confluence. At low confluency, MEX3A inhibition increased CDX2 expression, but this effect was reverted when the cells were highly confluent(Pereira et al. 2013). Taken together, these studies demonstrate that RBPs represent a complex regulatory network and their functional roles depend on the tissue type, microenvironment and the transcriptome of cells in which they are expressed. Therefore, understanding the precise, context-dependent mechanisms by which RBPs regulate protein expression in combination with other factors will be essential to understanding their complex roles in gastrointestinal cancers.

Identifying binding targets of RBPs

Crosslinking Immunoprecipitation – Sequencing (CLIP-Seq)

There are multiple experimental methods to unravel the landscape of RBP biology and their roles in disease (Figure 4). One method for identifying direct roles of RNA binding proteins has been to determine their target transcripts, using crosslinking immunoprecipitation (CLIP). The RBP under study is crosslinked *in vivo* to its target transcripts via a crosslinking agent, such as UV light, that forms covalent bonds between the RNA and protein. Cells are then lysed and the RBP precipitated using an antibody. Proteinase K is used to digest the RBP and leave the bound transcripts intact. After ligating adapters and linkers to the RNA, the transcript is reverse transcribed to cDNA and identified via high-throughput sequencing(Ule et al. 2003). CLIP techniques have been refined over the years to increase precision and sensitivity.

Several high precision crosslinking immunoprecipitation (CLIP) techniques in conjunction with sequencing have been developed, including HITS-CLIP(high-

throughput sequencing of RNA isolated by crosslinking immunoprecipitation)(Darnell 2010), PAR-CLIP(photoactivatable ribonucleoside–enhanced cross-linking and immunoprecipitation) (Hafner et al. 2010) and iCLIP (individual nucleotide–resolution cross-linking and immunoprecipitation) (Konig et al. 2010), among others. These can provide single nucleotide level resolution *in vivo*. These protocols can be technically challenging, with complex library preparations and difficulty in identifying targets when binding domains are not clearly understood. Newly improved eCLIP protocols have overcome some of these challenges(Van Nostrand et al. 2016). Although CLIP protocols can induce mutations due to UV-crosslinking and resulting in reduced sensitivity, it can be overcome by using PAR-CLIP techniques that incorporate photoactivatable ribonucleoside analogs into nascent transcripts as a means to decrease background noise(Ascano et al. 2012). A comparison between these techniques are listed in Table 1 (adapted from (Wang et al. 2015b)).

CLIP- Seq libraries have been generated for several RBPs in different cell types, including LIN28B(Madison et al. 2013b), IMP1(Conway et al. 2016) and MSI1(Bennett et al. 2016). While CLIP studies have been essential in our understanding of basic RBP biology, there are limitations. For example, several RBPs are only expressed in undifferentiated cells and their expression is very low in differentiated intestinal cells and therefore CLIP studies become a challenge unless the RBPs are genetically overexpressed or induced during stress or disease models. Although these analyses are feasible, the presence of non-physiological levels of these RBPs with several RNA binding sites may promote non-specific interactions or false positive binding targets. Furthermore, depending on the cell lines or tissues used, the transcriptome varies and thus the context-specificity of strength and intensity of binding may not be recapitulated.

RNA-Sequencing: evaluating the transcriptome in cells with over-expression or deletion of RBPs

Another technique to study the role of RBPs is to evaluate the transcriptome after modulation of RBP expression. This has been especially useful in genome wide association studies for human cancers. Whole genome RNA sequencing has been used to generate libraries for several cancers to identify genes that are amplified or silenced at transcription level(Lee et al. 2015). These libraries have been made publicly available using the Cancer Genome Atlas (TCGA) databases(Tomczak et al. 2015). RNA levels can be used along with DNA sequencing and clinical data for a variety of association studies to identify potential therapeutic targets. These targets can then be studied functionally to understand their roles. TCGA uses an Illumina based RNA sequencing platform and helps identify and quantify rare and common transcripts, isoforms, novel transcripts, gene fusions, and non-coding RNAs, among a wide range of samples, including low-quality samples(Wang et al. 2009). Transcriptome analysis provides information on RNA sequence coverage, sequence variants (e.g. fusion genes), expression of genes, exon, or junction. This can further be correlated to somatic mutation status, disease stage, prognosis and other clinical data(Brody and Dixon 2018).

Functional effects of RBPs can be studied by overexpressing or deleting the RBP gene followed by high-throughput RNA sequencing. This generates a snapshot of total RNA abundance in the presence or absence of a given RBP. Since RBPs can regulate the stabilization, degradation, localization and post-transcriptional modification (for example, splicing) of their targets, RNA sequencing provides a robust tool to study these changes in an unbiased, genomic way. However, since proteins are the functional effectors in cells, RNA sequencing may not serve as a direct indication of the functional role of the RBP. For example, some RBPs may bind to their target transcripts and cage them in RNP granules, making them inaccessible to the translation machinery(Bley et al.

2015). In these cases, mRNA abundance does not correlate to translation/functional effects. Therefore, RNA sequencing should be combined with additional analyses to determine functional roles of RBPs.

Ribosome profiling: Studying the 'translatome'

To completely understand the functional effect of RBP expression or deletion, evaluation of the protein landscape is required. Proteomics encompasses the study of the function and structure of proteins in a complex biological sample. Mass spectrometry(Whitelegge et al. 1999) and Edman degradation(Edman and Begg 1967) remain the two major techniques used for protein sequencing or to identify post-translational modifications. There are several challenges with these techniques including technical challenges (such as protein solubility, separation, detection of intact proteins), scalability, difficulty in sample preparation, high expense, low sensitivity and limitations in bioinformatics tools(Chandramouli and Qian 2009; Gregorich and Ge 2014). In recent years, ribosome footprint profiling (RFP) has been developed as a powerful tool to obtain a global snapshot of actively translating transcripts within a cell(Ingolia et al. 2013; Ingolia et al. 2014; Ingolia 2016).

This ribosome-centric technique uses binding and density of ribosomes on a transcript as an indicator of active translation. Profiling is done by deep sequencing of ribosome bound transcripts as well as sequencing total RNA abundance. Polysomes (a cluster of ribosomes held together by a strand of messenger RNA that each ribosome is translating) are stabilized by blocking translation elongation using cyclohexamide before cell lysis(Ingolia et al. 2011). This technique detects relative changes, so it relies on cells or tissues with deletion or overexpression of the desired RBP. This technique can help distinguish between genes regulated at the transcriptome and translatome levels. The ratio of RFP to total mRNA abundance for each transcript reveals the translation

efficiency for that gene that can be compared across genotypes or conditions(Zhou et al. 2013a) (Figure 5).

Incorporating multiple techniques to understand the global function

To completely understand the function of a RBP in a cell, we need to understand what target transcripts it binds to, the context-dependent binding, and downstream effect on transcription and translation of the transcript. To that end, combining CLIP-seq with ribosome profiling or proteomics would provide a more complete functional snapshot for a given RBP. Furthermore, genetic engineering studies can be used to overexpress or delete the RBP in different cell types at homeostasis and injury conditions to further increase our understanding of the dynamic role of RBPs *in vivo*. In conclusion, we have discussed a number of GI-relevant RBPs and their roles in homeostasis and disease. Furthermore, we highlight emerging techniques that may be employed *in vivo* to understand the context (cell type and disease state)-dependent function of RBPs. Identifying mechanisms of RBP biology in GI diseases may provide a foundation for new therapies to target or modulate RBP-RNA interactions.

The LIN28B - IMP1 axis – The hypothesis

The intestinal epithelium is in a dynamic equilibrium of proliferation, differentiation and apoptosis along the crypt-villus gradient. Normal intestinal homeostasis is disturbed during states of infection, inflammation and malignant transformation (adenomatous polyps, colorectal cancer). The pathogenesis of sporadic colorectal cancer (CRC) involves distinct pathways with characteristic genomic and genetic alterations. Despite significant advances in leveraging our understanding of these pathways for diagnostic, prognostic, and therapeutic strategies, colorectal cancer remains a top cause of cancer-related mortality, resulting in greater

than 50,000 deaths per year in the United States. This underscores a specific need to identify and understand novel, therapeutically tractable pathways in intestinal homeostasis that may drive CRC. Our work has introduced and elucidated the role of mRNA binding proteins in intestinal/colonic epithelial homeostasis, as well as aberrations including hyperproliferation, altered metabolism and transformation (1-6). Regulation of cellular identity and behavior via RNA binding proteins represent a unique layer of signaling control, where individual RNA binding proteins or networks represent the novel paradigm of "RNA regulons" (7). My thesis seeks to parse the individual and cooperative roles of two essential RNA binding proteins, LIN28B and IMP1, in gastrointestinal homeostasis and disease.

LIN28B plays a functional role in embryonic stem cells (ESCs) and induced pluripotent stem cells (iPSCs), where Oct4, Sox2, and Nanog occupy its promoter (8). LIN28B binds to and promotes the translation of multiple mRNA targets, including IGF2, OCT4, CCNB1, and BMP4 (9-11). In addition to regulating mRNAs, LIN28B post-transcriptionally regulates the Let-7 microRNA family via binding to pri-Let-7 in the nucleus, where it prevents Drosha-mediated cleavage and maturation resulting in suppression of differentiation (12). Let-7

microRNAs have diverse mRNA targets, including IMP1 (Igf2 mRNA binding protein-1), another mRNA binding protein with diverse functional roles. IMP1 binds to and promotes the translation of several mRNAs, including MYC, ACTB, and IGF2 mRNAs (13-16). Mice with global Imp1 gene deletion exhibit dwarfism and decreased survival, suggesting a critical role for Imp1 in development (17). Taken together, the LIN28B/Let-7/IMP1 axis represents a powerful signaling node with broad, yet incompletely understood functional roles. Furthermore, despite their association via Let-7, the overlapping and divergent targets of LIN28B and IMP1 have yet to be determined and

functionally characterized. Mechanistically, LIN28B and IMP1 have been associated with translation (via localization in polysomes) and mRNA localization (based upon localization in RNA particles and RNA granules), respectively (18). Subcellular localization of RNA binding proteins and their respective mRNA targets indicate that a subset of transcripts may be protected from degradation or repressed (rather than actively translated), the basis of which is not known for LIN28B and IMP1. As such, strategies to understand the effects of LIN28B and IMP1 on both transcript and protein abundance are highly relevant.

We have demonstrated that LIN28B drives tumor-initiating cell phenotype however, it remains unclear if LIN28B-mediated hyperproliferation, altered differentiation, and associated tumorigenesis is functionally dependent on IMP1. In addition, it remains unknown if the roles of IMP1 depend entirely on its regulation by Let-7 downstream of LIN28B. Taken together, published data from our own and other laboratories support the scientific premise that LIN28B and IMP1 represent functionally interdependent signaling modulators that may play critical roles in normal intestinal homeostasis and disease. The current Aims will address the hypothesis that LIN28B and IMP1 comprise cooperative roles in controlling post-transcriptionally the pathways associated with epithelial cell fate, which may favor malignant

transformation.

Studies herein will reveal new insights into how synergy within the LIN28B-Let-7-IMP1 axis

modulates intestinal epithelial homeostasis and cancer and will identify the specific mechanistic underpinnings. These findings have the potential to introduce a new paradigm of dose-dependent roles for mRNA binding proteins within the same axis as new prognostic indicators. In addition, the LIN28B-Let-7-IMP1 axis has emerged recently

as a novel therapeutic target for RNA-based therapies, which could be directly

applicable to the treatment of multiple GI diseases (i.e. IBD, CRC).

Figures and figure legends

Figure 1: Schematic representation of the crypt-villus axis and the major intestinal cell types for small intestine and colon
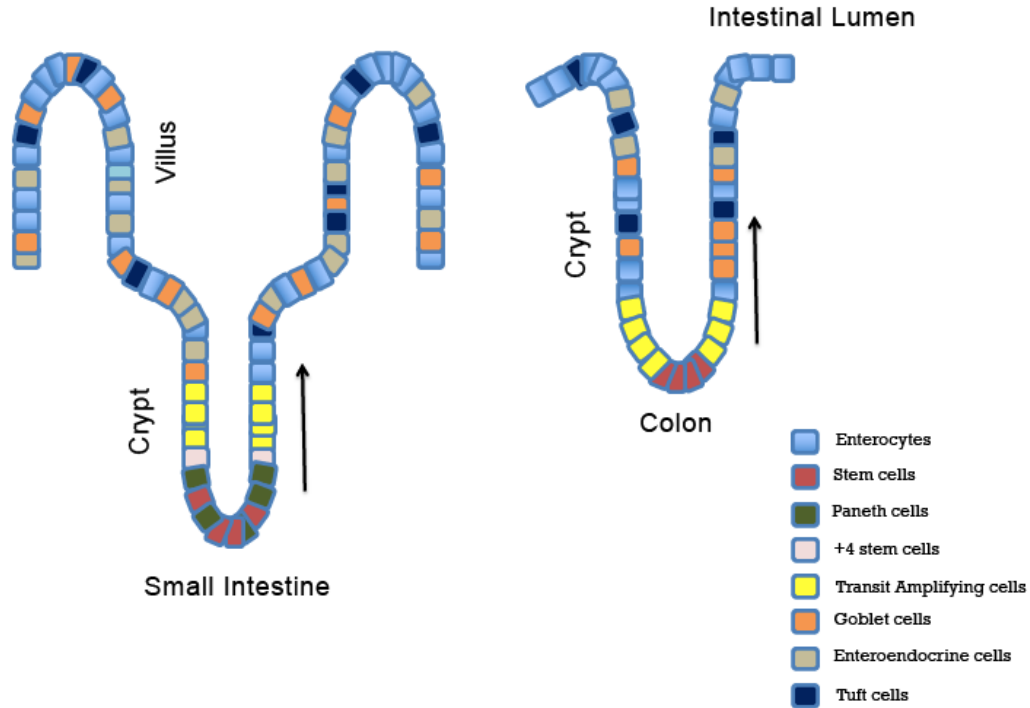
The figure depicts the major cell types in the small intestine and colon. The stem cells reside at the crypt base and proliferate (transit amplifying cells) and differentiate into secretory (Paneth, enteroendocrine, goblet, tufts cells) and absorptive lineages (enterocytes). These differentiated cells migrate towards the villi (in the small intestine).

Figure 2: Schematic representation of the different functional roles of RBPs
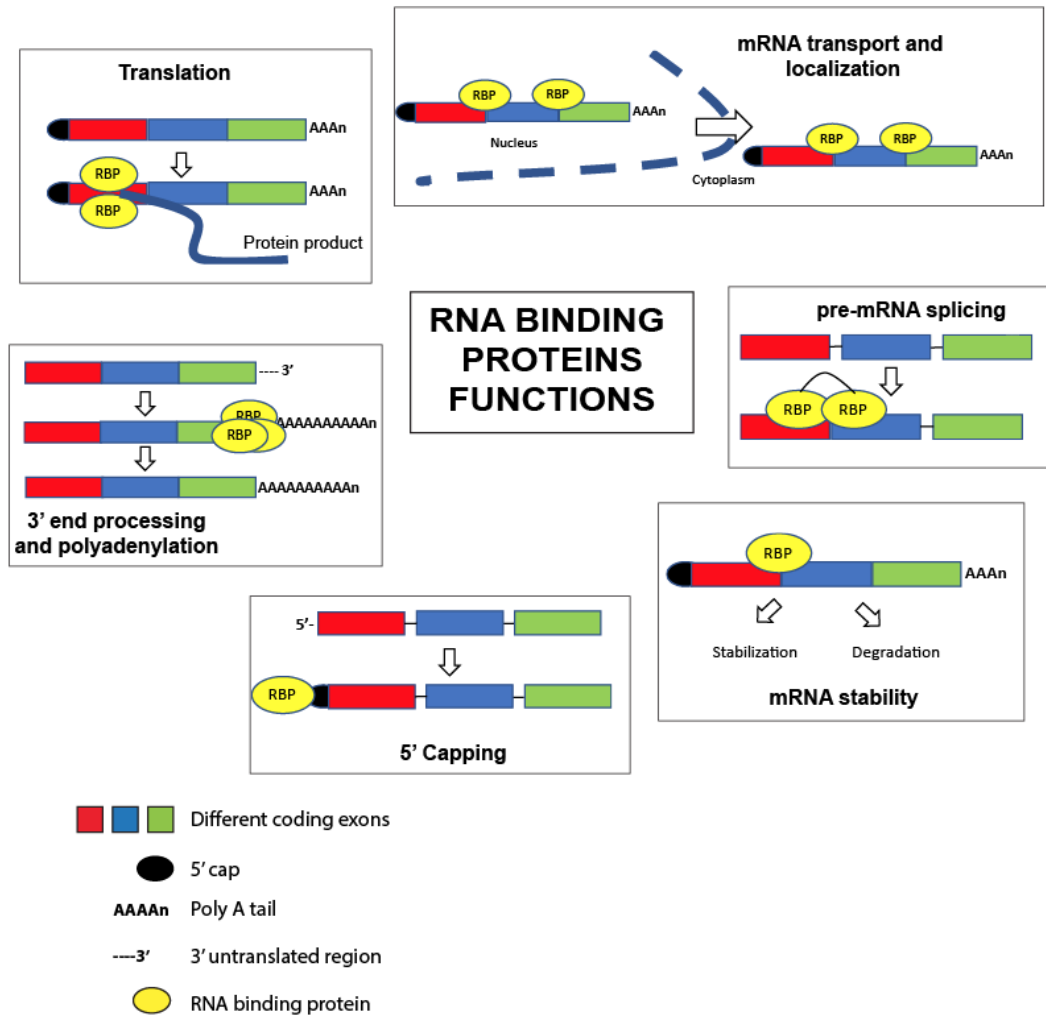
The figure depicts the major functional roles of the RBPs discussed in this chapter. The majority of the RBPs discussed here bind to mRNAs and regulate their processing (5' capping, 3' end processing, splicing), stability, localization and translation. This figure does not depict the non-conventional RBPs.

Figure 3: Schematic representation of the structural domains of LIN28 and IMPs
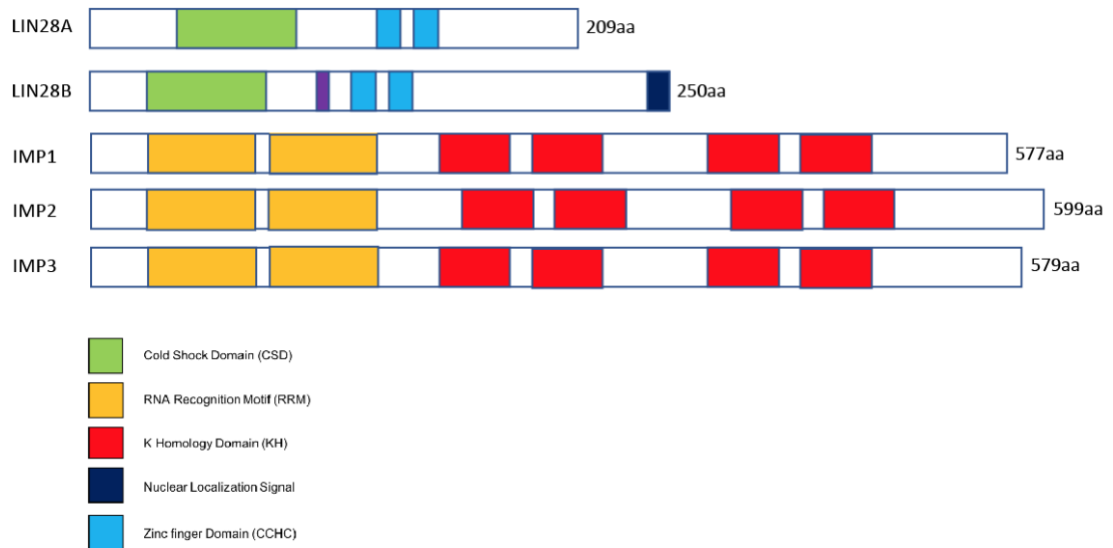
The figure shows a simplistic representation of the different structural domains of the RBPs that help them bind to their target RNAs and regulate their function. The amino acid length of the RBPs are also indicated. The RBPs contain different types of RNA binding and catalytic domains including RRMs, KH domains, zinc finger domains and cold shock domains. LIN28 proteins also contain localization signals to help them shuttle in and out of the nucleus.

Figure 4: Different experimental methods to unravel the landscape of RBP biology and their roles in disease
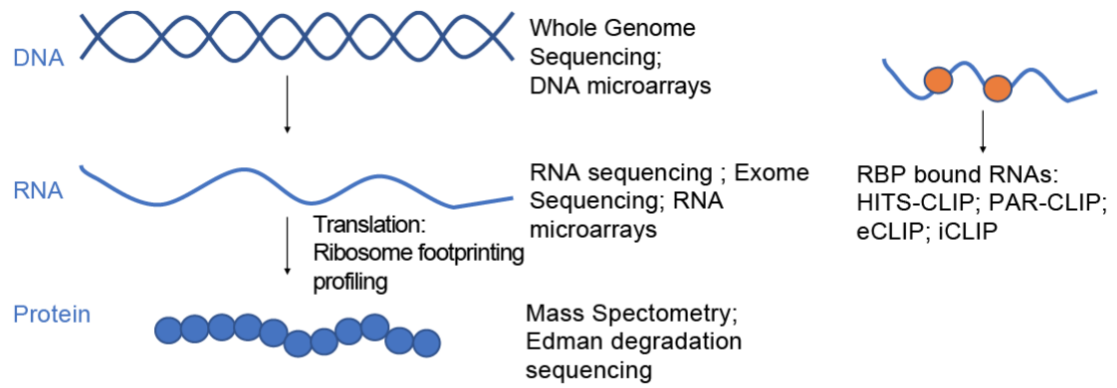
Figure 5: Schematic representation of Ribosome profiling
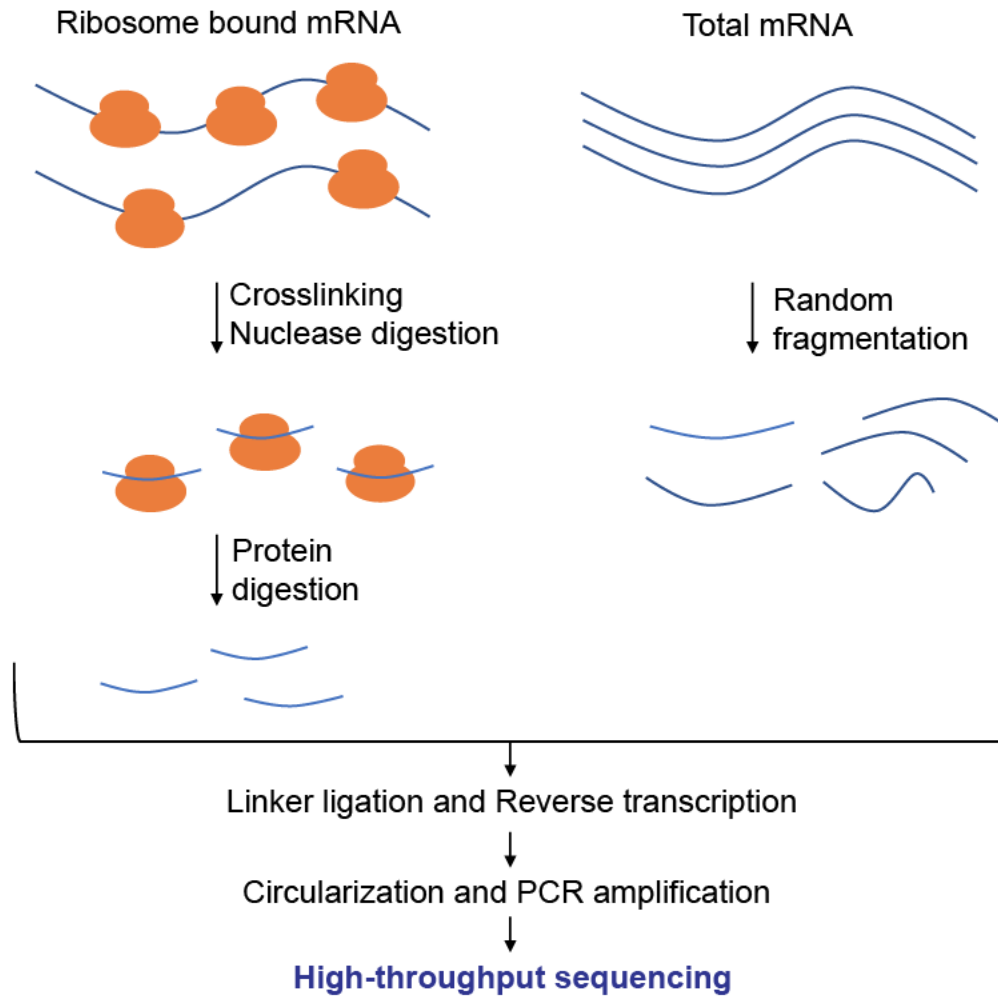
Ribosome profiling produces a "global snapshot" of all the ribosomes active in a cell at a particular moment, known as a translatome. It enables researchers to identify the location of translation start sites, the complement of translated ORFs in a cell or tissue, the distribution of ribosomes on a messenger RNA, and the speed of translating ribosomes. Ribosome profiling involves similar sequencing library preparation and data analysis to RNA-Seq, but unlike RNA-Seq, which sequences all of the mRNA of a given sequence present in a sample, ribosome profiling targets only mRNA sequences protected by the ribosome during the process of decoding by translation.

CHAPTER II: THE LIN28B-IMP1 POST-TRANSCRIPTIONAL REGULON HAS OPPOSING EFFECTS ON ONCOGENIC SIGNALING IN THE INTESTINE

(This section has been accepted for publication at Genes and Development (*Chatterji,Hamilton et. al, 2018*)

Abstract

RNA binding proteins (RBPs) are expressed broadly during both development and malignant transformation, yet their mechanistic roles in epithelial homeostasis or as drivers of tumor initiation and progression are incompletely understood. Here we describe a novel interplay between RBPs LIN28B and IMP1 in intestinal epithelial cells. Ribosome-profiling and RNA-sequencing identifies IMP1 as a principle node for gene expression regulation downstream of LIN28B. *In vitro* and *in vivo* data demonstrate that epithelial IMP1 loss increases expression of WNT target genes and enhances LIN28B-mediated intestinal tumorigenesis, which was reversed when we overexpressed IMP1 independently *in vivo*. Together, the data provides new evidence for the opposing effects of the LIN28B-IMP1 axis on post-transcriptional regulation of canonical WNT signaling, with implications in intestinal homeostasis, regeneration and tumorigenesis.

Keywords

Introduction

Post-transcriptional regulation of key growth and oncogenic pathways by RNA binding proteins (RBPs) is an emerging hallmark of cancer. Understanding the relative contribution and regulation of gene transcription and translation to functional and phenotypic outcomes is essential for generating effective therapeutics. Given the large number of putative binding targets and effector pathways downstream of RBPs, their evaluation *in vivo* is critical to understanding the prevailing effects of specific RBP:RNA target interactions in variable biological contexts. Intestinal epithelial cells exhibit remarkable plasticity in their ability to rapidly proliferate, differentiate, and undergo repair- processes that are aberrantly regulated during tumorigenesis. While the critical cellular pathways for epithelial injury repair and tumor development are well studied, the relative contribution of RBPs as key, functional regulators of these pathways are just beginning to be understood. A primary role of RBPs is to bind to and regulate functionally interrelated target transcripts, forming functional units referred to as "regulons" (Keene 2007; Morris et al. 2010). The integration of transcriptional and translational data has revealed that a significant number of genes are highly regulated at the translational level, underscoring the potential significant contribution of RBPs to numerous basic biological functions (Schafer et al. 2015). Pathways critical to epithelial homeostasis, such as WNT signaling, are aberrantly activated in and can contribute to colorectal cancer (CRC) pathogenesis, resulting in challenges for direct therapeutic targeting.

As a master regulator of the let-7 family of microRNAs, LIN28B exerts its effects via suppression of let-7 processing and thus up-regulation of let-7 targets, including *HMGA2* and *IGF2BP1* (*IMP1*) (Boyerinas et al. 2008; Piskounova et al. 2011). In addition, LIN28B acts as a pluripotency factor and promotes tumorigenesis in multiple tissues (Viswanathan et al. 2009; Tu et al. 2015; Rahkonen et al. 2016; Zhang et al.

2016). We demonstrated previously that LIN28B overexpression promotes migration and invasion *in vitro* and that CRC cells overexpressing LIN28B exhibit smaller, yet more metastatic tumors in subcutaneous xenograft mouse models. (King et al. 2011a; King et al. 2011b). In addition, we and others have established LIN28B is a *bone fide* oncogene in the intestinal epithelium (Madison et al. 2013b); (Tu et al. 2015). Furthermore, tumorigenesis was accelerated in mice with specific deletion of *let-7c2/let-7b*, suggesting that the oncogenic effects of LIN28B are predominantly via its regulation of let-7. In support of this notion, deletion of a single allele of the let-7 target *Hmga2* repressed Lin28b-driven tumorigenesis (Madison et al. 2015). Other key let-7 targets upregulated in *VillinLin28b* mice included *Igf2bp1*, *Igf2bp2*, *E2f5*, *cyclinD1* and *Acvr1c*. Recognizing that LIN28B functions as an oncogene in CRC and blocks processing of pre/pri -*let-7*, we reasoned that let-7 mRNA targets may be effectors of LIN28B-mediated oncogenic transformation. Specifically, we hypothesized that IMP1 may be a critical effector of LIN28B's actions.

IMP1 is a RBP with oncofetal functions that is minimally expressed in adult tissues during homeostasis. We demonstrated previously in subcutaneous xenografts that IMP1 overexpression in SW480 CRC cells exhibit increased tumor volume and elevated levels of its mRNA-binding target *CD44* (Hamilton et al. 2013). Conversely, loss of both *Imp1* alleles in stromal cells led to enhanced tumor load in colitis-associated colon tumorigenesis (Hamilton et al. 2015) indicating a tumor-suppressive role for IMP1 in this context. Others have reported diverse findings in other cancers; for example, overexpression of the IMP1 mouse homolog CRD-BP in mammary epithelial cells resulted in mammary tumor formation with a subset of mice exhibiting metastasis (Tessier et al. 2004). Conversely, studies in orthotopic breast fat pad xenografts demonstrated that IMP1 overexpression suppressed the growth of MDA231 cell-derived tumors and subsequent lung metastasis, as well as an associated decrease in IMP1

mRNA-binding targets *PTGS2*, *GDF15*, and *IGF2* (Wang et al. 2016a). Finally, ectopic

Imp1 expression in the *MMTV-PyMT* breast cancer mouse model significantly reduced

metastatic tumors (Nwokafor et al. 2016). Based upon these functional studies, we

conclude that IMP1 may exhibit oncogenic or tumor suppressive functions in a context-

dependent manner. Furthermore, these studies demonstrate that IMP1 may enhance or

suppress its mRNA-binding targets.

 In the current study, we utilize the intestinal epithelium as a prototypical model for

understanding the tissue-specific roles of two key RBPs, LIN28B and IMP1, in the

context of fundamental homeostasis and tumorigenesis. We performed novel and

unbiased transcriptome and translatome studies as a function of LIN28B expression and

found that IMP1 is a top regulator of differentially expressed transcripts with LIN28B

overexpression. We next evaluated the *in vivo* consequences of LIN28B expression with

and without IMP1 expression, elucidating their functional relevance in intestinal

homeostasis and tumorigenesis with pivotal involvement of WNT signaling. Taken

together, our studies reveal a LIN28B-IMP1 axis governing a post-transcriptional regulon

capable of modulating epithelial cell growth via global control of the WNT pathway.

Results

**IMP1 loss is a significant regulator of translation in the context of LIN28B
overexpression**

 To understand how LIN28B may modulate translation of the transcriptome, and

how this is impacted by IMP1, we used ribosome profiling to obtain a genome-wide

snapshot of translation in the context of LIN28B overexpression. First, we evaluated

SW480 CRC cells overexpressing LIN28B (King et al. 2011a; King et al. 2011b)

(Supplemental Figure 1A). We used tRanslatome (Tebaldi et al. 2014) to identify

putative regulatory factors upstream of differentially translated genes in LIN28B overexpressing versus control cells. This method computes a Fisher test p-value indicating whether binding sites for each regulator are significantly enriched in differentially expressed genes lists. This analysis allows the user to identify possible regulatory factors responsible for the translational regulation of differentially expressed genes in the experiment under consideration. The list of genes regulated by each post-transcriptional element was obtained from the Atlas of UTR Regulatory Activity (AURA) database (Dassi et al. 2014). Through this analysis, we identified IMP1 as a significant post-transcriptional regulator in LIN28B overexpressing cells (Figure 6A).

Next, we analyzed differential gene expression between LIN28B overexpressing lines with and without CRISPR/Cas9-mediated IMP1 deletion (Supplemental Figure 1A) and calculated log fold-changes between ribosome-bound RNAs (ribosome protected fragments, RPF) and total mRNA. A total of 1284 genes were regulated by IMP1 exclusively at the translational level, whereas 264 genes were regulated only at the transcriptional level. Additionally, 458 genes were regulated via translational antagonism, where genes exhibited increased mRNA levels, but lower translational efficiencies or *vice versa,* or translational reinforcement –where translational changes amplified the changes at the mRNA level (Figure 6B). These data demonstrate IMP1 is a major translational regulator of target genes. Translational regulation can occur through differential translation efficiencies (TE) of transcripts, which is calculated as the ratio of RPF reads to total mRNA abundance. We observed several transcripts with significantly different TE values between cells overexpressing LIN28B with or without IMP1 deletion (Figure 6C). Pathway enrichment analysis for TE genes differentially expressed in LIN28B cells with or without IMP1 deletion revealed a significant representation of pathways linked to cancer, including the WNT signaling pathway (Figure 6D, Supplemental Table 3). Finally, gene-set enrichment analysis (GSEA) of RNA-seq data

from the same cells suggest that IMP1 deletion upregulates WNT signaling at the mRNA level as well (Supplemental Table 1), demonstrating IMP1 modulation of WNT at both transcript abundance/stability and TE levels in this context. We further validated this in the SW480 cells overexpressing LIN28B with and without IMP1 deletion (Supplemental Figure 1C,D). We saw a significant upregulation of Wnt targets with IMP1 deletion via qPCR and upregulation of ß-catenin protein levels via western blot in these cells. Finally, to validate upregulation of Wnt targets identified via RNA sequencing, we used siRNA to knockdown IMP1 in Caco2 cells (Supplementary Figure 4A,B) that endogenously express LIN28B (Mizuno et al. 2018). We observed significant upregulation of multiple WNT targets with IMP1 knockdown, corroborating our findings in a second, independent cell line (Supplemental Figure 4A,B).

In an attempt to elucidate if direct binding may correlate with TE, we compared binding intensities of IMP1 targets identified via previously published enhanced UV crosslinking and immunoprecipitation (eCLIP) in human pluripotent stem cells (hPSCs) (Conway et al. 2016) with differential translational efficiency (TE) of these targets from the present study (in human CRC cells). However, we found no correlation between binding intensities and TEs (Supplemental Figure 1B). In addition, a large number of targets identified in eCLIP studies did not change significantly in our TE dataset and *vice versa* (Supplemental Table 2). While we cannot exclude the possibility that differences between mRNA-binding and TEs may be due in part to comparing hPSCs to CRC cells, these data nevertheless reinforce the concept that eCLIP-identified IMP1-bound targets may not necessarily correlate with gene expression changes (Conway et al. 2016).

IMP1 loss enhances LIN28B-mediated tumorigenesis *in vivo*

Gene expression and ribosome profiling data suggest that IMP1 loss causes dysregulation of several key signaling pathways that are involved in cellular proliferation

and maintenance. To understand the phenotypic consequence of these changes, we used LIN28B-overexpressing CRC cells with and without IMP1 loss in subcutaneous xenograft experiments (Supplemental Figure 2A). Consistent with our prior published studies, LIN28B overexpression caused a significant decrease in tumor volume as compared to controls, irrespective of IMP1 status (Supplemental Figure 2B) (King et al. 2011a). LIN28B overexpressing tumors exhibited a more differentiated phenotype as compared to controls, which had poorly differentiated tumors. This differentiation phenotype was reversed with IMP1 loss in LIN28B overexpressing cells (Supplemental Figure 2C), suggesting that IMP1 loss may promote an in increased stemness markers and/or downregulate differentiation pathways in CRC cells. We also observed an upregulation of nuclear ß-catenin staining with IMP1 loss and a significant increase in Wnt signature in these tumors (Supplemental Figure 2C,D).

To confirm that LIN28B expression in transformed cells can promote differentiation, we evaluated LIN28B expression and differentiation status in human colon tumors in colon cancer tissue microarrays(King et al. 2011a). We found that the majority of LIN28B overexpressing tumors were either moderately or well differentiated (Supplementary Figure 2E). The mechanistic explanation for this is not known; however, recent studies have demonstrated that in some CRC cell lines, overexpression of pluripotency factors (OCT3/4, SOX2 and KLF4) can lead to tumors with increased differentiation(Oshima et al. 2014). This is in line with our finding, since LIN28B is also a pluripotency factor (Rahkonen et al. 2016; Zhang et al. 2016; Tsanov et al. 2017), although this does not mean that pluripotency and differentiation are necessarily linked in this context.

We next evaluated transgenic mice with intestinal epithelial overexpression of Lin28b (*Villin-Lin28b*) and intestinal epithelial-specific deletion of *Imp1* (*VillinCre; Imp1fl/fl*) (Hamilton et al. 2013; Madison et al. 2013b) (Supplemental Figure 2F). Our prior work

demonstrated *de novo* intestinal tumor growth in *Villin-Lin28b* mice, confirming that Lin28b can act as an oncogene in the intestine (Madison et al. 2013b). *Imp1* expression is enhanced significantly in *Villin-Lin28b* mice and completely eliminated in the intestinal epithelium of *Villin-Lin28b; VillinCre;Imp1$^{fl/fl}$* mice (Figure 7A). We found that at 12 months of age, 18/25 *Villin-Lin28b* mice (72%) had at least one tumor, while 10/12 (83.33%) of *Villin-Lin28b; VillinCre;Imp1fl/fl* mice had tumors, the majority of which had multiple lesions. Aged mice overexpressing LIN28B exhibit a significant increase in number of proliferating cells (Figure 7B,C) in normal tissue. *Villin-Lin28b; VillinCre;Imp1$^{fl/fl}$* mice exhibit a significant increase in intestinal tumor number/mouse compared to *Villin-Lin28b* mice (Figure 7D). We did not observe hyperplasia or tumor growth with *Imp1* loss alone, evaluated out to 12 months of age. Histological grading revealed a higher percentage of adenocarcinoma lesions in *Villin-Lin28b;VillinCre;Imp1$^{fl/fl}$* compared to *Villin-Lin28b* mice (Figure 7E,F), demonstrating that *Imp1* loss promotes higher tumor number and grade in the context of *Lin28b* overexpression.

Our prior studies demonstrated that *Lin28b* overexpression results in increased expression of other let-7 targets, including *Hmga2*, *Arid3a*, *Igf2bp2*, and *CycD1*, as well as enhanced expression of stem cell-related genes (Madison et al. 2015). We evaluated isolated epithelia from aged mice and found no significant change in *Arid3a*, *Igf2bp2, Hmga2* and *CycD1* expression in *Villin-Lin28b;VillinCre;Imp1$^{fl/fl}$* mice compared to *Villin-Lin28b* mice (Figure 7G). We found a robust increase in stem cell and broader crypt cell markers including *Prom1, Hopx, Bmi1, Lgr5*, and *Olfm4* (van der Flier et al. 2009; Zhu et al. 2009; Takeda et al. 2011; Tian et al. 2011; de Sousa e Melo et al. 2017), suggesting an expansion of the stem cell compartment in *Villin-Lin28b;VillinCre;Imp1$^{fl/fl}$* compared to *Villin-Lin28b* mice (Figure 7H). Consistent with an expansion of the crypt base stem cell compartment, we observed an increase in WNT target gene expression with *Imp1* loss,

both at the mRNA and protein levels (Figure 7I-K and Supplementary Figure 3D). This effect was also observed *ex vivo* in enteroids generated from isolated crypts, where *Villin-Lin28b;VillinCre;Imp1*^{fl/fl} enteroids exhibit increased AXIN2 expression compared to wildtype or *Villin-Lin28b* mouse enteroids (Supplementary Figure 2G). Together, these data support the hypothesis that IMP1 may modulate stem cell signature and canonical WNT target gene expression in the intestine and that these effects persist in isolated crypt enteroid cultures.

To understand these findings in the context of patients with CRC, we evaluated the Cancer Genome Atlas (Cline et al. 2013) for *LIN28B* and *IMP1* expression levels in colon and rectal adenocarcinoma patients (COADREAD). We found a positive correlation between the two transcripts in patient tumors (Pearson's coefficient=0.266, p<0.0001; Supplemental Figure 3A). However, tumor stage-wise evaluation revealed higher *IMP1* expression in all tumor stages, whereas LIN28B expression increased in Stage IV, supporting the concept that IMP1 expression is regulated via additional mechanisms beyond LIN28B (Supplemental Figure 3B).

IMP1 regulates intestinal epithelial regeneration

Building upon our observation that *Imp1* loss upregulates stem cell and WNT target genes in the context of LIN28B overexpression, we sought to understand broader roles for IMP1 in the context of intestinal homeostasis and injury repair. Radiation injury has been increasingly used to study stem cell function and regeneration of the intestinal epithelium (Potten 2004; Zhou et al. 2013b; Gregorieff et al. 2015). *Imp1* expression is low in the adult intestinal crypt but is increased in regenerating epithelium following whole body irradiation (Figure 8A). We observed IMP1 protein expression specifically in regenerative foci 4 days following irradiation, a time point where surviving stem cells are undergoing rapid proliferation to replenish the epithelium and restore barrier function

(Figure 8B). We observed that *Villin-Lin28b* mice lose significantly more weight at day 4 post-irradiation as compared to wildtype controls. This phenotype is reversed in *Villin-Lin28b;VillinCre;Imp1^{fl/fl}* mice, where *Imp1* deletion results in significantly less weight loss as compared to *Villin-Lin28b* mice, returning to wildtype levels (Figure 8C). Furthermore, the number of regenerative crypts at day 4 following radiation is significantly higher in *Villin-Lin28b;VillinCre;Imp1^{fl/fl}* mice compared to *Villin-Lin28b* mice (Figure 8D). *Villin-Lin28b;VillinCre;Imp1^{fl/fl}* mice also display decreased H2AX foci (Zhou et al. 2015) as compared to *Villin-Lin28b* mice, thus indicating less DNA damage at day 4 after radiation (Supplementary Figure 3C).

Evaluating IMP1 separately from its function downstream of LIN28B, we observed that *VillinCre;Imp1^{fl/fl}* mice exhibit less weight loss following irradiation compared to control *Imp1^{fl/fl}* mice (Figure 8E) and that the number of regenerative crypt foci is increased in *VillinCre;Imp1^{fl/fl}* mice (Figure 8F & G). Crypt regeneration in *VillinCre;Imp1^{fl/fl}* mice was evaluated further by plating post-irradiated crypts in 3D enteroid culture (Fuller et al. 2012) (Figure 8H). Crypt enteroids from untreated *Imp1^{fl/fl}* and *VillinCre;Imp1^{fl/fl}* mice establish and grow at similar rates under homeostasis (Supplemental Figure 4A); however, post-irradiated crypt from *VillinCre;Imp1^{fl/fl}* mice exhibit a significant increase in enterosphere formation as well as growth into enteroids 4 days after plating (Figure 8I).

Our data demonstrating that *Imp1* deletion enhances Lin28b-mediated tumorigenesis and regeneration in both wild type and *Villin-Lin28b* mice may counter current views of IMP1 function. We therefore generated mice in which *Imp1* is overexpressed in the intestinal epithelium (*VillinCre Imp1^{OE}*; Supplemental Figure 4B&C) to evaluate mechanistic reversal of phenotypes observed in *VillinCre;Imp1^{fl/fl}* mice. We analyzed aged mice (10-12 months) and found no tumors (Figure 9A) or any significant difference in intestinal morphology or Ki67+ proliferating cells between *VillinCre Imp1^{OE}*

and control mice (Figure 9B). We did not observe a significant difference in Paneth, goblet or enteroendocrine cell numbers (Supplemental Figure 5). Intriguingly, irradiated *VillinCre;Imp1^{OE}* mice did not exhibit significant differences in weight loss compared to control mice at day 4, though there was a trend for increased weight loss in *VillinCre Imp1^{OE}* mice (Figure 9C). Taken together, these data confirm that IMP1 overexpression by itself is insufficient to initiate tumors in the intestine.

We observed upregulation of Wnt targets in *Lin28b;VillinCre;Imp1$^{fl/fl}$* mice. To evaluate whether *VillinCre; Imp1^{OE}* mice exhibit opposing effects, we analyzed gene expression in *Villin-Lin28b;VillinCre;Imp1^{OE}* mice. Analysis of 3-month old mice revealed a trend for decreased Wnt target gene expression in *Villin-Lin28b;VillinCre;Imp1^{OE}* compared to *Villin-Lin28b* mice, supporting the hypothesis that Imp1 may serve as a "switch" for canonical Wnt target gene regulation in the context of Lin28b overexpression (Figure 9D). Finally, analysis of aged *Villin-Lin28b;VillinCre;Imp1^{OE}* mice revealed a suppression of tumor incidence compared to *Villin-Lin28b* mice (Figure 9A). In summary, the functional effects observed in mice with *Imp1* loss or overexpression provide evidence that Imp1 acts as a suppressor of the epithelium's proliferative response under non-transformed conditions, due in part via regulation of Wnt signaling. In this regard, high IMP1 in CRC patients is likely an "effect" rather than a "cause" of tumor initiation.

IMP1 plays a functional role in reserve intestinal stem cells

We performed RNA-Seq followed by GSEA on isolated crypts from *Imp1$^{fl/fl}$* and *VillinCre;Imp1$^{fl/fl}$* mice to evaluate baseline changes in gene expression with *Imp1* loss. Similar to *Villin-Lin28b;VillinCre;Imp1$^{fl/fl}$* mice, crypt gene expression analysis in *VillinCre;Imp1$^{fl/fl}$* mice revealed an increase in intestinal stem cell and Wnt target gene expression (Supplemental Figure 6A and Figure 10A). GSEA revealed enrichment of gene targets involved in proliferation, regeneration and Wnt signaling in *VillinCre;Imp1$^{fl/fl}$*

mice compared to control mice (p-value < 0.001, FDR < 0.001).

VillinCre;Imp1fl/fl mice lack *Imp1* in all intestinal epithelial cells, including stem, progenitor, and differentiated cells. Based upon the upregulation of stem cell-related and Wnt target genes in *VillinCre;Imp1fl/fl* mice, we reasoned that Imp1 may exhibit a functional role within the intestinal crypt compartment. To confirm *Imp1* gene expression in small intestine crypt cells, we utilized *Sox9-EGFP* reporter mice, in which sub-populations of intestinal epithelial cells are fractionated by their relative EGFP expression using fluorescent activated cell sorting (FACS). *Sox9-EGFP* negative, sublow, low, and high segregate into populations of differentiated cells, progenitor/ transit-amplifying cells, active crypt base stem cells, and a mixed population of reserve stem cells/secretory progenitors/enteroendocrine cells, respectively (Formeister et al. 2009; Gracz et al. 2010; Van Landeghem et al. 2012; Roche et al. 2015). Subpopulations were validated previously with gene expression and functional assays. In *Sox9-EGFP* mice, *Imp1* expression is significantly higher *Sox9-EGFP* low and high cells as compared to differentiated lineages (*Sox9-EGFP* negative cells) (Figure 10B). Furthermore, *Imp1* expression is upregulated in all cell populations following whole body irradiation with a significant increase in *Sox9-EGFP* high cells relative to other cells types (Supplementary Figure 6B).

To determine if the protective effect of *Imp1* loss persists in a more restricted epithelial population, we crossed *Imp1fl/fl* to mice harboring the *HopxCreERT2* knockin allele (Wang et al. 2016a), which is expressed specifically in Wnt[Negative] quiescent reserve stem cells (Li et al. 2014; Yousefi et al. 2016) (Takeda et al. 2011). Similar to *VillinCre;Imp1fl/fl* mice, we found that *HopxCreERT2;Imp1fl/fl* mice exhibit less weight loss following irradiation compared to controls (Figure 10C) and an increase in regenerative crypt foci, consistent with enhanced recovery following injury (Figure 10D&E). Taken together, these data support a role for IMP1 induction to negatively regulate WNT

signaling during homeostasis, putatively in crypt cells with an inactive canonical Wnt signaling pathway during homeostasis.

In total, we propose a model in which LIN28B overexpression promotes increased proliferation and tumorigenesis and enhances IMP1 expression, which may then feedback and suppress these pathways during homeostasis (Figure 11). This mechanism is reinforced by data in *Lin28b;VillinCre;Imp1^{fl/fl}* mice, where *Imp1* loss enhances Lin28b-mediated tumorigenesis and upregulates Wnt signaling, and in *Villin-Lin28b;VillinCre;Imp1^{OE}* mice, where high Imp1 expression reduces Lin28b-mediated tumorigenesis.

Discussion

In the current study, we use ribosome profiling to demonstrate that IMP1 acts as a pivotal regulator downstream of LIN28B and that IMP1 deletion promotes changes to both mRNA levels and translational efficiency. Globally, there is partial overlap in genes that are regulated at the mRNA and translation levels, suggesting that IMP1 may regulate both homeostatic transcript abundance and translational efficiency for a subset of target transcripts. In addition, we found no correlation between the binding efficiencies of targets from eCLIP studies (Conway et al. 2016) and the changes in their translation efficiencies through ribosome profiling. This notion is supported by recent studies comparing eCLIP-identified IMP1-bound targets with gene expression changes in IMP1-depleted cells, where there was no significant correlation between binding and trends in genes expression changes (Conway et al. 2016). Additionally, there are targets that are not revealed in the eCLIP studies but are found to be differentially regulated by ribosome profiling, highlighting the tissue-specific as well as potentially direct/indirect roles of IMP1 on gene expression. Our data support the significance of evaluating both the transcriptome and translatome simultaneously to understand RBP function and that

evaluating translational reinforcement, antagonism, and buffering may uncover additional roles for RBPs to refine the functional outcome of a gene or pathway.

LIN28B is a critical pluripotency factor and is engaged in diverse cancer types, including colorectal cancer(Rahkonen et al. 2016; Zhang et al. 2016; Tsanov et al. 2017). LIN28B acts to a major extent through the post-transcriptional downregulation of the *let-7* microRNA (miR) family. This enables the induction of let-7 mRNA targets, which are normally suppressed. In most contexts, this should lead to enhanced proliferation, growth and presumably a pathway towards transformation. While the let-7 mRNA targets are many, e.g. *CyclinD1*, *HMGA2*, *IMP1*, *IMP2*, it is remains elusive how precisely LIN28B exerts its actions through the *let-7* mRNA targets. Herein, we find that IMP1 regulates the translation efficiency of genes downstream of LIN28B, with one node through Wnt signaling pathway components. Pathway analyses highlight several pathways involved in cancer (affecting proliferation, migration, differentiation, and apoptosis), including WNT signaling, are significantly enriched with *Imp1* deletion and concurrent Lin28b expression. These genes are regulated by changes in translational efficiencies by differential binding of ribosomes on the transcripts, a finding that expands substantially our knowledge about IMP1 and WNT signaling, building upon previous studies that β-catenin induces IMP1 transcription and IMP1 stabilizes β-catenin mRNA(Gu et al. 2008).

We demonstrate that *Imp1* loss in *Lin28b* transgenic mice promotes a robust increase in high-grade tumors exhibiting phenotypically less differentiation and a more invasive phenotype, upregulation of stem/progenitor cell genes, and enhanced nuclear β-catenin, suggesting *Imp1* loss may promote expansion of the intestinal stem cell compartment. This is in contrast to data in neural stem cells, where *Imp1* deletion promoted differentiation(Nishino et al. 2013). Similarly, the finding that *Imp1* loss promotes tumorigenesis in the intestinal epithelium is in contrast to prior studies

suggesting IMP1 may act as an oncogene in different tissues (Tessier et al. 2004; Kobel et al. 2007; Mayr and Bartel 2009; Hamilton et al. 2013; Gutschner et al. 2014). However, more recent studies have identified tumor-suppressive roles of IMP1 as well (Hamilton et al. 2015; Wang et al. 2016a). These divergences likely depend upon numerous factors, including age, the compartment in which Imp1 is expressed (for example epithelial versus mesenchymal), the specific tissue type (intestinal, breast, brain, etc.) and whether Imp1 loss is acting alone or in concert with known oncogenes. IMP1 stabilizes β-catenin mRNA in breast cancer cells (Gu et al. 2008) and is in turn activated by it in a feedback mechanism(Gu et al. 2009). In other studies, IMP1 was shown to bind and stabilize beta-TRCP1, a β-catenin antagonist (Elcheva et al. 2009) . Hence, we used unbiased approaches (RNA sequencing and ribosome profiling/sequencing) to evaluate global changes in pathways with IMP1 loss and then used *in vivo* mouse models to understand the net effects upon WNT pathway signaling. However, our data do not necessarily exclude a role for IMP1 in tumor progression, where it may exhibit different roles based upon target transcript abundance.

Although LIN28B has been reported to range from 30-75% of colorectal cancer tumors (Piskounova et al. 2011) (Tu et al. 2015), IMP1 is overexpressed in up to 80% (King et al. 2011a) (Mongroo et al. 2011). This suggests that the LIN28B-Let7-IMP1 axis may function under certain scenarios, but other LIN28B-independent factors, yet to be identified in colorectal cancer, may still regulate IMP1 expression. This is supported by our TCGA analysis where LIN28B and IMP1 expression do not positively correlate at all stages of colon cancer. Importantly, our finding that *VillinCre;Imp1^{OE}* mice do not exhibit spontaneous tumor initiation suggest that IMP1 overexpression is itself insufficient to drive tumor initiation. To that end, it is possible that IMP1 overexpression may serve as a "brake" or "checkpoint" to the oncogenic effects of LIN28B. The "checkpoint" regulation may be achieved through a variety of mechanisms ascribed to IMP1, such as

sequestration of transcripts in IMP1 containing RNP granules (Weidensdorfer et al. 2009) (Jonson et al. 2007) (to avoid mRNA degradation and/or release the transcripts for translation at critical time points), reduction of miRNA mediated silencing of mRNA transcripts (Elcheva et al. 2009; Nishino et al. 2013; Busch et al. 2016; Degrauwe et al. 2016a) (for review see (van Kouwenhove et al. 2011)), or displacing miRNA containing RISCs (Elcheva et al. 2009). IMP1 may also enhance the expression of LIN28B by shielding *LIN28B* mRNA from regulation by let-7 *in vitro* (Busch et al. 2016). Additionally, Lin28b and drosophila Imp1 (dImp1) cooperate for mitotic activity and oncogenesis (Narbonne-Reveau et al. 2016). Furthermore, LIN28B and IMP1 may cooperate to augment cellular bioenergetics, and in the case of LIN28B, cell metabolism (Tu et al. 2015).

Targeting key pathways in colorectal cancer remains challenging as so many of these pathways are important for normal epithelial homeostasis. The targeting of RBPs can be refined to interrupt specific RBP:RNA transcript interactions. LIN28B and IMP1 exhibit low expression in most adult tissues, suggesting that targeting them may have few deleterious effects. Inhibitors for LIN28B would prevent aberrant blockade of tumor suppressor let-7, whereas a specific IMP1 inhibitor would require targeting of tumor-promoting interactions while sparing tumor suppressor functions. For example, a novel IMP1 inhibitor that targets c-Myc specifically has demonstrable effects on melanoma and ovarian cell proliferation; however, studies have been limited to *in vitro* assays thus far (Mahapatra et al. 2014; Mahapatra et al. 2017). In summary, our findings highlight the LIN28B/IMP1 signaling axis as a key regulon for normal homeostasis and tumorigenesis in the intestinal epithelium, providing mechanistic insight into the basic biology of RBPs as well as underscoring the importance of understanding post-transcriptional regulation of principle oncogenic pathways *in vivo.*

Figures and figure legends

Figure 6: IMP1 is a significant translational regulator downstream of LIN28B
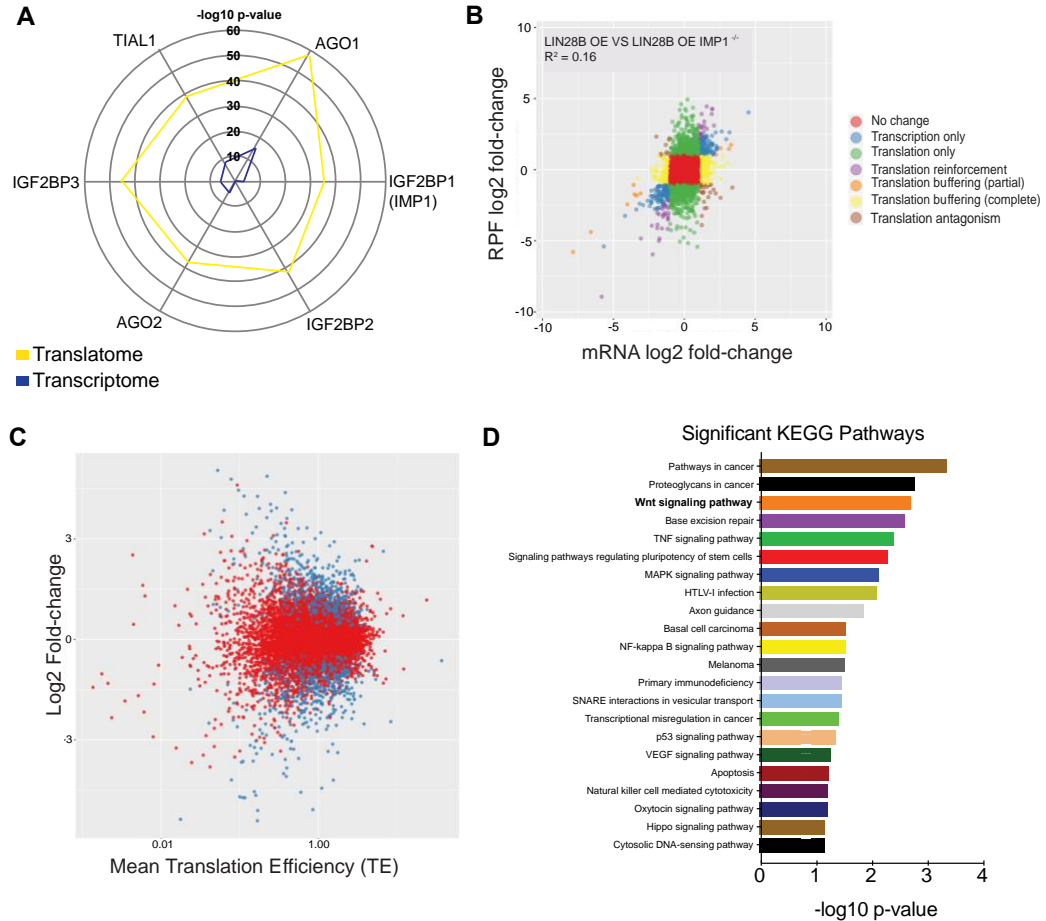
A. Radar map demonstrating top post-transcriptional regulators of differentially expressed genes with LIN28B overexpression in SW480 cells as compared to control cells. A single point on the radar map indicates -10 log p-value of enrichment of any post-transcriptional regulator. Differentially expressed genes at each level were identified using the DEGseq and the list of post-transcriptional regulators was obtained from the AURA database (see methods).

B. Scatterplot of differential expression between LIN28B overexpressing lines with and without IMP1 deletion.

The log2 fold changes between ribosome-bound RNAs (ribosome protected fragments, or RPF) and total mRNA are plotted. The plot indicates that IMP1 regulates both mRNA abundance and translation. C. Scatterplot of genes with significant (in blue) differential translational efficiencies between LIN28B overexpressing cells with and without IMP1 deletion. Translation efficiencies (TE) of the transcripts are calculated as the ratio of reads of ribosome-protected fragments to the reads in total mRNA abundance. D. Pathway analysis using DAVID software of the differentially expressed genes from C to see what signaling/effector pathways are enriched with IMP1 deletion. (Note the Wnt signaling pathway)

Figure 7: IMP1 loss enhances LIN28B-mediated tumorigenesis in vivo.
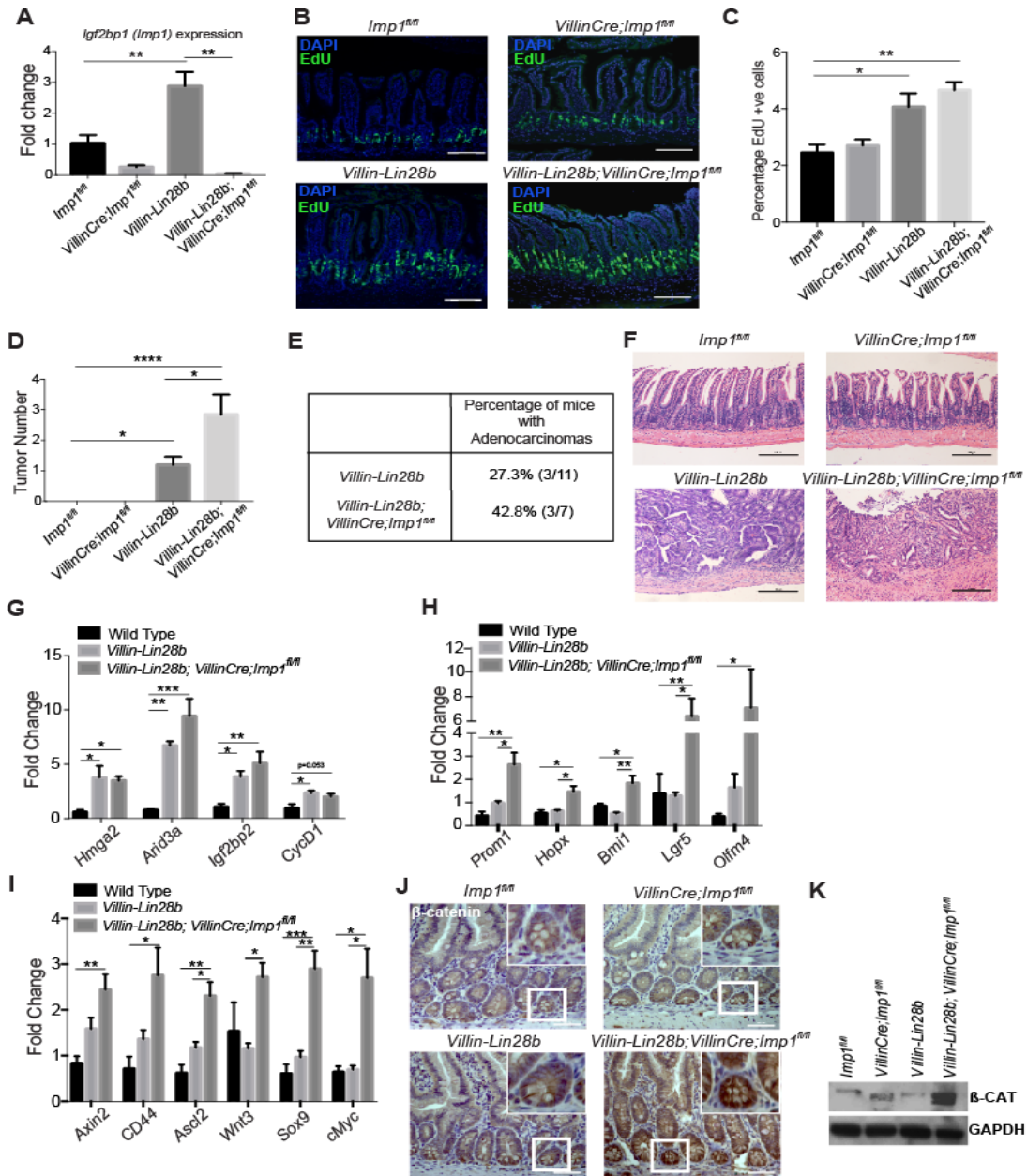
Imp1$^{fl/fl}$ (Wild Type), *Villin-Cre;Imp1$^{fl/fl}$* , *Villin-Lin28b* , *Villin-Cre;Villin-Lin28b;Imp1$^{fl/fl}$* were

aged up to one year and then sacrificed to evaluate tumor growth. A. *Igf2bp1/Imp1*

expression in the epithelium isolated from jejunum of 12-month-old mice (n>4 mice per

genotype). B. Representative immunofluorescence staining for EdU incorporation in

mouse intestinal epithelium. (Scale bars = 500μm) C. Quantification of EdU+ve cells

using flow cytometry (n=3 mice per genotype) D. Number of intestinal tumors in mice with or without *Imp1* in the context of *Lin28b* overexpression (n> 9 mice per genotype). E. Percentage of tumors classified as adenocarcinomas by histological scoring. F. Representative H&E staining of intestinal epithelium in aged mice. Mice lacking *Lin28b* overexpression exhibited normal intestinal morphology at 12 months of age. Mice with *Lin28b* overexpression exhibited tumor development that worsened with *Imp1* loss. (Scale bars = 500μm) G. Relative expression of different let-7 targets in the intestinal epithelium via qPCR (n> 5 mice per genotype). H. Relative expression of stem cell markers in the intestinal epithelium via qPCR expressed as fold change with respect to *Imp1*$^{fl/fl}$ mice (n> 5 mice per genotype). I. Relative expression of *Wnt* target genes in intestinal epithelium via qPCR expressed as fold change with respect to *Imp1*$^{fl/fl}$ mice (n> 5 mice per genotype). J. Representative immunohistochemical staining for β-catenin in mouse intestinal epithelium (magnified in inset). K. Representative β-catenin protein levels in mouse intestinal crypts from the four genotypes.

(All data are expressed as mean ± SEM. *, $p < 0.05$; **, $p < 0.01$; ***, $p < 0.001$; ****, < 0.0001 by ordinary one-way ANOVA test followed by Tukey's multiple comparison test. The significance is shown compared to control/wildtype samples unless indicated otherwise)

Figure 8: IMP1 regulates intestinal epithelial regeneration following irradiation.
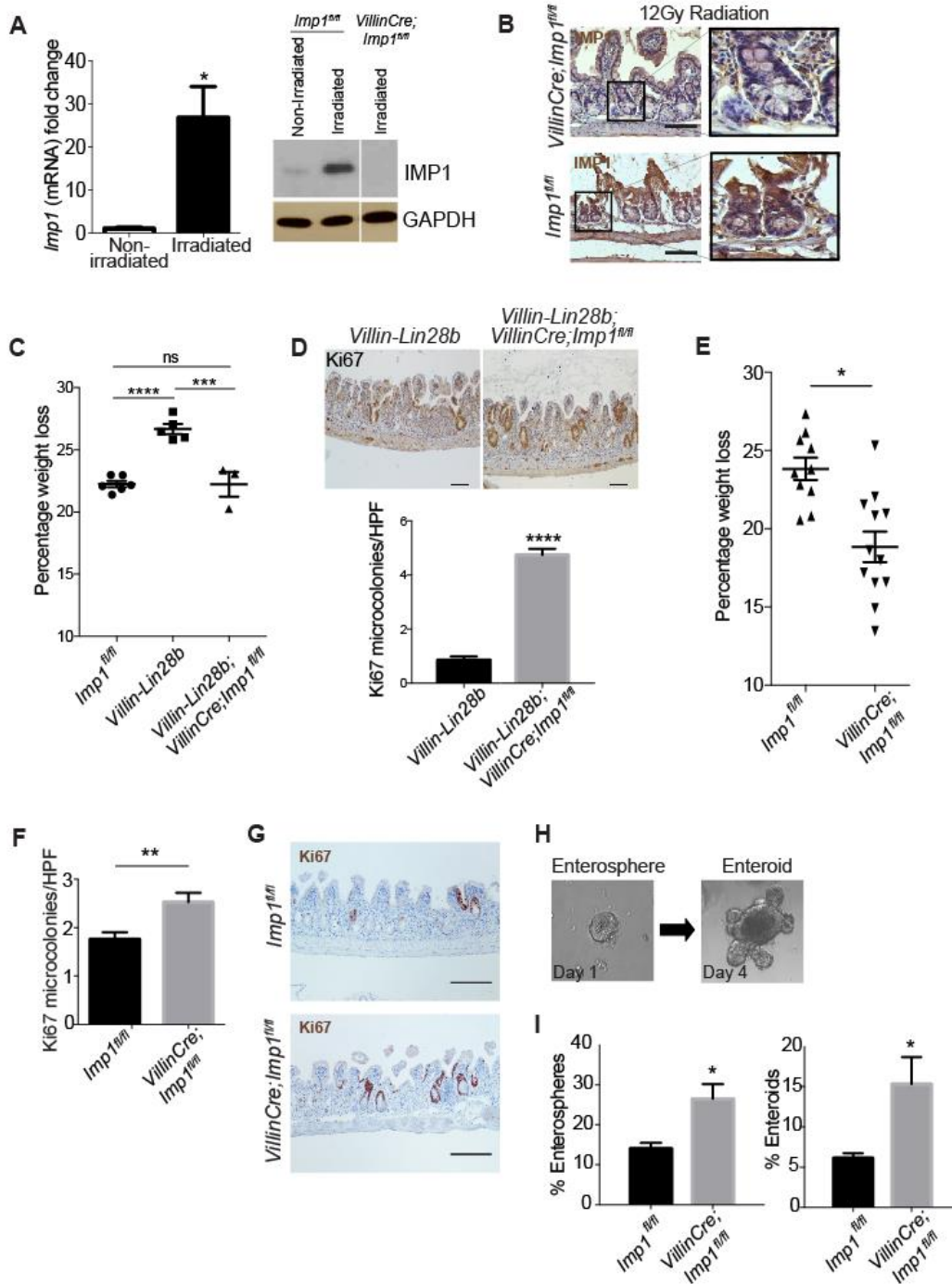
Mice were evaluated for Imp1 expression in non-irradiated (non-IR) and 4-days post 12 Gy whole body IR. A. qRT-PCR and representative western blot for *Imp1* in isolated crypts from these mice. *P<0.05 vs. non-IR, N=3-4 mice per genotype. B.

Representative immunohistochemical staining showing Imp1 increase in wildtype (Imp1$^{fl/fl}$) mice following radiation. *VillinCre;Imp1 $^{fl/fl}$* mice are used as controls (Scale bars = 500µm). C. *Villin-Lin28b; Villin-Cre;Imp1$^{fl/fl}$* mice lost significantly less weight at sacrifice following irradiation than *Villin-Lin28b* mice (22.23 ± 0.9905% mean weight loss in *Villin-Cre;Villin-Lin28b;Imp1$^{fl/fl}$* mice (n=3) versus 26.68 ± 0.4076% in *Villin-Lin28b* (n=5)) The weight loss in *Villin-Lin28b* mice was significantly higher than in controls (22.24 ± 0.2556% mean weight loss). D. Analysis of Ki67+ cells revealed a significant increase in Ki67+ regenerative crypt foci in *VillinCre Villin-Lin28b;Imp1 $^{fl/fl}$* mice at 4 days following irradiation(n=3-4 mice per genotype, 20-30 HPF per mouse). Representative immunohistochemical staining for Ki67+ foci in the mouse intestinal epithelium is shown. (Scale bars = 500µm). E. *VillinCre;Imp1 $^{fl/fl}$* mice lost significantly less weight at sacrifice following irradiation than controls (18.83 ±0.98% in *VillinCre;Imp1 $^{fl/fl}$* mice versus 23.34 ±0.56% mean weight loss in controls). (n =14 *Imp1$^{fl/fl}$* and 12 *VillinCre;Imp1 $^{fl/fl}$* mice). F. Analysis of Ki67+ cells revealed a robust increase in Ki67+ regenerative crypt foci in *VillinCre;Imp1 $^{fl/fl}$* mice at 4 days following irradiation (n=4 mice per genotype, 20-30 HPF per mouse). G. Representative immunohistochemical staining for Ki67+ foci in mouse intestinal epithelium. (Scale bars = 500µm) H. Representative pictures of enterosphere and enteroid with buds. Enhanced growth of post-irradiation enteroids from *VillinCre;Imp1 $^{fl/fl}$* mice. Regenerative crypt units were plated in enteroid culture on the day of sacrifice to evaluate *ex vivo* survival and growth. I. Evaluation of enterosphere growth 1 day following plating and enteroid growth 4 days after plating (revealed a significant increase in *VillinCre;Imp1 $^{fl/fl}$* compared to *Imp1$^{fl/fl}$*. (All data are expressed as mean ± SEM. *, $p < 0.05$; **, $p < 0.01$; ***, $p < 0.001$; ****, < 0.0001 by ordinary one-way ANOVA test followed by Tukey's multiple comparison test. The significance is shown compared to control/wildtype samples unless indicated otherwise)
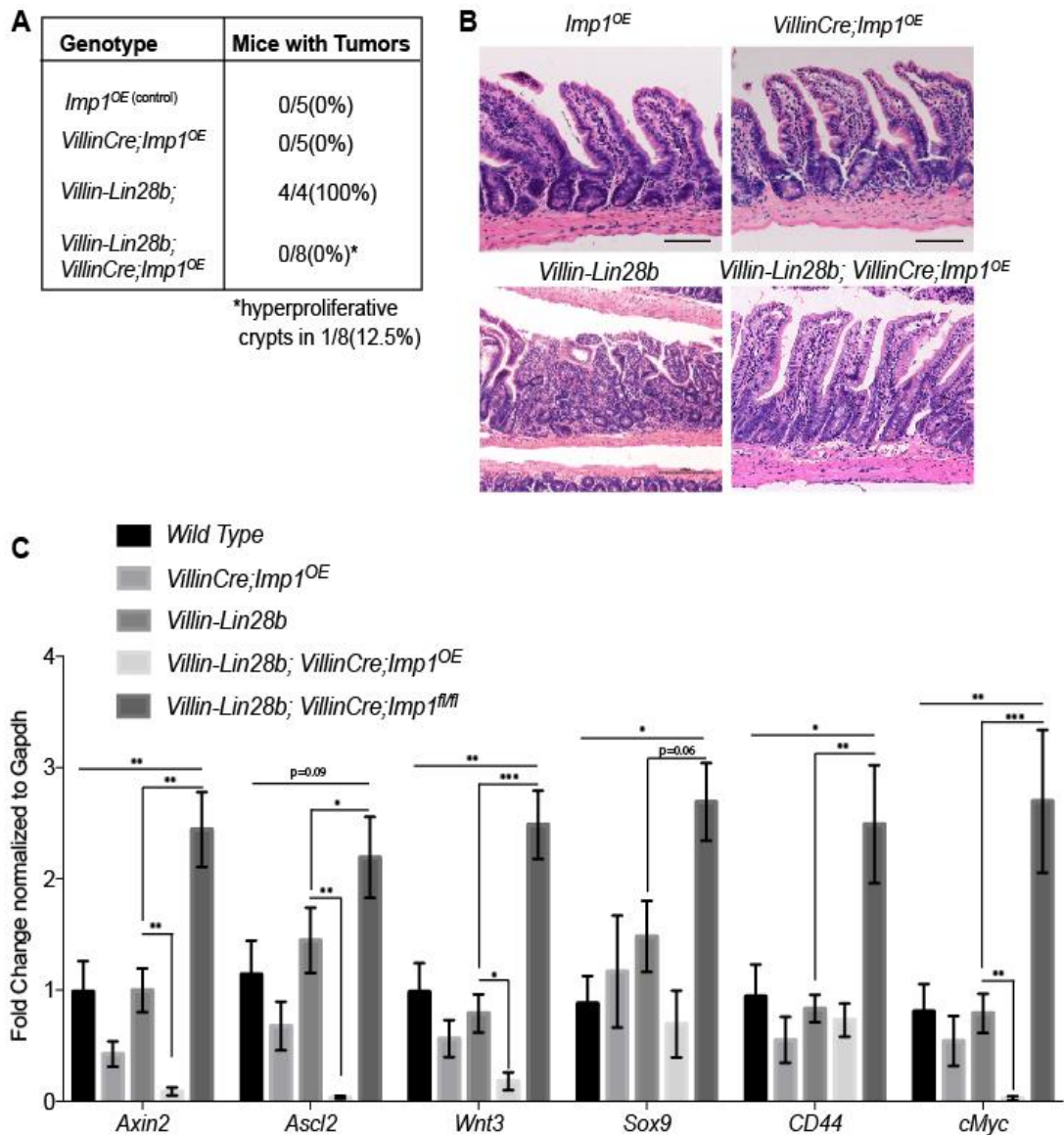
Figure 9: IMP1 overexpression does not initiate tumors in vivo.

A. *The VillinCre;Imp1OE* mice did not exhibit tumor formation between 10-12 months of age. B. Representative H&E and Ki67 staining of intestinal epithelium in aged (10-12 months) mice. Mice overexpressing IMP1 exhibited normal intestinal morphology and did not show a tumor phenotype (Scale bars = 500μm). C. Relative expression of Wnt target genes in the intestinal epithelium via qPCR expressed as fold change with respect to wildtype control mice at 10-12 months of age (n= >4 mice per genotype). (All data are expressed as mean ± SEM. *, p < 0.05;

, p < 0.01; ***, p < 0.001; **, < 0.0001 by ordinary one-way ANOVA test followed by

Tukey's multiple comparison test).

Figure 10: IMP1 plays a functional role in reserve intestinal stem cells.
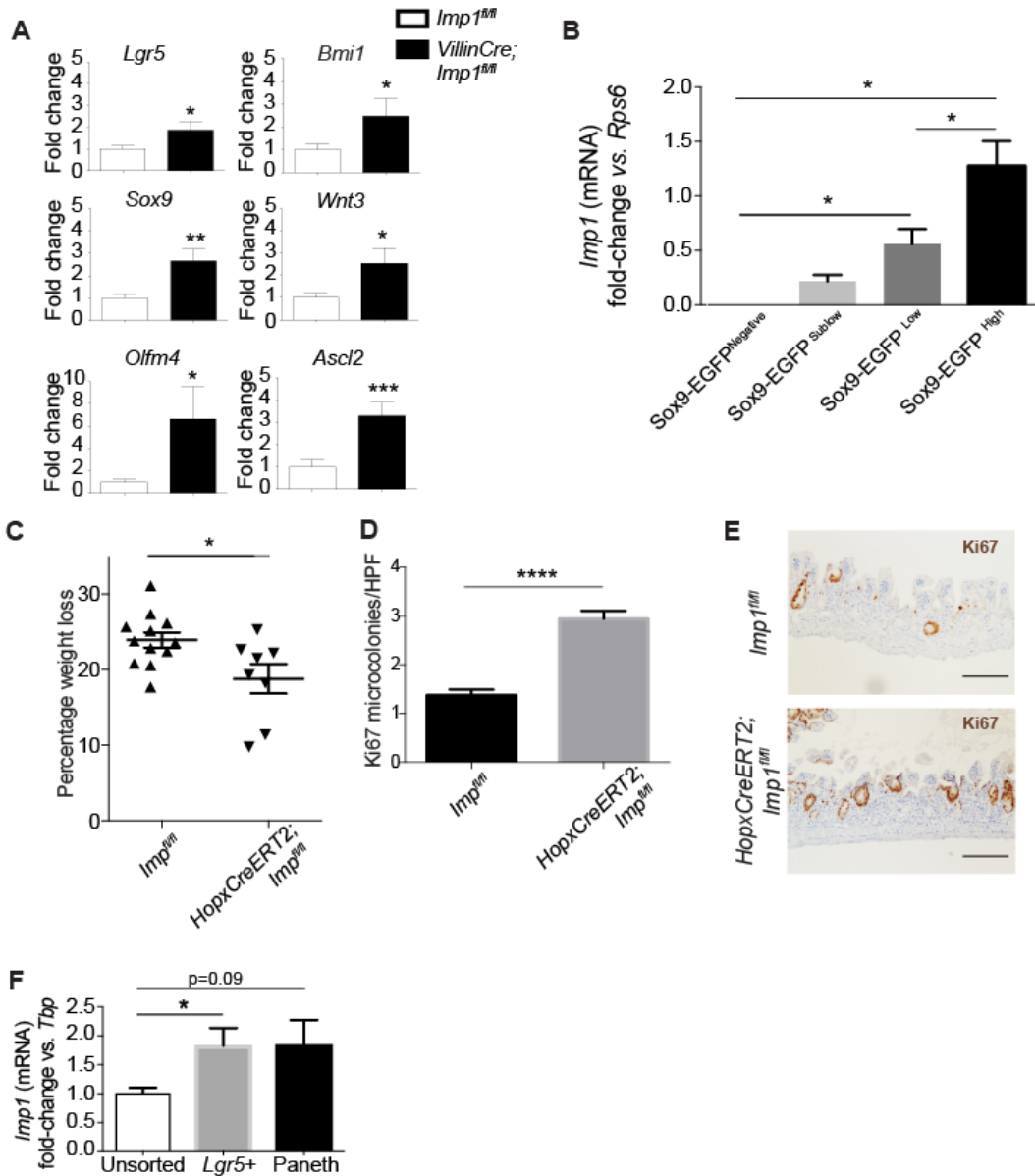
A. qRT-PCR for stem cell markers and Wnt target genes in isolated crypts from

VillinCre;Imp1fl/fl mice compared to *Impfl/fl* mice. (n=3-4 mice per genotype). B. qPCR in

Sox9-EGFP reporter mice, where epithelial cell populations are

sub-classified via FACS into *Sox9-EGFP* negative, sublow, low and high cells. *Imp1* is

expressed at low levels in all represented cell types except *Sox9-EGFP* negative cells

(white bars). Imp1 expression is significantly higher in

Sox9-EGFP low and high cells, which encompass intestinal stem cells (n=5 animals per

group). C. *HopxCreERT2;Imp1fl/fl* mice lost significantly less weight at sacrifice following

irradiation than controls (18.8 ± 1.951% mean weight loss in *HopxCreERT2;Imp1fl/fl*

mice versus 23.92 ± 1.015% in controls). (n =8 *HopxCreERT2;Imp1fl/fl* and n=12 control

mice). D. Analysis of Ki67+ cells revealed there was a robust increase in Ki67+

regenerative crypt foci at 4 days following irradiation in *HopxCreERT2;Imp1fl/fl* mice

compared to control mice, (n=4 mice per genotype, 20-30 HPF per animal) (Scale bars =

500μm). E. Representative immunohistochemical staining for Ki67+ foci in mouse

intestinal epithelium quantified in D. F. qPCR for Imp1 expression in Lgr5+ and Paneth

(CD24/cKit/SSC high) cells sorted from Lgr5-eGFP-IRES-CreERT2 mouse crypts. All

data are expressed as mean ± SEM. *, $p < 0.05$; **, $p < 0.01$; ***, $p < 0.001$; ****, $p <$

0.0001 by unpaired t-test.

Figure 11: IMP1 is the principal node for post-transcriptional regulation downstream of LIN28B.
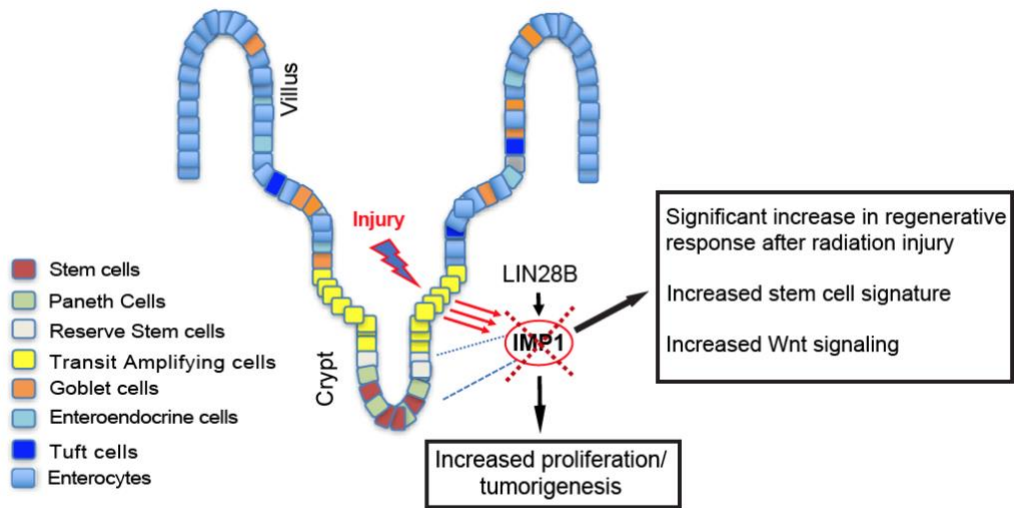
We propose a model in which IMP1 plays an important regulatory role downstream of

LIN28B. Both LIN28B overexpression and whole-body irradiation enhance IMP1

expression in the intestinal epithelium. Deletion of IMP1 causes a significant increase in

LIN28B-mediated tumorigenesis, likely due in part to observed increases in Wnt

signaling and potentially stem cell signature. Furthermore, IMP1 loss (specifically in

Hopx+ stem cells) causes increased regeneration following radiation injury. Taken

together, these data suggest IMP1 as a regulator of intestinal epithelial

homeostasis downstream of both LIN28B and radiation.

Supplemental Figures

Supplementary Figure 1
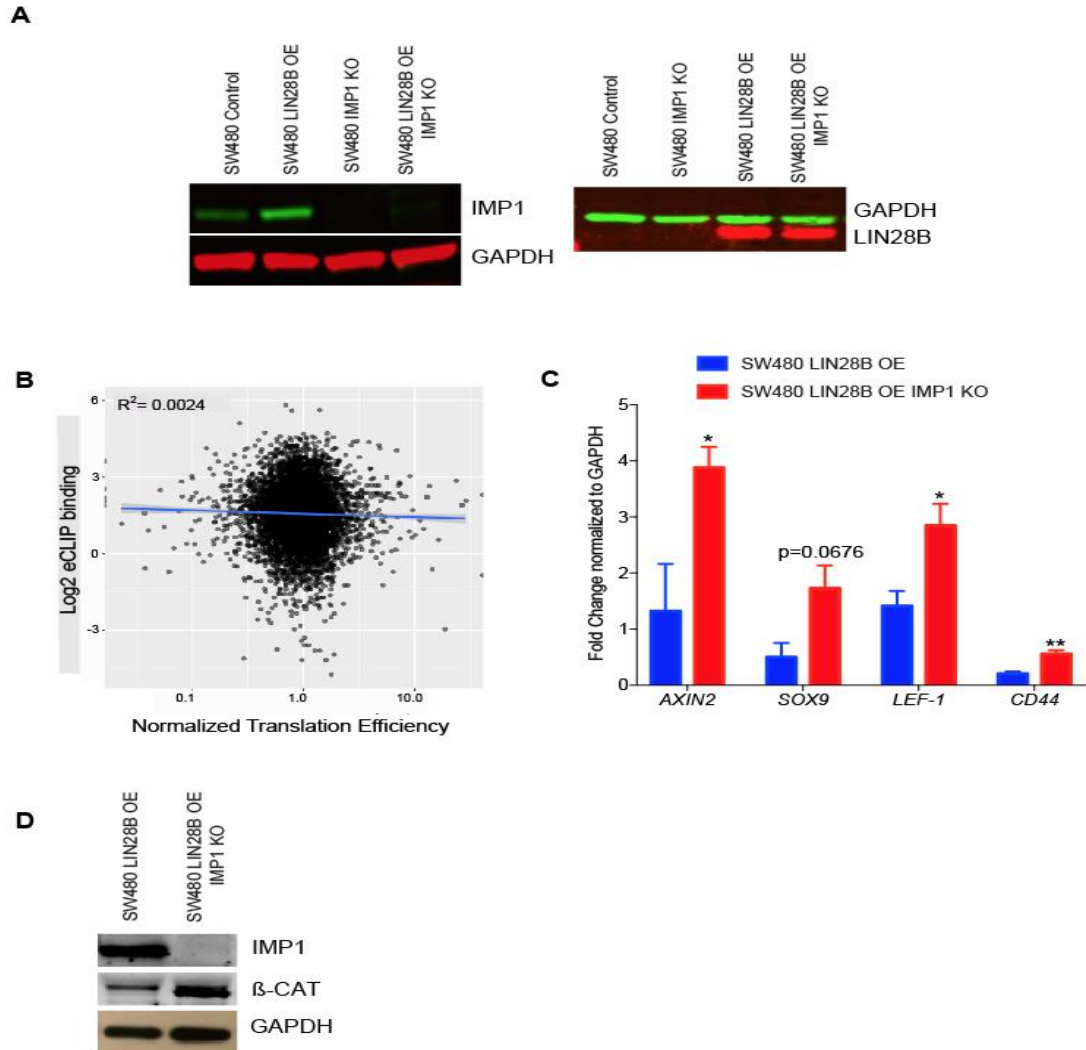
A. Representative western blot demonstrating LIN28B and IMP1 expression in SW480 cells. Wild type SW480 cells express endogenous IMP1 that increases with LIN28B overexpression (OE). CRISPR-cas9-mediated deletion of IGF2BP1 (IMP1) in SW480 cells (WT and LIN28B OE). SW480 cells do not express LIN28B endogenously. B. Scatterplot of binding efficiencies of RNA targets of IMP1 identified by enhanced UV crosslinking and immunoprecipitation (eCLIP) (Conway et al. 2016) with differential translational efficiency of the targets identified in 1C. We find no significant correlation

between the two (R2=0.0024). C. qRT-PCR for Wnt target genes in SW480 cells overexpressing LIN28B with and without IMP1 deletion. (n=3 passages). Several Wnt targets are significantly upregulated with IMP1 deletion. D. Western blot showing ß-CATENIN increase with IMP1 deletion in SW480 cells with LIN28B overexpression. (* p<0.05 by Student's t-test)

Supplementary Figure 2
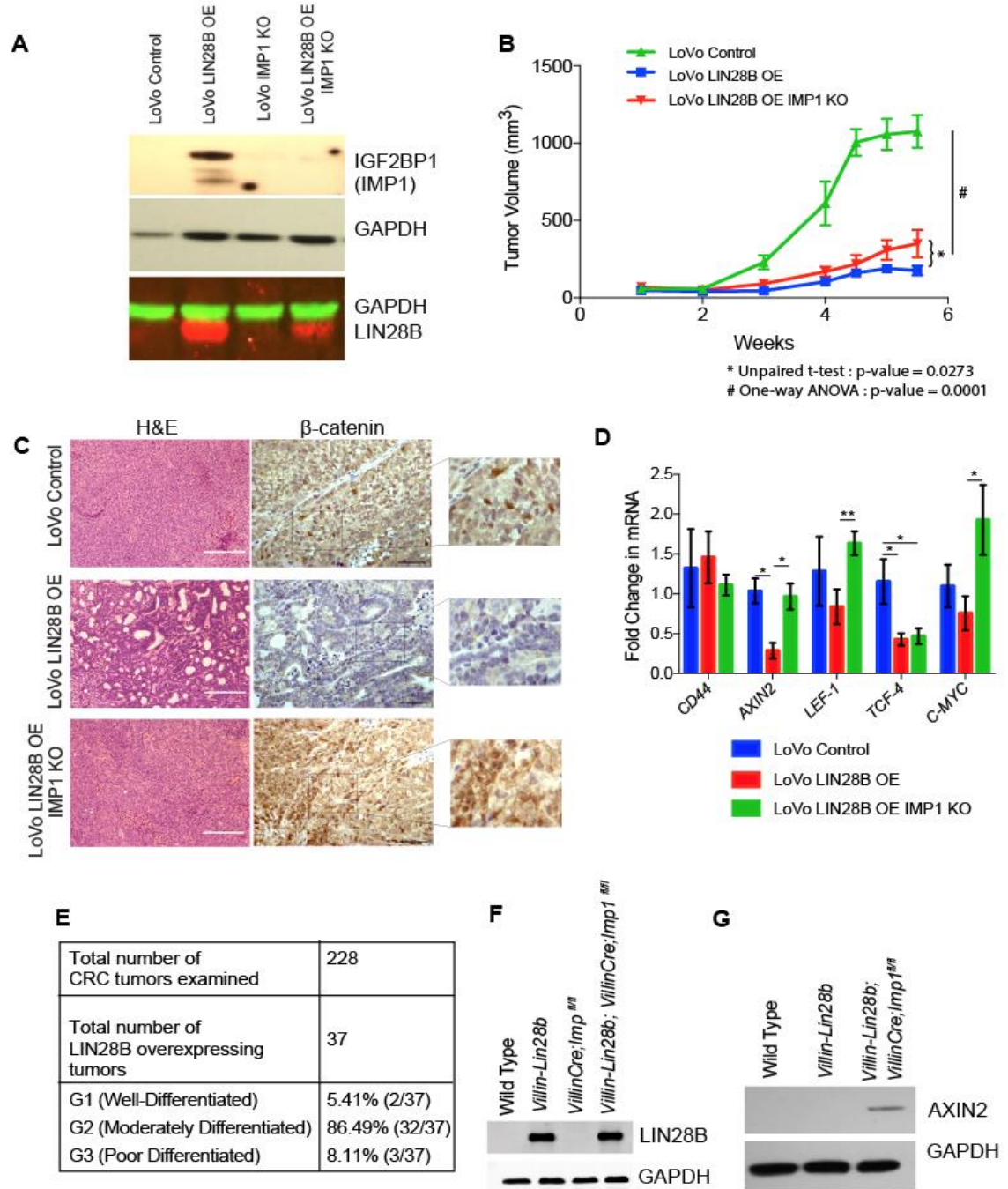
A. Representative western blots demonstrating LIN28B and IMP1 expression in LoVo

cells. Wild type (WT) LoVo cells show undetectable IMP1 expression that was increased

with LIN28B OE. CRISPR-cas9-mediated deletion of *IGF2BP1* (*IMP1*) in LoVo cells (WT

and *LIN28B* OE). B. Xenograft (subcutaneous) experiments with LoVo cells (n=10 per

cell type) show a significant decrease in tumor size with LIN28B overexpression (169.9 ± 31.12 mm^3 at sacrifice) as compared to WT cells (1145 ± 120.3 mm^3 at sacrifice). This effect is partially rescued with IMP1 knockout (417.6 ± 107.7 mm^3 at sacrifice). C. Representative histological sections of the xenografts from B show highly differentiated tumors in LoVo cells with LIN28B overexpression. This is not observed in tumors from WT LoVo cells or LIN28B overexpressing LoVo cells with IMP1 deletion where the tumors are poorly differentiated and express more ß-catenin staining (Scale bars = 500µm). D. Relative expression of *Wnt* target genes in xenograft tumors from B (n> 4 tumors per genotype). E. Table showing differentiation status of LIN28B overexpressing human colorectal tumors from tumor tissue microarray (matched normal and tumor samples n=37). A majority of the tumors show increased differentiation. F. Representative western blot showing LIN28B expression in the intestinal epithelium of the 4 genotypes. G. Representative western blot showing increased AXIN2 expression in the 3D organoids/enteroids cultured from crypts of *Villin-Cre;Villin-Lin28b;Imp1$^{fl/fl}$* mice.

Supplementary Figure 3
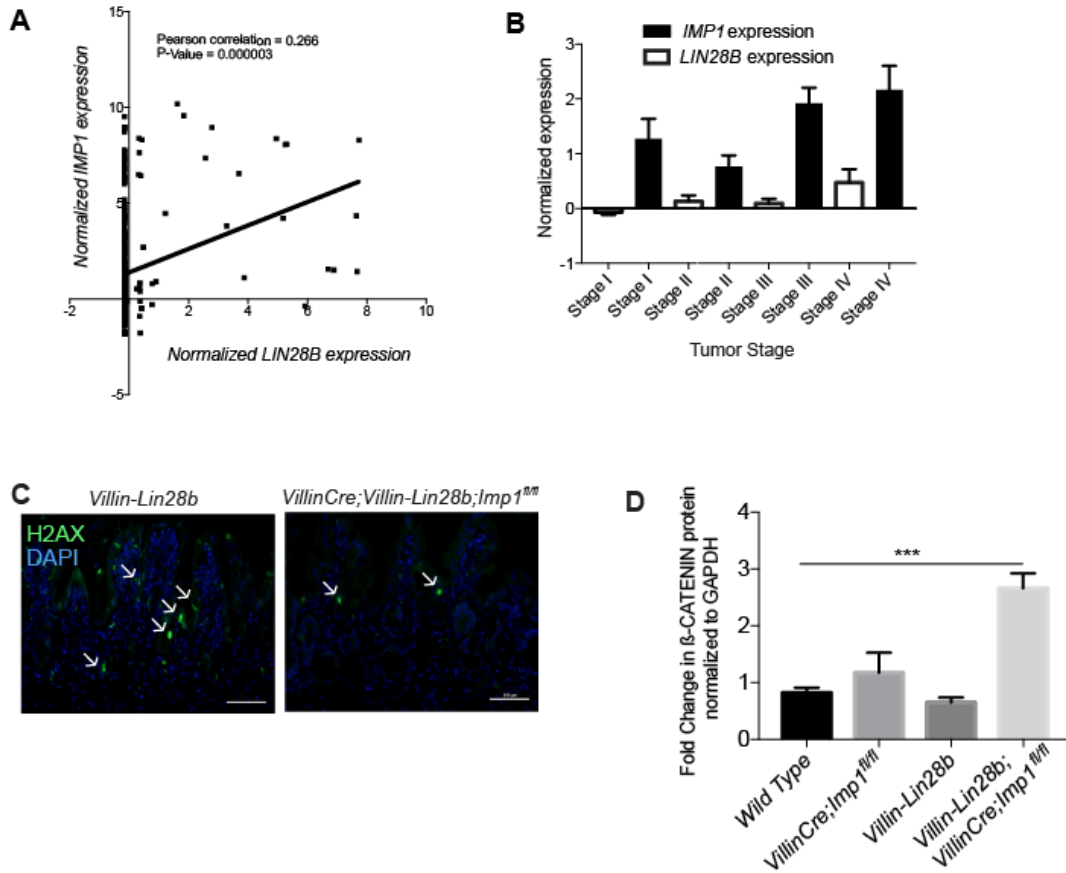
A. Correlation graph between normalized mRNA expression intensities of LIN28B and

IMP1 in the colon adenocarcinoma and rectal adenocarcinoma (COADREAD) datasets

in the Cancer Genome Atlas (Cline et al. 2013) (n=300 patients). LIN28B expression

significantly correlates positively with IMP1 expression. B. TCGA analysis showing

LIN28B and IMP1 expressions in different stages of colorectal cancer. IMP1 is

expressed highly in all four stages irrespective of LIN28B expression levels showing that

IMP1 expression is potentially regulated by factors in a LIN28 dependent and

independent fashion. C. Representative H2AX staining in *Villin-Lin28b* and *Villin-*

Cre;Villin-Lin28b;Imp1fl/fl mice 4 days after 12Gywhole body radiation. Arrows indicate

H2AX foci. (Scale bars = 500μm) D. Quantification of ß-CATENIN protein via western blots of the crypts cells of the mice of the 4 genotypes (n=3 per genotype)

Supplementary Figure 4
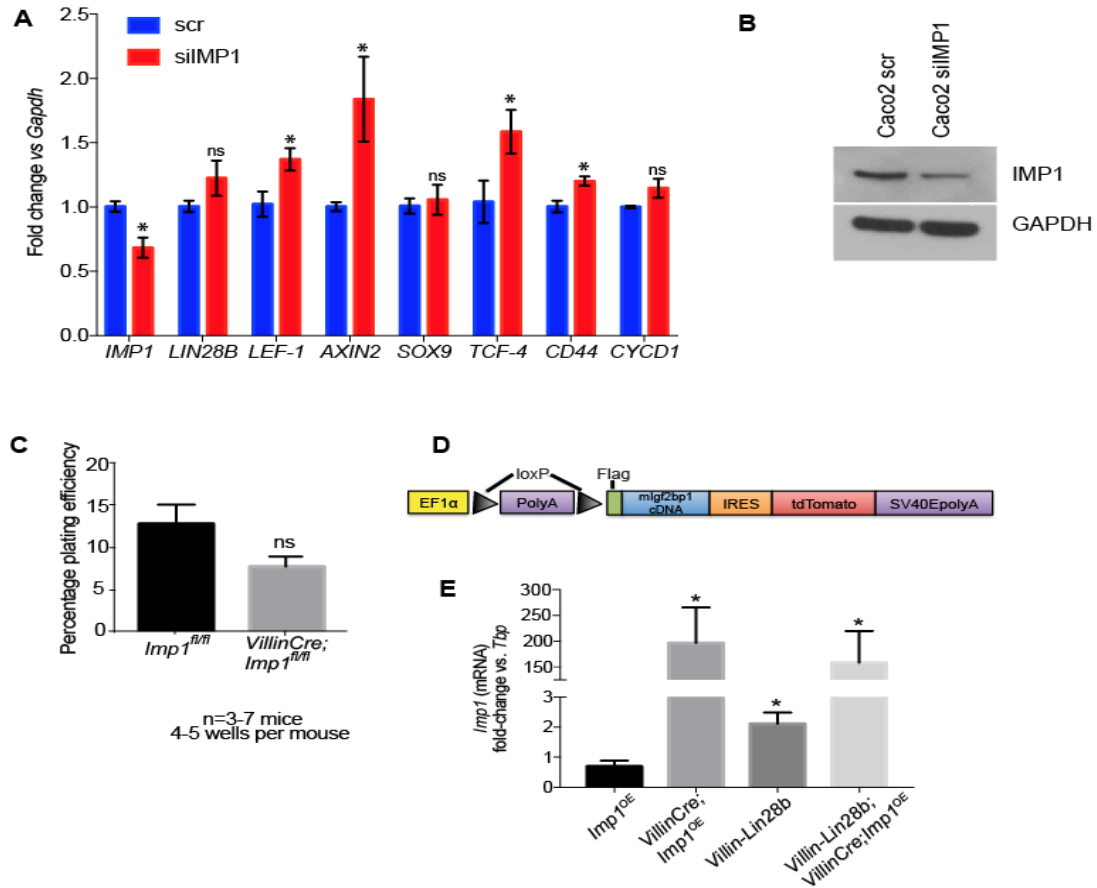
A. qRT-PCR for Wnt target genes in CaCo2 cells with IMP1 knockdown as compared to controls. (n=3 independent experiments). Several Wnt targets are significantly upregulated with IMP1 knockdown. B. Western blot showing IMP1 knockdown using siIMP1 in CaCo2 cells. C. Enteroid plating efficiency from *Imp1 fl/fl* and *VillinCre;Imp1fl/fl* mice at homeostasis revealed no significant difference between genotypes. N=3-7 mice per genotype with 4-5 wells per mouse analyzed. D. Construct for *Imp1OE* mice, which were then crossed with *VillinCre* mice. E. The *VillinCre;Imp1OE* mice were verified for

intestinal IMP1 expression by qRT-PCR in isolated epithelia from these mice. *P<0.05,

N=3-4 mice per genotype.

Supplementary Figure 5
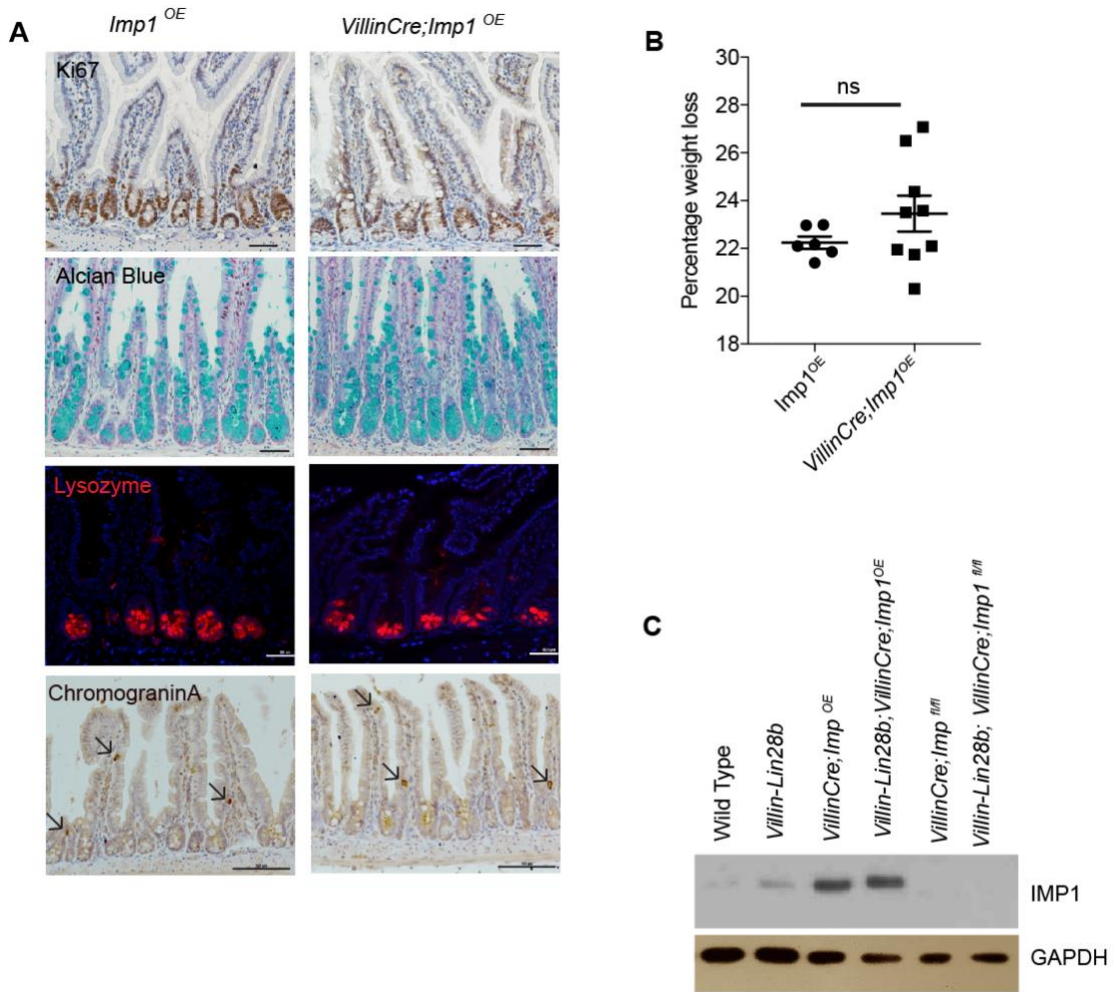
A. Representative staining for Ki67 (proliferation), Lysozyme (Paneth cells), Alcian blue (goblet cells) and chromogranin A (enteroendocrine cells) in *VillinCre;Imp1OE* mice as compared to controls. (Scale bars = 500µm). B. *Villin-Cre;Imp1OE* mice lost similar weight at sacrifice following irradiation compared to *Imp1OE* controls. (23.46 ± 0.7485% mean weight loss in *Villin-Cre;Imp1OE* mice (n=9) versus 22.24 ± 0.2556% in *Imp1OE* (n=6)). C.Western Blot for IMP1 in isolated epithelia from all the genotypes .

Supplementary Figure 6
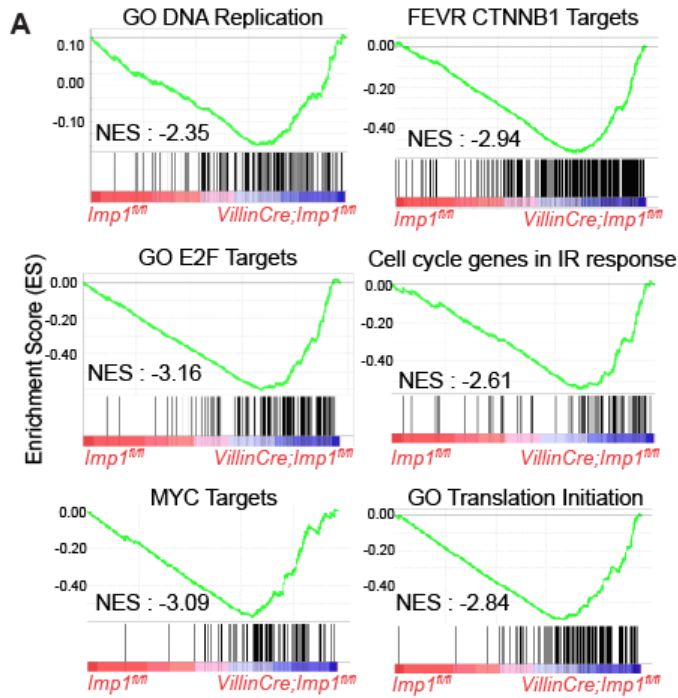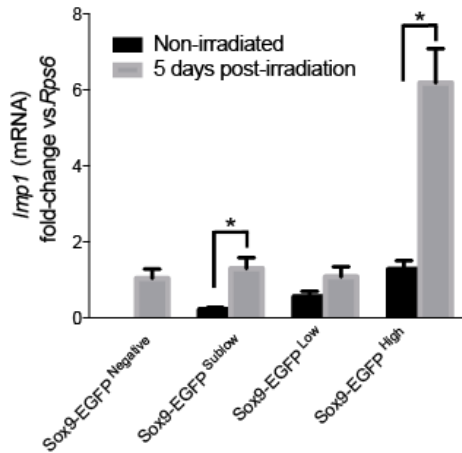
A. Crypts cells from *Imp1fl/fl* and *VillinCre;Imp1fl/fl* mice were isolated and RNA-Seq

performed N=3 mice per group. Gene set enrichment analysis (GSEA) revealed

enrichment of gene targets involved in proliferation, regeneration and Wnt signaling in

VillinCre;Imp1fl/fl mice as compared to control mice (p-value < 0.001, FDR < 0.001)

(NES = Normalized Enrichment Score; It reflects the degree to which a gene set is overrepresented at the top or bottom of a ranked list of genes). B. Imp1 expression is upregulated in all the different *Sox9-EGFP* cell fractions five days following 14Gy irradiation and significantly upregulated in the Sublow and High populations (n=5 animals per group).

Supplemental Tables

Supplemental Table 1: Pathways enriched in SW480 cells with LIN28B overexpression and IMP1 deletion

Name	NOM p-value	FDR q-value
Hallmark_E2F_Targets	0	0
Hallmark_G2M_Checkpoint	0	0
Hallmark_MYC_Targets_V1	0	0
Hallmark_Oxidative_Phosphorylation	0	0.0022
Hallmark_Notch_Signaling	0.002053388	0.00265
Hallmark_Fatty_Acid_Metabolism	0	0.0084
Hallmark_Wnt_Beta_Catenin_Sig	0.01705757	0.0167
Hallmark_MYC_Targets_V2	0.015625	0.0267
Hallmark_UV_Response_Up	0	0.0386
Hallmark_DNA_Repair	0.012987013	0.0443
Hallmark_Spermatogenesis	0.006593407	0.0405
Hallmark_Peroxisome	0.027253669	0.061803464
Hallmark_MTORC1_Signaling	0.013888889	0.06772548
Hallmark_Adipogenesis	0.008602151	0.06409443
Hallmark_Cholesterol_Homeostasis	0.055900622	0.0648
Hallmark_Mitotic_Spindle	0.04954955	0.1625
Hallmark_Estrogen_Response	0.0771028	0.1671
Hallmark_Hedgehog_Signaling	0.17038539	0.17756905
Hallmark_Glycolysis	0.08	0.19207256
Hallmark_Angiogenesis	0.21111111	0.20649734
Hallmark_Bile_Acid_Metabolism	0.18518518	0.21454285
Hallmark_Androgen_Response	0.20177384	0.2415668
Hallmark_Hypoxia	0.2488372	0.3487353
Hallmark_PI3K_AKT_MTOR_Signaling	0.3325792	0.40959582
Hallmark_Pancreas_Beta_Cell	0.40169132	0.5057253

Hallmark_Kras_Signaling_Dn	0.518847	0.5805789
Hallmark_Xenobiotic_Metabolism	0.5788337	0.6075719
Hallmark_ROS_Pathway	0.5813449	0.72866654
Hallmark_IL2_STAT5_Signaling	0.8098434	0.75037533

Supplemental Table 2: Comparison of fold change of transcripts between the eCLIP studies(Conway et al. 2016) and our TE studies.

Translational efficiency changes	eCLIP dataset		
	< 2 fold change	> 2 fold increase	> 2 fold decrease
< 2 fold change	2492	4019	111
> 2 fold increase	90	235	5
> 2 fold decrease	153	428	12

Supplemental Table 3: List of Wnt signaling pathway genes differentially regulated by IMP1 loss with LIN28B overexpression in SW480 cells

ID	Gene Name	Function
CTBP2	C-terminal binding protein 2(CTBP2)	Corepressor targeting diverse transcription regulators. Acts as a scaffold for specialized synapses. Phosphorylated upon DNA damage. Phosphorylation by HIPK2 on Ser-428 induces proteasomal degradation. Ubiquitous expression. Highest levels in heart, skeletal muscle, and pancreas.
FBXW11	F-box and WD repeat domain containing 11(FBXW11)	Substrate recognition component of a SCF (SKP1-CUL1-F-box protein) E3 ubiquitin-protein ligase complex which mediates the ubiquitination and subsequent proteasomal degradation of target proteins. Probably recognizes and binds to phosphorylated target proteins. SCF(FBXW11) mediates the ubiquitination of CTNNB1 and participates in Wnt signaling.

WNT10A	Wnt family member 10A(WNT10A)	Ligand for members of the frizzled family of seven transmembrane receptors. Probable developmental protein. May be a signaling molecule important in CNS development.
CTNNBIP1	catenin beta interacting protein 1(CTNNBIP1)	Prevents the interaction between CTNNB1 and TCF family members and acts as negative regulator of the Wnt signaling pathway.
DKK1	dickkopf WNT signaling pathway inhibitor 1(DKK1)	
DVL2	disheveled segment polarity protein 2(DVL2)	May play a role in the signal transduction pathway mediated by multiple Wnt genes.
DVL3	disheveled segment polarity protein 3(DVL3)	May play a role in the signal transduction pathway mediated by multiple Wnt genes.
FZD6	frizzled class receptor 6(FZD6)	Receptor for Wnt proteins. Lys-Thr-X-X-X-Trp motif is involved in the activation of the Wnt/beta-catenin signaling pathway. The FZ domain is involved in binding with Wnt ligands.
NKD2	naked cuticle homolog 2(NKD2)	Cell autonomous antagonist of the canonical Wnt signaling pathway. May activate a second Wnt signaling pathway that controls planar cell polarity (By similarity). Required for processing of TGFA and for targeting of TGFA to the basolateral membrane of polarized epithelial cells.
NLK	nemo like kinase(NLK)	Acts downstream of MAP3K7 and HIPK2 to negatively regulate the canonical Wnt/beta-catenin signaling pathway and the phosphorylation and destruction of the MYB transcription factor. Involved in TGFbeta-mediated mesoderm induction, acting downstream of MAP3K7/TAK1 to phosphorylate STAT3.
PRKCA	protein kinase C alpha(PRKCA)	
PRKCG	protein kinase C gamma(PRKCG)	This is a calcium-activated, phospholipid-dependent, serine- and threonine-specific enzyme.
PRKACA	protein kinase cAMP-activated catalytic subunit alpha(PRKACA)	Phosphorylates a large number of substrates in the cytoplasm and the nucleus.
PPP3CC	protein phosphatase 3 catalytic subunit gamma(PPP3CC)	Calcium-dependent, calmodulin-stimulated protein phosphatase. This subunit may have a role in the calmodulin activation of calcineurin.

RHOA	ras homolog family member A(RHOA)	
RAC1	ras-related C3 botulinum toxin substrate 1 (rho family, small GTP binding protein Rac1)(RAC1)	
TP53	tumor protein p53(TP53)	

Materials and Methods

Cell Lines and Cell Culture

Colorectal cancer cell lines were obtained from ATCC that STR authenticates them. Stable *LIN28B* expression in SW480 and LoVo cells was achieved using MSCV-PIG-*LIN28B* and empty vector control plasmids (gifts from Dr. Joshua Mendell) using the protocol described previously (King et al. 2011b). *IMP1* was knocked out by co-transfecting cells with IMP-1 CRISPR/Cas9 KO Plasmid (h) (Santa Cruz; sc-401703) and IMP-1 HDR Plasmid (h) (Santa Cruz ; sc-401703 HDR) followed by sorting and clonal expansion of RFP+ve cells. The knockout was verified by western blotting for IMP1. *IMP1* was knocked down in CaCo2 cells by siRNA transfection using Lipofectamine RNAiMax as per the manufacturer's guidelines. Silencer select negative control #1 siRNA from ThermoFisher was used as a negative control. qRTPCR was used to validate knockdown. Cell lines were cultured in DMEM (Thermo Fisher Scientific) supplemented with 10% FBS (GE Healthcare Life Sciences) and 1% Penicillin-Streptomycin (P/S; Thermo Fisher Scientific) in a 37 °C incubator with 5% CO_2 under puromycin selection. Cells are tested for mycoplasma at least every 2 months in the laboratory.

Animal Models

VillinCre;Vil-Lin28b;Imp1^{fl/fl} were obtained by mating *Vil-Lin28b^{Med}* and *VillinCre;Imp1^{fl/fl}* mice that have been described previously (Hamilton et al. 2013; Madison et al. 2013b), and were maintained via backcrosses to C57BL/6J. *Imp1^{fl/fl}* mice were considered wild type and express LIN28B and IMP1 insignificantly different from wild type mice. *Lgr5-EGFP-IRES-creERT2* mice were purchased from Jackson Laboratories. The *HopxCreERT2;Imp1^{fl/fl}* mice were generated by crossing *Imp1^{fl/fl}* mice with tamoxifen inducible *Hopx-CreERT2* (JAX strain 017606) mice that were generated at the University

of Pennsylvania in the laboratory of J. Epstein (Philadelphia, PA) and have been characterized previously (Yousefi et al. 2016). *Sox9-EGFP* mice were maintained as previously described (Van Landeghem et al. 2012). We utilized Cyagen (Santa Clara, CA) to generate Imp1 overexpressing (Imp1^{OE}) mice. Briefly, the knockin construct was generated by amplification of mouse genomic fragments from a BAC clone using high-fidelity DNA polymerase. The targeting vector was assembled to include Flag-tagged Imp1 (Igf2bp1) cDNA targeted to the Rosa locus downstream of the EF1α promoter and PolyA sequence flanked by loxP sites (Supplemental Figure 4B). In addition, we included an IRES;tdTomato;SV40EpolyA following the Imp1 cDNA. We crossed these mice with *Villin-Cre* mice in order to specifically overexpress Imp1 in intestinal epithelial cells. All experimental analyses were performed on three or more individual mice (male or female mice at 12 months of age for tumor studies and 8-12-week-old mice for irradiation studies). Controls and experimental groups were either sex-matched littermates or age-matched, sex-matched non-littermates. To ablate *Imp1* in *HopxCreERT2;Imp1$^{fl/fl}$* mice, tamoxifen (Sigma-Aldrich) was dissolved in peanut oil at 10 mg/ml, and 200µg/g of body weight tamoxifen was injected intraperitoneally for each dose. A total of 2 doses were administered 24 hours apart before the irradiation experiments. 12 Gy whole-body γ-IR was administered to at least three mice in each group. For irradiation experiments utilizing *VillinCre;Imp$^{fl/fl}$* mice, animals were given a whole body, single dose of 12Gy using the Gammacell 40 Cesium 137 Irradiation Unit. Irradiation of *Sox9-EGFP* mice was performed as described previously (Van Landeghem et al. 2012). Body weights were recorded daily, and mice were euthanized before losing a maximum of 25% total body weight at day 4 post-irradiation. All mouse protocols were approved by the Institutional Animal Care and Use Committee at the University of Pennsylvania under protocol 804607.

Ribosome Profiling

Ribosome profiling libraries from 3 pooled cell culture plates were prepared using a standard protocol (McGlincy and Ingolia 2017), with minor modifications. Separate 5' and 3' linkers were ligated to the RNA-fragment instead of 3' linker followed by circularization (Subtelny et al. 2014). 5' linkers contained 4 random nt unique molecular identifier (UMI) similar to a 5 nt UMI in 3' linkers. During size-selection, we restricted the footprint lengths to 18-34 nts. Matched RNA-seq libraries were prepared using RNA that was randomly fragmentation by incubating for 15 min at 95C with in 1 mM EDTA, 6 mM Na_2CO_3, 44 mM $NaHCO_3$, pH 9.3. RNA-seq fragments were restricted to 18-50 nts. Ribosomal rRNA were removed from pooled RNA-seq and footprinting samples using RiboZero (Epicenter MRZH116). cDNA for the pooled library were PCR amplified for 15 cycles.

Ribosome profiling data processing and analysis

RNA-seq and footprinting reads were mapped to the human transcriptome using the riboviz pipeline(Oana Carja 2017b). Sequencing adapters were trimmed from reads using Cutadapt 1.10 (Martin 2011) (--trim-n -O 1 –minimum-length 5). The reads from different samples were separated based on the barcodes in their 3' linkers using fastx_barcode_splitter (FASTX toolkit, Hannon lab) with utmost one mismatch allowed. UMI and barcodes were removed from reads in each sample using Cutadapt (--trim-n -m 10 -u 4 -u -10). Trimmed reads that aligned to human/mouse rRNA were removed using Bowtie v1.1.2 (Langmead et al. 2009). Remaining reads were mapped to a set of 19,192 principal transcripts for each gene in the APPRIS database (Rodriguez et al. 2013) (using HISAT2 v2.1.0 (Kim et al. 2015)). Only reads that mapped uniquely were used for all downstream analyses. For genes with multiple principal transcripts, the first one in the list was chosen. Codes for selecting these transcripts were obtained from riboviz

package (https://github.com/shahpr/RiboViz, (Oana Carja 2017a)). Radar map: The list of post-transcriptional regulators was obtained from the AURA database (Dassi et al. 2014) and the plot was generated using modified functions of tRanslatome (Tebaldi et al. 2014) package in R. The tRanslatome package was modified to restrict the list of post-transcriptional regulators to regulators of 19,192 genes used for mapping reads. All analyses of ribosome profiling datasets were performed in R. We restricted analyses to genes with at least one dataset (RNA-seq or footprinting across conditions) with 64 mapped reads and genes with 0 read counts in any dataset were ignored unless the mean read counts across all 8 datasets was above 64. Differentially expressed genes were identified using DEGseq package (Wang et al. 2010) using an FDR cutoff of 0.001. GO enrichment analyses and identification of post-transcriptional regulators of differentially expressed genes at the transcriptome and translatome levels was performed using tRanslatome package.

RNA Sequencing

RNA was isolated from freshly isolated mouse intestine crypts and cell lines using the GeneJET RNA Purification Kit according to the manufacturer's instructions, with DNase treatment. The cDNA libraries were then generated using Illumina TruSeq Stranded mRNA Library Preparation Kit with Ribo Zero treatment (RS-122-2201). The cDNA was sequenced using HiSeq 50 Cycle Single-Read Sequencing version 4 by the High Throughput Genomics core at the Huntsman Cancer Institute, University of Utah for a fee. All sequencing reads were first trimmed to remove 3' sequencing adapters, and aligned to the hg19 human genome with STAR using the default parameters(Dobin et al. 2013). Read counts for each gene were measured using HTSeq run in "intersection-strict" mode(Anders et al. 2015), and differential expression analysis was performed using DESeq2(Love et al. 2014). Taking all differentially expressed genes with a false

discovery rate (FDR) < 0.05, GO analysis was performed using DAVID(Huang da et al. 2009b; Huang da et al. 2009a). Genotypes were run in triplicates and DESeq2 analysis was performed on them. GO Analysis was performed on the differentially expressed genes. GSEA was performed according to previously established guidelines (Subramanian et al. 2005).

TCGA Analyses

Publicly available gene expression data from The Cancer Genome Atlas (TCGA) were downloaded from the Genomic Data Commons (GDC) Data Portal and graphs generated using GraphPad Prism. Tumor type and stage data were acquired from the University of California Santa Cruz (UCSC) Xena at http://xena.ucsc.edu. Pooled Colon and rectal adenocarcinoma (COADREAD) data contained 433 samples in different tumor stages. For staging, high expression and low expression groups were determined by cutoff at the 75th percentile.

Correlation of expression was determined via Chi-square analysis; 95% confidence interval calculated for confirmation of statistical significance in GraphPad Prism.

Tumor Tissue Microarray Analysis

A tumor tissue microarray comprised of a uniform cohort of 228 (133 males and 95 females) patients with colon carcinoma (88 in stage 2, and 140 in stage 3) diagnosed between November 1993 and October 2006 was used. Rectal tumors were excluded(King et al. 2011a). LIN28B staining intensity was scored by a pathologist (A.J.K.S.) - 1 was used to signify low Lin28b intensity, 2 for intermediate intensity, and 3 for high. We used the high expressing samples and analyzed the differentiation status by the three-tier tumor grading system recommended by the American Joint Commission (Edge and Compton 2010).

Enteroid Culture and Analyses

The proximal jejunum (6cm) was flushed with cold PBS and cut lengthwise to expose the luminal surface. Tissue was placed in calcium-magnesium-free HBSS (CMF-HBSS) with 1 mM N-acetyl cysteine, vortexed briefly, and placed on ice. The tissue was then transferred to CMF-HBSS containing 10 mM EDTA and 1 mM NAC and incubated for 45 minutes at 4°C with end-to-end rotation. Epithelial cells were then mechanically dissociated by vortexing for 30 seconds, following a rest on ice for 30 seconds, repeated for a total of 4 times. The villi were removed by filtering over a 70μm filter. Crypts were pelleted at 100 x g for 4 minutes and resuspended in Basal+ Media (Advanced DMEM/F12 containing: 2mM, 10mM HEPES, 1X Penicillin/Streptomycin, 5μM CHIR99021, 1mM NAC, 1X N2 supplement, and 1X B27 supplement for quantification. Crypts were defined as small, U-shaped structures (or partial U-shaped structures for irradiated mice). Crypts were plated in 4 wells of a 48-well plate per mouse at a density of 150 crypts per well in an 80/20 mixture of Matrigel Matrix and Basal+ Media also containing 50ng/mL mouse epidermal growth factor and 2.5% Noggin/R-spondin conditioned media (Sato et al. 2009). After Matrigel solidified, crypt-containing patties were overlaid with ENR media. The number of surviving crypt spheres (enteroids) were counted on day 1-4 following plating to determine enteroid plating efficiency. On day 4 after plating the number of surviving enteroids was scored. All counting was performed at 10X magnification using the Olympus IX81 inverted microscope. A crypt sphere was defined as a 3-D sphere or oval shape surrounding a lumen (ie enterosphere). A "budded" enteroid was defined as a 3-D structure with one or more *de novo* projections of any length representing crypts emerging from the spheroid body.

qRT-PCR

Small intestine crypt RNA was isolated using the GeneJet RNA purification kit. Equal amounts of total RNA were reverse-transcribed using the Taqman RT Reagents kit and resulting cDNA used with Power SYBR Green PCR Master Mix and validated primer sets listed in the table below. Non-reverse transcribed samples were used as negative controls, and gene expression was calculated using the $R = 2^{(-\Delta\Delta Ct)}$ method, where changes in C_t values for the genes of interest were normalized to housekeeping genes *Tbp, Rsp6* or *Gapdh*. Gene expression data are expressed as fold-change versus mean values for wild type or no treatment controls. All experiments were replicated in at least 3 independent experiments with technical replicates (duplicates) in each experiment. For analyses of *Sox9-EGFP* mice, FACS-isolation of *Sox9-EGFP* cell populations was performed as described previously (Van Landeghem et al. 2012). Total RNA from all Sox9-EGFP populations and non-sorted epithelial cells were extracted and reverse transcribed. qRT-PCR was performed using Platinum Quantitative PCR SuperMix-UDG and the following TaqMan probes: Mm00501602_m1 (*Igf2bp1*) and Mm02342456_g1 (*Rsp6*). Samples were run in duplicate and expression was determined by a standard curve of pooled non-sorted intestinal epithelial cells and normalized to the invariant control gene *Rps6.*

Histology, Immunohistochemistry and Tissue Analyses

Tissues were fixed in zinc formalin fixative overnight at 4°C, washed in PBS, and moved to 70% ethanol before paraffin embedding and sectioning. Hematoxylin and eosin (H&E) staining was performed according to standard procedures in the Molecular pathology and imaging core of the Penn Center for Molecular Studies in Digestive and Liver Diseases. For immunostaining, antigen retrieval was performed by heating slides in 10mM citric acid buffer (2.1g Citric Acid Monohydrate in 1L di H_2O, pH 6.0) in a pressure cooker. The images were taken using Nikon Eclipse E600 Microscope and analyzed with

the NIS-Elements Basic Research software version 4.51. Imaging was performed at RT. The following primary antibodies were used for immunostaining: anti-Ki67 antibody (1:200), anti-LYSOZYME (1:1000), anti-CHROMAGRANIN A (1:1000), anti-H2AX (1:1000), anti-IMP1 antibody (1:1000), anti-AXIN2 (1:4000), anti–β-CATENIN antibody (1:1000). Cy2- or Cy3-, conjugated secondary antibodies were obtained from Jackson ImmunoResearch Laboratories, Inc. Biotinylated secondary antibodies and DAB substrate kit for immunohistochemistry were purchased from Vector Laboratories. All quantifications were done across at least 30 high-powered fields per animal that were randomly selected areas throughout the small intestine of at least four mice in each genotype. For quantifying regeneration after irradiation, regenerative microcolonies/foci were defined as a cluster of ≥5 Ki67-positive cells from a single clone (colony or hyperproliferative crypt).

Flow cytometry and sorting

For analysis of EdU positive cells, the mice were injected with 20mg/kg of EdU intraperotoneally. The mice were sacrificed 2 hours after the injection. The single cell suspensions of crypt-enriched intestinal epithelium from the small intestine (jejunum) of the mice were then stained for EdU following the manufactures instructions. For sorting, mouse intestinal epithelial cells were isolated into single cells. CD24-PE (Biolegend) and cKit PE-Cy7 (eBioscience) staining was done for sorting as per manufacturer's instructions.Flow cytometry was performed using a FACS LSR (BD Biosciences) with a 100μm nozzle. Sorting was done using FACS Aria (BD Biosciences) sorter. Gating and compensation were performed using a negative and single-color controls. Three biological replicates (and three technical replicates) for each genotype were used.

Quantification and Statistical Analysis

Statistical analysis was performed using GraphPad Prism software version 7.0. One-way

ANOVA with Tukey's post-hoc test was performed to compare the differences among

groups in all studies. Unpaired t-test (two-tailed) was used when two groups were

compared. For all experiments with error bars, the standard error of the mean was

calculated, and the data are presented as mean ± SEM. The sample size for each

experiment is included in the figure legends.

Data and Software Availability

See above Ribosome profiling and data processing. The accession numbers for all new

RNA-sequencing data and ribosome-profiling data reported in this manuscript will be

deposited via GEO upon acceptance.

CHAPTER III: POST-TRANSCRIPTIONAL REGULATION OF THE INTESTINAL EPITHELIAL CELL RESPONSE TO COLITIS

Abstract

RNA binding proteins (RBPs) are emerging as critical regulators of intestinal development and cancer. IMP1 (*IGF2* mRNA Binding Protein 1) hypomorphic mice exhibit severe intestinal growth defects, yet it's role in adult epithelium is unclear. We investigated the mechanistic contribution of epithelial IMP1 to intestinal homeostasis and repair. We evaluated IMP1 expression in Crohn's disease patients followed by unbiased ribosome profiling in IMP1 knockout cells. Concurrently, we evaluated mice with intestinal epithelial-specific *Imp1* deletion (*Imp1$^{\Delta IEC}$*) following dextran sodium sulfate (DSS)-colitis. Based on ribosome profiling data, evaluated autophagy in *Imp1$^{\Delta IEC}$* mice, as well as *in silico* and *in vitro* approaches to determine direct protein:RNA interactions. Finally, we analyzed the consequence of genetic deletion of essential autophagy protein, *Atg7,* in *Imp1$^{\Delta IEC}$* mice using colitis and irradiation models. IMP1 was upregulated robustly in Crohn's disease patients and *Imp1* loss lessened DSS-colitis severity. Unbiased ribosome-profiling revealed that IMP1 may coordinate translation of multiple pathways important for intestinal homeostasis, including autophagy, which we verified by western blotting. Mechanistically, we found evidence for increased autophagy flux in *Imp1$^{\Delta IEC}$* mice, reinforced through *in silico* and biochemical analyses revealing direct binding of IMP1 to autophagy transcripts. Finally, we found genetic deletion of *Atg7* reversed the phenotype observed in DSS- or irradiation-challenged *Imp1$^{\Delta IEC}$* mice. IMP1 acts as a post-transcriptional regulator of gut epithelial repair post-colitis and irradiation, in part through modulation of autophagy. This study provides a new perspective on post-transcriptional regulation of autophagy as a contributing factor to the pathogenesis of inflammatory bowel disease.

Keywords: RNA binding protein; IMP1; ribosome profiling; colitis; autophagy

Transcript Profiling: [GEO link]

Introduction

Intestinal epithelium maintains its integrity through orchestration of self-renewal, proliferation, differentiation, and cell death during homeostasis and in response to stress. The rapidity with which intestinal epithelium must respond to environmental stressors suggests a necessity for multiple layers of gene regulation. RNA binding proteins (RBPs) have emerged as critical regulators of intestinal proliferation and stem cell dynamics (Madison et al. 2013a; Li et al. 2015; Madison et al. 2015; Tu et al. 2015; Wang et al. 2015a; Yousefi et al. 2016). *IGF2* mRNA-binding protein 1 (IMP1) is a RBP with primary roles in mRNA trafficking, localization, and stability. Target mRNAs of IMP1 (also called IGF2BP1, CRD-BP, ZBP1) include *IGF2*, *ACTB*, *MYC*, *H19*, *CD44*, *GLI1 and PTGS2* (Leeds et al. 1997; Ross et al. 1997; Nielsen et al. 1999; Runge et al. 2000; Lemm and Ross 2002; Vikesaa et al. 2006; Noubissi et al. 2009; Manieri et al. 2012). *In vitro* studies demonstrate that IMP1 forms stable complexes with its target mRNAs, confining these transcripts to ribonucleoprotein particles (RNPs) and stabilizing mRNA or inhibiting translation (Bernstein et al. 1992; Huttelmaier et al. 2005; Noubissi et al. 2006; Stohr et al. 2006; Vikesaa et al. 2006; Gu et al. 2008; Elcheva et al. 2009; Noubissi et al. 2009; Weidensdorfer et al. 2009; Stohr et al. 2012). IMP1 also plays a functional role in mRNA transport to aid in various cellular processes, including movement and polarity (Vikesaa et al. 2006; Gu et al. 2012). Finally, PAR-CLIP and eCLIP studies have identified a myriad of IMP1 targets, providing important insight into the diverse and context-specific roles of IMP1 via regulation of specific transcripts or transcript groups (Hafner et al. 2010; Conway et al. 2016).

In mice, *Imp1* is expressed in the small intestine and colon during embryonic development through postnatal day 12 and at low levels during adulthood (Hansen et al. 2004). *Imp1* hypomorphic mice exhibit dwarfism, intestinal defects and perinatal lethality (Hansen et al. 2004; Fakhraldeen et al. 2015). Recent studies in the fetal brain implicate

Imp1 as a regulator of differentiation of stem/progenitor cells, where *Imp1* deletion leads to neural stem cell depletion (Nishino et al. 2013). In adult mouse colon, IMP1 is expressed in the epithelial crypt base and in mesenchymal cells following injury (Dimitriadis et al. 2007a; Manieri et al. 2012). Our prior published studies demonstrated that IMP1 may promote or suppress colon tumorigenesis based upon its expression and function in the epithelial or mesenchymal compartments, underscoring the notion that IMP1 may exhibit opposing effects in different contexts (Hamilton et al. 2013; Hamilton et al. 2015). Taken together, *in vivo* studies suggest IMP1 as a key regulator of development and cancer, potentially via regulation of stem/progenitor cell maintenance (Degrauwe et al. 2016b).

Finally, prior reports have suggested a role for IMP1 in cellular stress response. Studies of the IMP1 chicken orthologue, ZBP1, revealed an essential role in the integrated stress response (ISR) via differential regulation of mRNA fates in non-stressed versus stressed cells (Stohr et al. 2006). Characterization of IMP1 RNP granules *in vitro* revealed enrichment of mRNAs encoding proteins involved in the secretory pathway, ER stress, and ubiquitin-dependent metabolism (Jonson et al. 2007). Despite its considerable importance in normal development and its role in coordinating cellular stress, the specific functional roles of IMP1 in adult tissues have yet to be elucidated *in vivo.* In the present study, we tested the hypothesis that IMP1 functions as a regulator of epithelial response to damage in adult tissues.

Results

IMP1 is upregulated in adult and pediatric Crohn's disease patients

Based upon prior studies, we reasoned that IMP1 may play a role during damage or stress conditions in the gut. In whole tissue biopsies from adult Crohn's disease

patients (Table 1), we observed a >5-fold increase in *IMP1* compared to control patients (1±0.12 versus 5.3±1.81, Figure 12A). This was confirmed via IMP1 immunohistochemistry, where we observed both epithelial and stromal IMP1 staining in adult Crohn's disease patients (Figure 12B). Consistent with these findings, analysis of published RISK RNA-sequencing data from pediatric inflammatory bowel disease (IBD) patients revealed that *IMP1* is upregulated significantly compared to control patients, and that this effect is specific to *IMP1* (i.e. other distinct isoforms, *IMP2* and *IMP3,* are not changed; Figure 12C) (Haberman et al. 2014).

Mice with intestinal epithelial cell deletion of *Imp1* exhibit increased recovery following colitis

We next evaluated the functional consequence of Imp1 deletion during chronic colitis using *VillinCre; Imp1$^{fl/fl}$* mice (*Imp1$^{\Delta IEC}$* mice; Supplementary Figure 7A). *Imp1$^{\Delta IEC}$* mice lost significantly less weight following 3 cycles of dextran sodium sulfate (DSS) compared to controls (*Imp1$^{fl/fl}$*, denoted as *Imp1^{WT}*; Figure 13A). *Imp1$^{\Delta IEC}$* mice exhibited an overall decrease in colitis score, hyperplasia, inflammation, and mononuclear cell score (Figure 13B-F). In addition, cytokine expression was decreased in *Imp1$^{\Delta IEC}$* mice (Figure 13G). *Imp1$^{\Delta IEC}$* mice further displayed a modest decrease colon shortening compared to controls (Supplementary Figure 7B). Together, these observations suggest that Imp1 loss in intestinal epithelium may promote recovery from damage in the setting of DSS-colitis.

IMP1 knockout reveals global changes in translation

Transcriptome-wide approaches provide a global snapshot of transcript abundance within a given context; however, the functional effects of RBPs are not

captured fully by RNA-sequencing alone. To define the putative molecular basis for phenotypic differences between $Imp1^{\Delta IEC}$ and control mice, we examined the effect of IMP1 loss upon translation efficiency. Due to technical challenges in performing ribosome-profiling *in vivo*, we utilized CRISPR-mediated IMP1 deletion in the SW480 colorectal cancer cell line to evaluate "translatome"-wide effects of IMP1 loss (Figure 14A; Supplementary Figure 8A&B). Following deep sequencing to compare total RNA abundance in SW480 cells with and without IMP1, RNA fragments protected by bound ribosomes were sequenced to define actively translating mRNAs (Data deposited in GEO (GSE112305) [NCBI tracking system #18999297]). We found that *IMP1* loss affected gene expression on both transcriptional and translational levels. Of the 10043 genes analyzed, we saw no change in RNA level or ribosome binding in 7386 genes (Figure 14B). 642 transcripts were exclusively differentially regulated at the transcription level whereas 1264 genes were only differentially regulated at the translational level. Furthermore, in 28 genes, translation direction was completely antagonistic to transcription, whereas translation reinforced transcriptional direction in 60 genes (Figure 14B). Additionally, in 663 genes translation acted as a buffering mechanism (McManus et al. 2014), whereby protein levels remain constant despite changes in mRNA levels.

Translational efficiency (TE) of a gene is defined as the ratio of abundance in ribosome protected fragments (RPF) to that of total mRNA abundance for a gene (Zhong et al. 2017). We compared TE changes between the two genotypes and observed differential TE for 1469 genes (Figure 14C). Pathway enrichment analysis for TE genes (Chen et al. 2009) differentially expressed in cells with IMP1 deletion revealed a significant representation of pathways linked to cell cycle, gene expression and RNA processing, post-translational modification, autophagy, and metabolism (Figure 14D). Enhanced TE of these pathways suggest a post-transcriptional program directed by IMP1 that may underlie the protective or regenerative effects observed in $Imp1^{\Delta IEC}$ mice.

Mice with *Imp1* loss exhibit morphological changes in Paneth cells and enhanced autophagy

Evidence in *Imp1* hypomorphic mice, which express 20% of wild type Imp1, suggests that its expression is critical for normal growth and development, as these mice exhibit high perinatal mortality and morphological defects in intestine epithelium (Hansen et al. 2004; Fakhraldeen et al. 2015). We observe no gross phenotypic effects in *Imp1^ΔIEC^* mice, suggesting that intestinal epithelial IMP1 is dispensable during homeostasis (Supplementary 9A). We analyzed the number and morphology of differentiated epithelial cell types and although there was no difference in total Paneth, goblet, or enteroendocrine cell numbers between genotypes (Supplementary Figure 9B, C), diffuse lysozyme staining was apparent in Paneth cells of *Imp1^ΔIEC^* mice (Figure 15A&B). As autophagy gene mutations have been associated with Paneth cell granule defects in Crohn's disease patients (Liu et al. 2014b; VanDussen et al. 2014; Liu et al. 2016; Liu et al. 2017; Stappenbeck and McGovern 2017), we evaluated autophagy in *Imp1^ΔIEC^* mice. Freshly isolated, live crypt cells stained with the cationic amphiphilic tracer dye CytoID, which incorporates into autophagic structures, revealed an increase in basal autophagic vesicle content in *Imp1^ΔIEC^* mice via flow cytometry (Fig. 15C). Importantly, we validated CytoID as a tool to measure autophagy using *Atg7^ΔIEC^* mice (Supplementary Figure 10A, B). Ultrastructural analysis of crypts via transmission electron microscopy (TEM) revealed an increase in small, electron-dense lysozyme granules within areas of electron-lucent halos in *Imp1^ΔIEC^* mice compared to controls (Fig. 15E). As an additional measure of autophagy, we performed western blotting for cleaved LC3 in freshly isolated *Imp1^ΔIEC^* colon and jejunum crypt cells. A shift from the upper to lower LC3 band suggested enhanced autophagic vesicle content in *Imp1^ΔIEC^* mice (Figure 15E;

Supplementary Figure 9D). Furthermore, a concurrent decrease in autophagy cargo-associated protein p62 in $Imp1^{\Delta IEC}$ colon crypts, indicted increased autophagy flux (Figure 15E).

To confirm a direct role for IMP1 knockdown to induce autophagy, we evaluated Caco2 cells transfected with IMP1 siRNA and observed a robust increase in LC3-I/LC3-II (Figure 15F). Finally, in order to determine if changes in autophagy are maintained *ex vivo*, $Imp1^{\Delta IEC}$ and $Imp1^{WT}$ enteroids were treated with the lysosomal inhibitor chloroquine (CQ) and evaluated for CytoID puncta formation. Active autophagic flux is signified by an accumulation of CytoID–stained puncta upon CQ treatment, which we observed in both $Imp1^{\Delta IEC}$ and $Imp1^{WT}$ mice (Figure 15G). Intriguingly, we noted a broader CytoID staining pattern (not restricted to Paneth cells) in $Imp1^{\Delta IEC}$ mice. As such, we performed gene expression analysis for *Imp1* in *Lgr5+* and Paneth (CD24/cKit/SSC high) cells sorted from *Lgr5-eGFP-IRES-CreERT2* mouse crypt epithelium. We observed that *Imp1* is enriched in both *Lgr5+* and Paneth cells compared to unsorted crypts (Figure 15H).

Enhanced recovery from colitis in *Imp1^{\Delta IEC}* mice is reversed with genetic deletion of *Atg7*

Based upon our data that $Imp1^{\Delta IEC}$ mice exhibited decreased inflammation and colitis during chronic DSS, we aimed to determine if $Imp1^{\Delta IEC}$ mice fare better during acute colitis. Both $Imp1^{WT}$ and $Imp1^{\Delta IEC}$ mice exhibited significant weight loss following five days of DSS treatment, but $Imp1^{\Delta IEC}$ mice began to recover weight, whereas $Imp1^{WT}$ mice required sacrifice due to weight loss (Figure 16A). Acute DSS-treated $Imp1^{\Delta IEC}$ mice exhibited significantly lower total colitis and epithelial loss scores compared to controls (Figure 16B, C). Prior studies suggest enhanced susceptibility to colitis in mice

with genetic deletion of autophagy (Tsuboi et al. 2015). ATG7 is an essential component of the ATG conjugation system and is critical for early autophagosome formation (Komatsu et al. 2005). In addition, prior studies of intestinal epithelial-specific *Atg7* deletion demonstrated loss of autophagic vacuoles via TEM analysis and a phenotype similar to that of intestinal epithelial-specific knockout of the autophagy genes *Atg16L1* or *Atg5* (Cadwell et al. 2009; Adolph et al. 2013). To evaluate the relative contribution of enhanced autophagy to the phenotype in *Imp1^{ΔIEC}* mice, we generated *Imp1^{ΔIEC}* mice with genetic deletion of autophagy using *Atg7*-floxed alleles (*Imp1^{ΔIEC}Atg7^{ΔIEC}*). *Imp1^{ΔIEC}Atg7^{ΔIEC}* mice lost weight and became moribund more rapidly than *Imp1^{WT}* and *Imp1^{ΔIEC}* mice, requiring sacrifice prior to the recovery period (Figure 16A). Thus, autophagy loss offsets the beneficial effect of *Imp1* loss during acute colitis.

We next evaluated whether *Imp1* loss could promote enhanced recovery in a second damage/stress model. We challenged *Imp1^{ΔIEC}* mice with 12Gy whole body irradiation and evaluated tissue regeneration via quantification of EdU+ regenerative microcolonies. *Imp1^{ΔIEC}* mice loss less weight and exhibited a significant increase in number of EdU+ microcolonies compared to *Imp1^{WT}* mice (Fig. 16D, E). *Imp1^{ΔIEC}Atg7^{ΔIEC}* mice exhibited more weight loss and fewer regenerating microcolonies than *Imp1^{ΔIEC}* mice, suggesting that *Atg7* deletion reversed the beneficial effects of *Imp1* loss in this context. Taken together, these data suggest that IMP1 can regulate the autophagy pathway during homeostasis and in two injury models.

IMP1 interacts with autophagy transcripts

One way in which RBPs regulate post-transcriptional gene expression is via direct binding of target transcripts. We have demonstrated that Imp1 loss 1) enhances translation efficiency of genes in the autophagy pathway (Figure 14D), and 2) leads to increased LC3 protein expression (Figure 15E, F; Supplementary Figure 9D). We

therefore evaluated direct binding of IMP1 to autophagy transcripts. We first performed

in silico analyses to assess binding propensities of IMP1 for autophagy transcripts using

catRAPID, which predicts RNA:protein interactions based upon nucleotide and

polypeptide sequences as well as physicochemical properties (Cirillo et al. 2016). These

analyses predicted binding of IMP1 to *BECN1, MAP1LC3B and ATG3* transcripts (Figure

17A), as well as positive control *ACTB*. Lower relative binding scores were predicted for

ATG16L1, ATG7, and ATG5. This algorithm predicted no binding to negative targets

TNFRSF1B and ITGA7. We next evaluated published eCLIP data (Conway et al. 2016)

in human pluripotent stem cells for the same autophagy transcripts and found a

signification correlation between catRAPID-predicted binding and eCLIP binding (r =

0.9838465 Pearson correlation coefficient, Figure 17B). To confirm IMP1 binding to

these targets, we performed ribonucleoprotein (RNP)-immunoprecipitation with

antibodies to endogenous IMP1 in Caco2 cells. Previously confirmed IMP1 targets

ACTN and *PTGS2* and non-target *TNFRSF1B* were used as positive and negative

controls, respectively. We observed significant binding enrichment in autophagy genes

MAP1LC3B and *ATG3* with IMP1 (Figure 17C, Supplementary Figure 11A). *ATG7*,

BECN1, and *ATG5* all demonstrated enriched binding similar to *PTGS2*, which was

confirmed as an IMP1 binding target in prior published studies (Manieri et al. 2012). As

both *ATG3* and *ATG5* were enriched in ribosome-profiling, *in silico* predictions, and *in*

vivo binding, we evaluated protein levels in crypts isolated from *Imp1$^{\Delta IEC}$* mice. We

observed increased Atg3 and Atg5 in *Imp1$^{\Delta IEC}$* colon epithelium compared to controls,

suggesting that IMP1 may directly affect protein levels of key components in the

autophagy pathway (Figure 17D). In addition, *in silico* analysis of individual transcripts

predicted binding of IMP1 to 5' UTRs of *ATG3* and *ATG5* (Supplementary Figure 11B,

C) Taken together, we demonstrate via three independent methods that IMP1 binds

directly to specific autophagy transcripts required early in the autophagy cascade,

suggesting direct binding as one mechanism by which IMP1 regulates the autophagy pathway during homeostasis.

Discussion

In the current study, we describe a new role for the RBP IMP1 to regulate homeostasis in intestinal/colonic epithelium. We demonstrate that IMP1 is upregulated in Crohn's disease patients and that *Imp1* loss leads to enhanced repair following damage *in vivo*. Unbiased and phenotypic data revealed a mechanistic relationship between IMP1 and the autophagy pathway, underscoring post-transcriptional regulation as an additional layer of gut epithelial response to stress. Prior *in vivo* studies have implicated IMP1's critical role in development, and we and others have demonstrated diverse roles for IMP1 in cancer (Hansen et al. 2004; Hamilton et al. 2013; Hamilton et al. 2015). The present study is the first to uncover *in vivo* mechanisms for IMP1 during homeostasis. IMP1-containing RNP granules are localized around the nucleus and in cellular projections, containing mRNAs representing up to 3% of the transcriptome in HEK293 cells. These granules contain significant enrichment of transcripts encoding proteins involved in ER quality control, Golgi, and secretory vesicles, consistent with our finding that alterations in IMP1 affect the autophagy pathway (Jonson et al. 2007). While the functional roles of autophagy are context-dependent, the regulation of autophagy itself is an emerging field of investigation. Interplay between autophagy, homeostasis, and disease in the gut, as well as the associated regulatory cascades, may have important potential therapeutic implications as well.

In IECs, autophagy contributes to microbial handling through packaging and secretion of antimicrobial peptides by Paneth cells. Independent groups have demonstrated that mice with *Atg16l1* gene mutations are more sensitive to colitis or infection, exhibit increased serum IL-1β and IL-18, and display diffuse lysozyme staining

in Paneth cells (Cadwell et al. 2008; Saitoh et al. 2008; Cadwell et al. 2009; Matsuzawa-Ishimoto et al. 2017; Burger et al. 2018; Pott et al. 2018). In addition, several recent studies revealed that autophagy genotype-phenotype associations may be used to sub-classify Crohn's patients (Rioux et al. 2007; VanDussen et al. 2014; Liu et al. 2016). Evaluation of *Imp1*$^{\Delta IEC}$ mice revealed diffuse lysozyme staining. Intriguingly, we found evidence of enhanced autophagy flux in these mice, suggesting that additional pathways may be altered in *Imp1*$^{\Delta IEC}$ mice. Recent studies by Bel *et al.* demonstrated that Paneth cells secrete lysozyme via secretory autophagy during bacterial infection through activation of DC-ILC3 circuit (Bel et al. 2017); however, it remains unclear whether secretory autophagy is engaged as a homeostatic mechanism. As such, it would be interesting to determine whether IMP1 may regulate Paneth cell secretory autophagy in future studies. While a role for autophagy in Paneth cells is reasonably understood, other crypt cells, including crypt base columnar stem cells, may rely upon the autophagy stress response for survival. In support of this notion, deletion of *Atg5* in all IECs except Paneth cells (using *Ah-Cre*) revealed impaired recovery after irradiation, underscoring Paneth cell-independent roles of autophagy in the gut (Asano et al. 2017). Our observation that *Imp1* is expressed in both *Lgr5+* and Paneth cells suggests a broader role for Imp1 than in Paneth cells.

The levels of functional regulation of autophagy include transcriptional (e.g. TP53, STAT3 and NFκB), posttranscriptional (via miRNAs), and posttranslational (phosphorylation, ubiquitination and acetylation) (Copetti et al. 2009; Yee et al. 2009; Lipinski et al. 2010; Feng et al. 2015; Jing et al. 2015). To date, autophagy regulation by RBPs autophagy is largely unexplored. Recently, the Dhh1 mRNA decapping regulator and its mammalian homolog DDX6 were implicated as repressors of autophagy through direct modulation of LC3 transcript stability (Hu et al. 2015). This supports the premise that while autophagy activation is beneficial for cellular response to stress, post-

transcriptional repressors may play a critical role in attenuating autophagy to prevent prolonged activation. Our biochemical data suggest that IMP1 may represent a new post-transcriptional modulator of the autophagy pathway, acting as an "autophagy rheostat" in intestinal/colonic epithelium (Figure 18). IMP1 binds to and regulates the fate of target transcripts; in part via binding to different mRNA regions. Early biochemical studies demonstrated IMP1 binding to the 5′ UTR of the translationally regulated IGF-II leader 3 mRNA, leading to translational repression (Nielsen et al. 1999). More recently, IMP1 was demonstrated to bind primarily to 3'UTRs at the region-level (Conway et al. 2016). Our finding that IMP1 is predicted to bind to 5' UTRs of autophagy transcripts supports the model whereby IMP1 may bind to and repress the translation of pivotal autophagy transcripts.

Finally, our studies evaluating direct binding of IMP1 to autophagy mRNAs may lay the foundation for development of new therapies to selectively modulate autophagy (Kuo et al. 2015; Hooper et al. 2016). Indeed, it is feasible to identify small molecule inhibitors to disrupt IMP1 interactions with specific mRNA targets, permitting specific modulation of a desired pathway without disrupting other important functional roles (Mahapatra et al. 2014). What remains unknown are the upstream signaling pathways that may determine the fate of IMP1-bound transcripts (stabilization versus degradation) within specific contexts, as well as the ability of specific sequence motifs to confer IMP1 target specificity for autophagy (or other) transcripts. In addition, the role for cooperation between IMP1 and microRNAs to elicit specific phenotypes, including effects on autophagy, remain to be determined (Elcheva et al. 2009). In summary, the current study reveals that IMP1 may function as a mediator of homeostasis by regulating autophagy in gut epithelial cells. More broadly, these studies underscore the importance of evaluating post-transcriptional contributions to gastrointestinal homeostasis and disease.

Figures and Figure legends

Figure 12: IMP1 is upregulated in adult and pediatric Crohn's disease patients

Gene Name	Log Fold Change	p-Value
Igf2bp1	2.114	1.65E-10
Igf2bp2	0.313	0.142
Igf2bp3	-0.455	0.309

n=180 ileal CD and 43 non-IBD controls
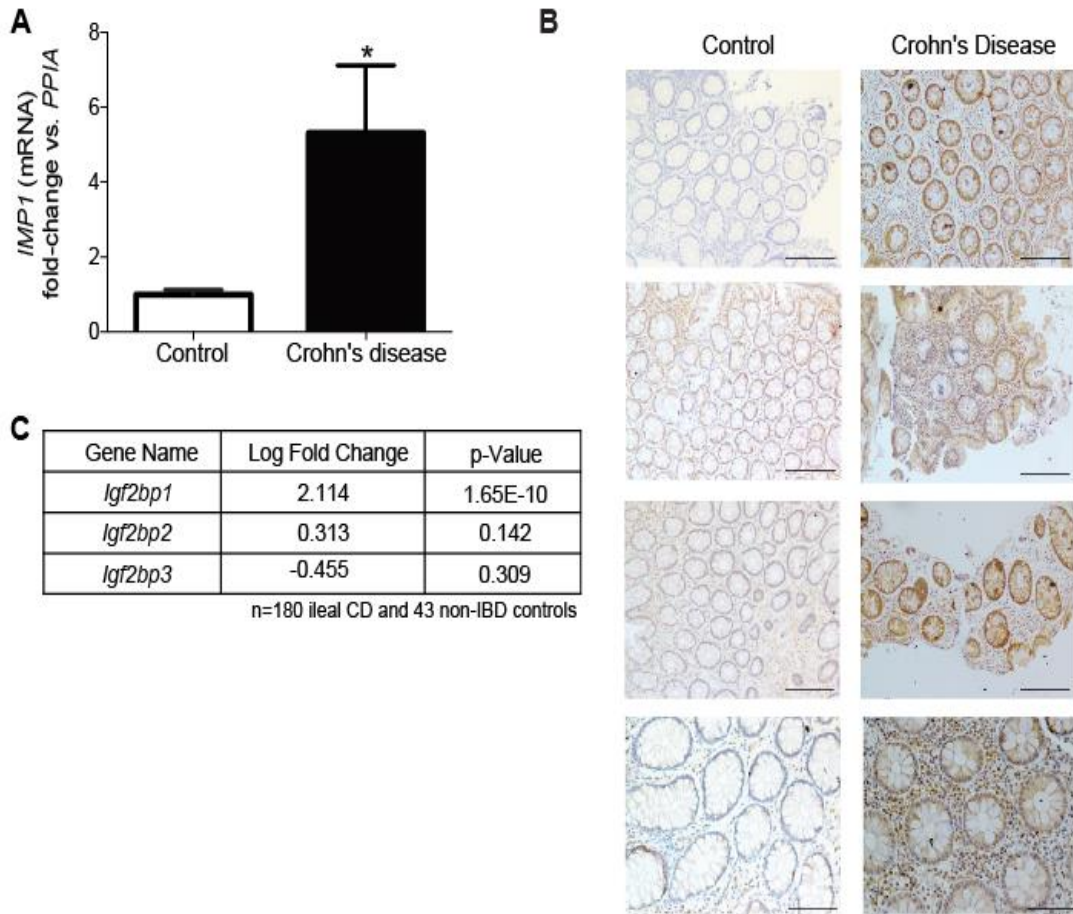
A. qPCR analysis for *IMP1* expression in colon biopsy samples from adult Crohn's disease (CD) patients. *IMP1* expression is >5 fold higher in CD samples (5.314 ± 1.807, n=8) as compared to control samples (1 ± 0.1245, n=7). **B**. Representative immunohistochemistry demonstrating IMP1 expression in colon biopsy samples from CD patients and normal adults. IMP1 expression is higher in CD samples (Scale bars = 500µm). **C**. Differential gene expression analysis of pediatric CD patient colon samples (n=180) show increased (>4 fold) *IMP1* expression as compared to non-inflammatory bowel disease (IBD) (n=43) pediatric samples. (All data are expressed as mean ± SEM.

*, p < 0.05; **, p < 0.01; ***, p < 0.001; ****, p < 0.0001 by ordinary one-way ANOVA test or standard t-test).

Figure 13: Mice with intestinal epithelial cell deletion of *Imp1* exhibit increased recovery following colitis
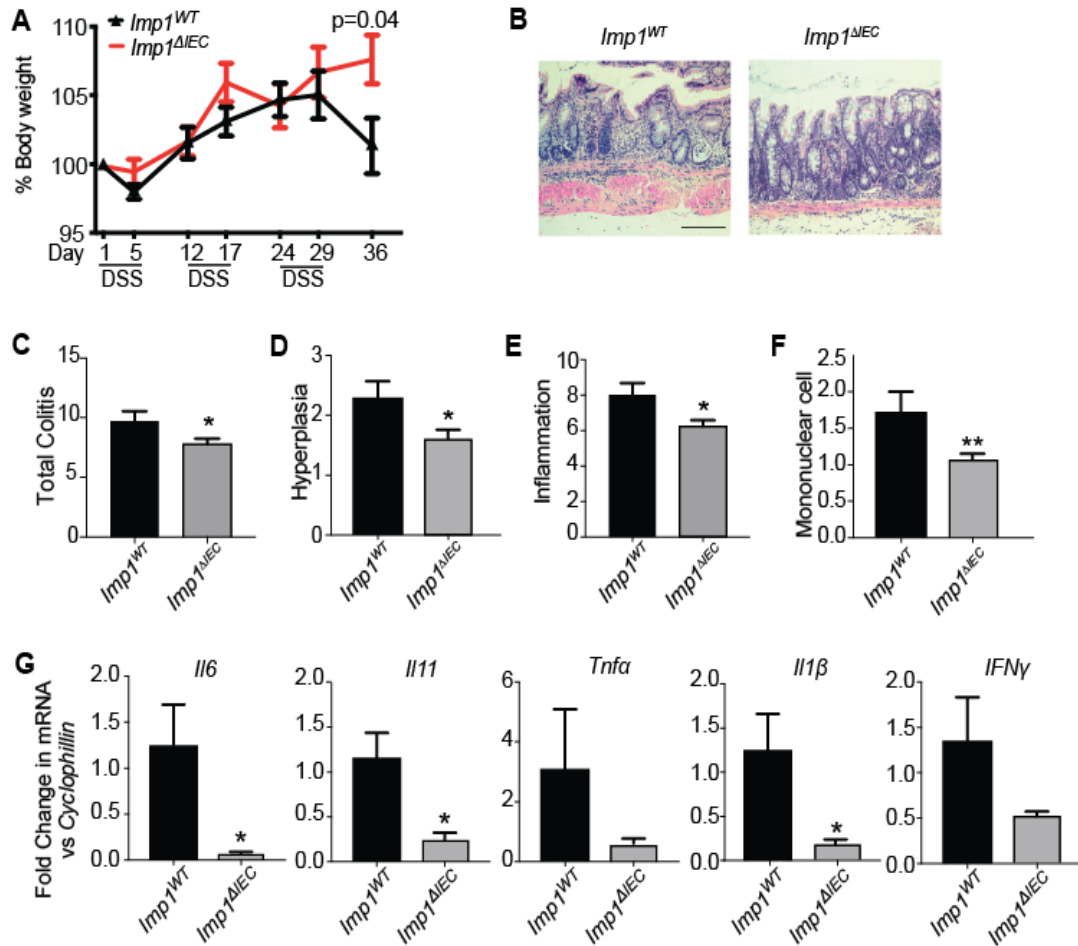
A. Mice were given 3 cycles of 2.5% DSS in drinking water for 5 days followed by a week of recovery. Mice with *Imp1* deletion lost significantly less weight as compared to controls at day 36. B. Representative H&E pictures of *Imp1^WT^* and *Imp1^ΔIEC^* mice at day 36 after chronic DSS treatment (Scale bars = 500μm). C. *Imp1^ΔIEC^* mice show significantly less total colitis (7.769 ± 0.4824, n=13; As scored blinded by a pathologist) as compared to *Imp1^WT^* mice (9.714 ± 0.8371, n=7). D. *Imp1^ΔIEC^* mice show significantly less hyperplasia (1.615 ± 0.1404, n=13) as compared to *Imp1^WT^* mice (2.286 ± 0.2857, n=7). E. *Imp1^ΔIEC^* mice show significantly less inflammation score (6.231 ± 0.3608, n=13) as compared to *Imp1^WT^* mice (8 ± 0.6901, n=7). F. *Imp1^ΔIEC^* mice show significantly less

mono-nuclear cell infiltration (1.077 ± 0.076, n=13;) as compared to $Imp1^{WT}$ mice (1.714

± 0.2857, n=7). **G**. qPCR data showing expression of different cytokines in colon

epithelium of $Imp1^{WT}$ and $Imp1^{\Delta IEC}$ mice at day 36 after chronic DSS treatment. (All data

are expressed as mean ± SEM. *, $p < 0.05$; **, $p < 0.01$; ***, $p < 0.001$; ****, $p < 0.0001$

by ordinary one-way ANOVA test or standard t-test).

Figure 14*: IMP1 **knockout reveals global changes in the "translatome"**
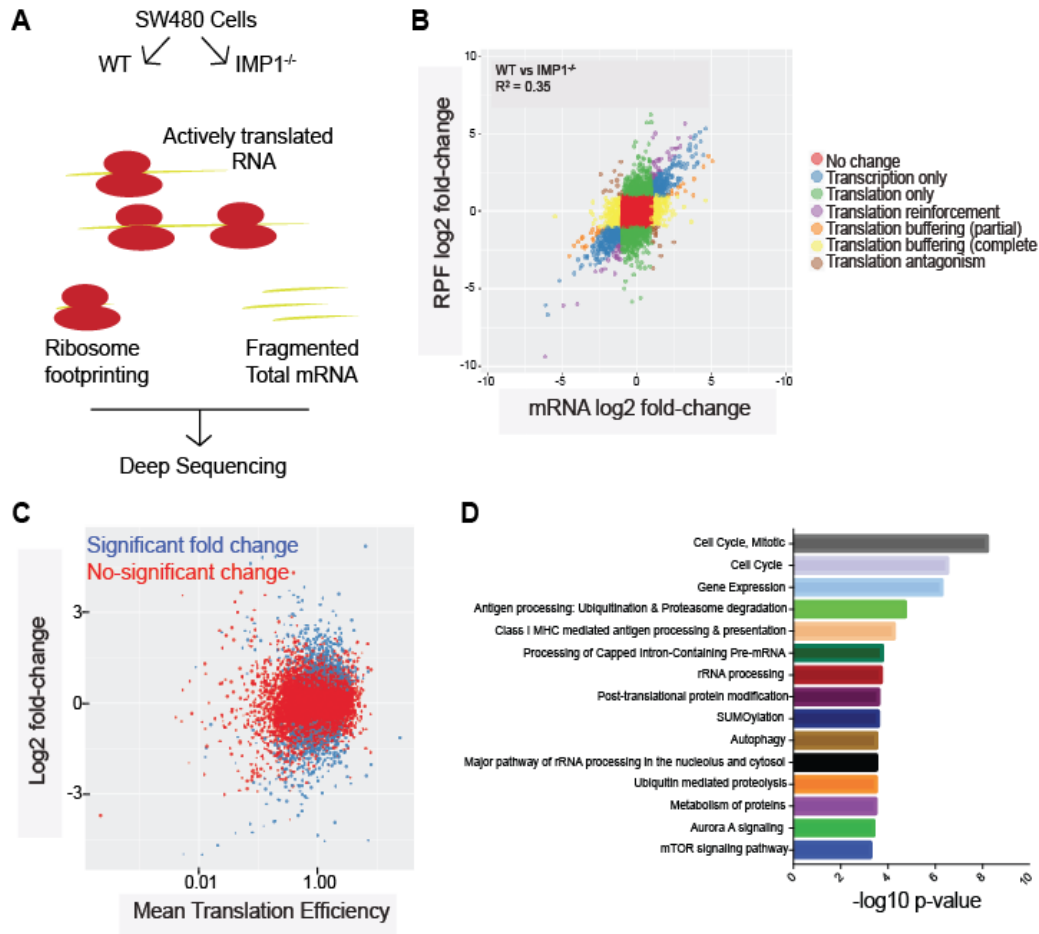
A. Simplistic schematic of ribosome profiling technique. **B**. Scatterplot of differential expression between SW480 cells with and without *IMP1* deletion. The log2 fold change between ribosome-bound RNAs (ribosome protected fragments, or RPF) and total mRNA is plotted. The plot indicates that IMP1 regulates both mRNA abundance and translation. **C**. Scatterplot of genes with significant (in blue) differential translational efficiencies between SW480 cells with and without *IMP1* deletion. Translation efficiencies of transcripts are calculated as the ratio of reads of ribosome-protected fragments to the reads in total mRNA abundance. **D**. Pathway analysis using Toppgene

gene enrichment analysis software of differentially expressed genes from **C** to define

which signaling/effector pathways are enriched with *IMP1* deletion.

Figure 15: Mice with *Imp1* loss exhibit morphological changes in Paneth cells and enhanced autophagy
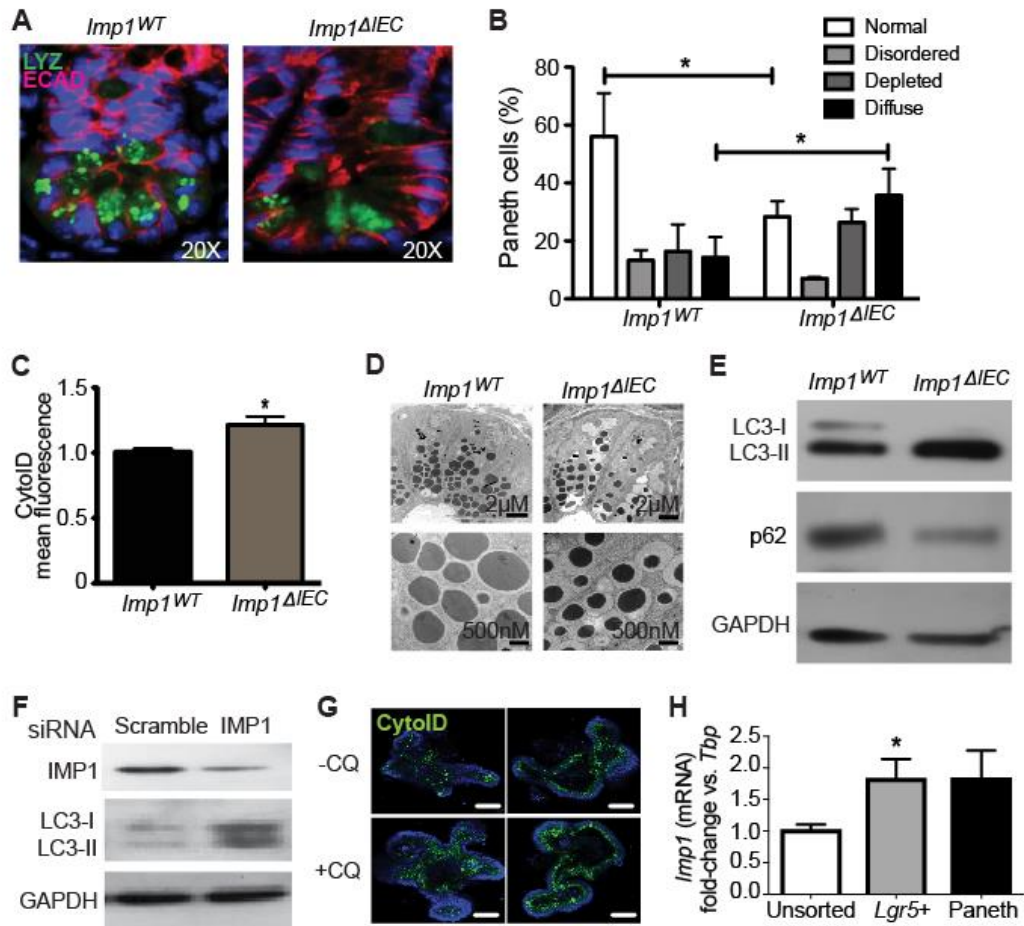
A. Paneth cells from *Imp1^{WT}* and *Imp1^{ΔIEC}* mice were evaluated histologically using IF for lysozyme (LYZ). E-cadherin (ECAD) staining was used to demarcate individual epithelial cells. Note presence of diffuse lysozyme staining in *Imp1^{ΔIEC}* mice. **B**. Published lysozyme scoring was utilized to evaluate specific Paneth cell phenotypes. *Imp1^{ΔIEC}* mice exhibit a significant shift from normal to diffuse lysozyme phenotype (n= 4 mice per genotype). **C**. Live cell staining of autophagic structures with the cationic amphiphilic tracer dye CytoID indicated a significant increase in autophagic vesicles in crypts from *Imp1^{ΔIEC}* mice (n=8) compared to *Imp1^{WT}* mice (n= 7) using flow cytometry. **D**. Transmission electron microscopy revealed an abundance of small, electron dense

granules in $Imp1^{\Delta IEC}$ mice. **E**. To confirm a direct role for IMP1 knockdown to induce autophagy, we evaluated epithelial cells from colon in $Imp1^{WT}$ and $Imp1^{\Delta IEC}$ mice. This confirmed a robust increase in LC3 and decrease in p62, which together indicate enhanced flux. Blots are representative of 3 independent experiments. **F**. Caco2 cells transfected with IMP1 siRNA demonstrated a robust increase in LC3-I/LC3-II indicating enhanced flux. Blots are representative of 3 independent experiments. **G**. Crypt enteroid cultures from $Imp1^{WT}$ and $Imp1^{\Delta IEC}$ mice were treated with the autophagy inhibitor chloroquine (CQ) for 3 hours and then stained with CytoID to evaluate autophagy flux, where increased CytoID puncta with CQ treatment represents active flux. There was a modest increase in basal CytoID in $Imp1^{\Delta IEC}$ enteroids compared to controls, as seen with FACS analysis of isolated crypts from $Imp1^{\Delta IEC}$ mice in **C**, and both genotypes exhibited an increase in CytoID puncta with CQ treatment. **H**. qPCR for $Imp1$ expression in $Lgr5+$ and Paneth (CD24/cKit/SSC high) cells sorted from $Lgr5\text{-}eGFP\text{-}IRES\text{-}CreERT2$ mouse crypt epithelium. (All data are expressed as mean ± SEM. *, $p < 0.05$; **, $p < 0.01$; ***, $p < 0.001$; ****, $p < 0.0001$ by ordinary one-way ANOVA test or standard t-test).

Figure 16*: Genetic deletion of *Atg7* reverses the *Imp1^{ΔIEC}* phenotype during colitis
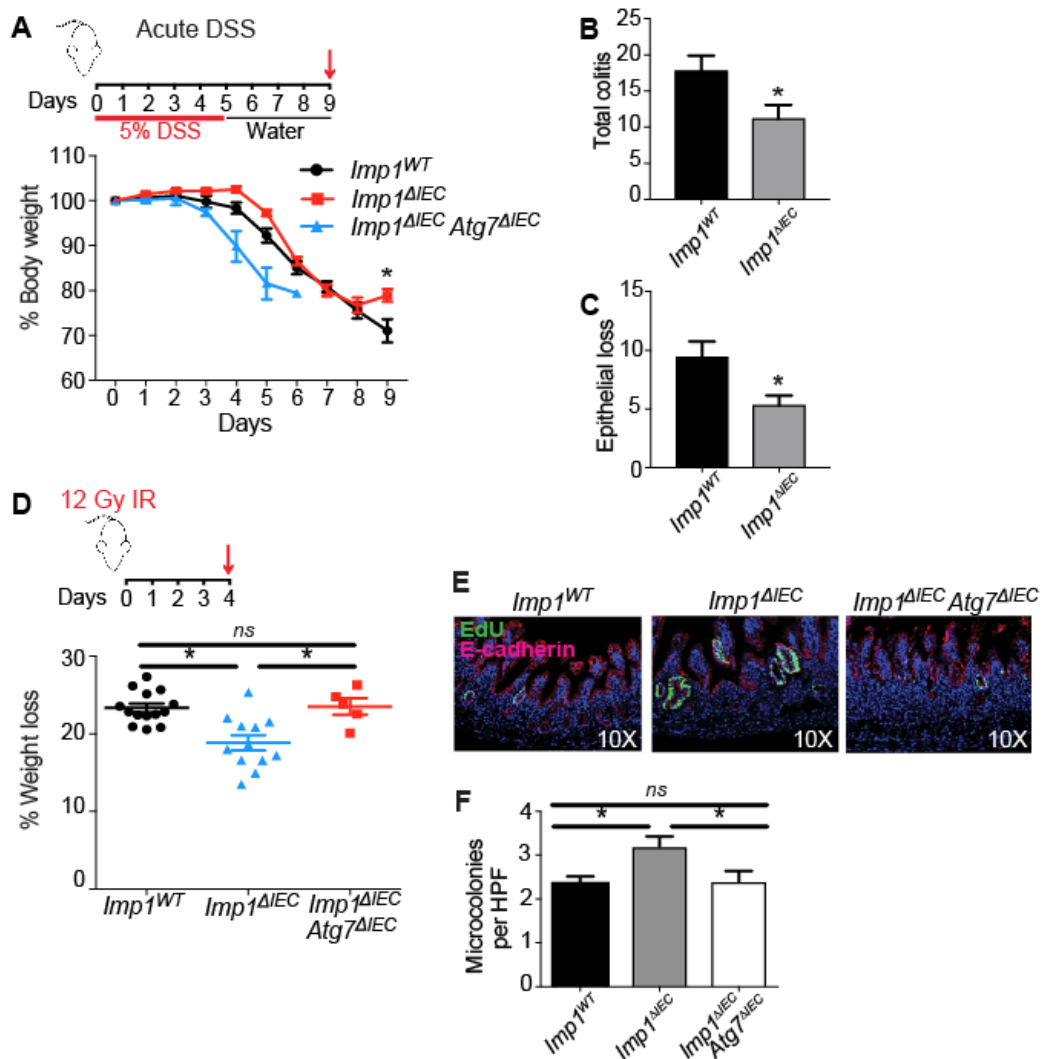
A. Mice were given 5% DSS in drinking water for 5 days followed by 4 days of recovery. Mice with *Imp1* deletion lost significantly less weight as compared to controls. *Imp1^{ΔIEC}Atg7^{ΔIEC}* mice lost weight and became moribund more rapidly than *Imp1^{WT}* and *Imp1^{ΔIEC}* mice, requiring sacrifice prior to the recovery period. **B**. *Imp1^{ΔIEC}* mice show significantly less total colitis (11.14 ± 1.933, n=7; As scored blinded by a pathologist) as compared to *Imp1^{WT}* mice (17.75 ± 2.144, n=8). **C**. *Imp1^{ΔIEC}* mice show significantly less epithelial loss (5.286 ± 0.865, n=7) as compared to *Imp1^{WT}* mice (9.375 ± 1.375, n=8). **D**. *Imp1* deletion confers protective effects following irradiation, which is reversed in the

context of *Atg7* deletion. *Imp1*$^{\Delta IEC}$ mice lost significantly less weight at sacrifice following irradiation than controls (18.83 ±0.98% in *Imp1*$^{\Delta IEC}$ mice(n=12*)* versus 23.34 ±0.56% mean weight loss in controls (n=14)*.* This phenotype was abrogated in *Imp1*$^{\Delta IEC}$*Atg7*$^{\Delta IEC}$ mice (23.5±1.05% mean weight loss, n=5). For untreated animals, there was no significant difference in mean body weights between groups (not shown). **E&F**. Analysis of EdU+, S-phase cells revealed similar staining in all non-IR mice; however, there was a robust increase in EdU+ regenerative crypt foci at 4 days following irradiation in *Imp1*$^{\Delta IEC}$ mice compared to *Imp1*^{WT} mice, and this effect was abolished in *Imp1*$^{\Delta IEC}$*Atg7*$^{\Delta IEC}$ mice (n=4 mice per genotype, 20-30 HPF per animal).(All data are expressed as mean ± SEM. *, $p < 0.05$; **, $p < 0.01$; ***, $p < 0.001$; ****, $p < 0.0001$ by ordinary one-way ANOVA test or standard t-test).
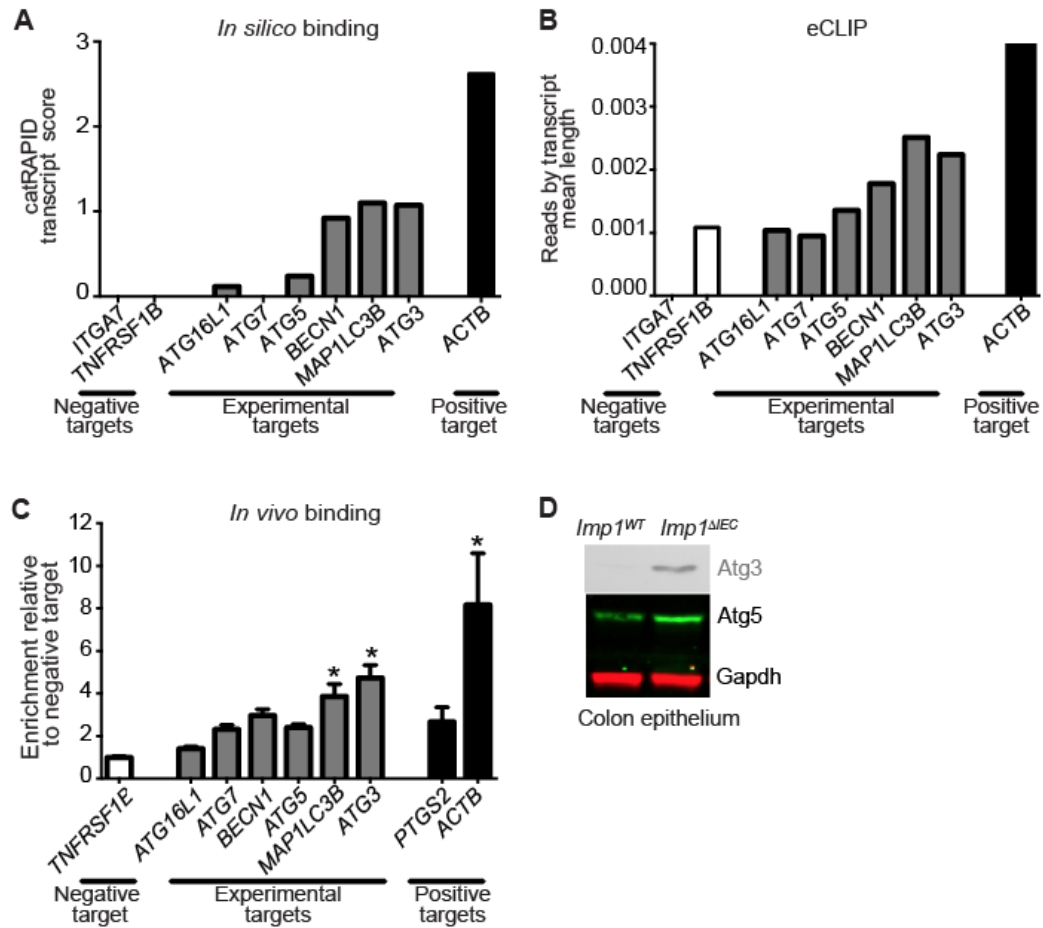
Figure 17: IMP1 directly binds autophagy mRNAs.

We utilized computational predictions, analyses of published CLIP-Seq data and ribonucleoprotein-immunoprecipitation (RIP) to identify direct interactions between IMP1 and autophagy transcripts. **A**. catRAPID Transcript Score. For each predicted transcript, we measured the IMP1 interaction propensity with respect to the negative control IgG. Negative targets (ITGA7 and TNFRSF1B) were also evaluated. **B**. We retrieved CLIP scores from published eCLIP data against the same set of autophagy-related transcripts analyzed in **A** and found a strong correlation between catRAPID scores and eCLIP data (r =0.9838465 Pearson correlation coefficient). The CLIP data scores were calculated as total number of reads corresponding to the transcript divided by the length of the

different isoforms. **C**. We evaluated binding of endogenous IMP1 to autophagy transcripts using RIP assays in Caco2 cells. Specific enrichment of IMP1 was confirmed by IP with either IMP1 or control IgG antibodies followed by western blot for IMP1. Enrichment of target transcripts over control is represented relative to negative target, TNFRSF1B. Positive controls were PTGS2 and ACTB. vs. negative target by 1-way ANOVA. n=3 independent experiments. **D**. Representative western blot showing upregulation of Atg3 and Atg5 in colon epithelium of $Imp1^{\Delta IEC}$ mice as compared to controls. (All data are expressed as mean ± SEM. *, $p < 0.05$; **, $p < 0.01$; ***, $p < 0.001$; ****, $p < 0.0001$ by ordinary one-way ANOVA test).

Figure 18: Model for IMP1 modulation of intestinal epithelial homeostasis.
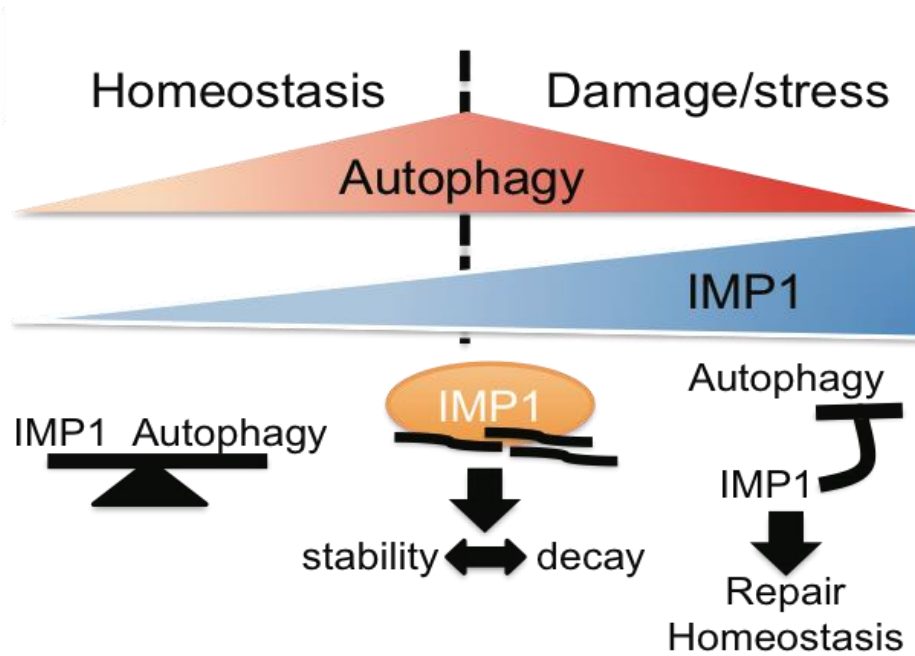
Schematic depicts proposed model for IMP1 function during homeostasis, where IMP1 binds autophagy transcripts and represses their translation post-challenge in order to return to baseline epithelial homeostasis.

Supplementary Figures

Supplementary Figure 7
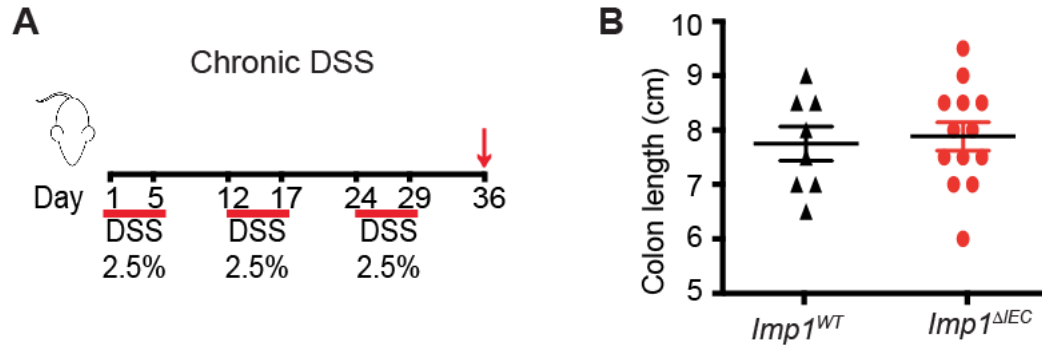
A. Schematic showing the chronic DSS experimental protocol. **B**. The colon lengths of

*Imp1^WT^* and *Imp1^ΔIEC^* mice showed no significant difference following chronic DSS.

Supplementary Figure 8
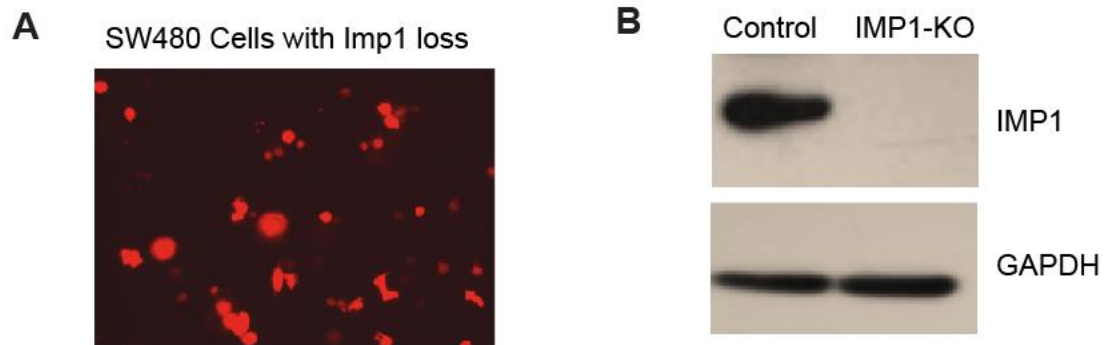
A. SW480 cells with RFP expression following incorporation of HDR plasmid after

CRISPR transfection. **B**. Representative western blot showing complete IMP1 deletion in

SW480 cells after CRISPR transfection.
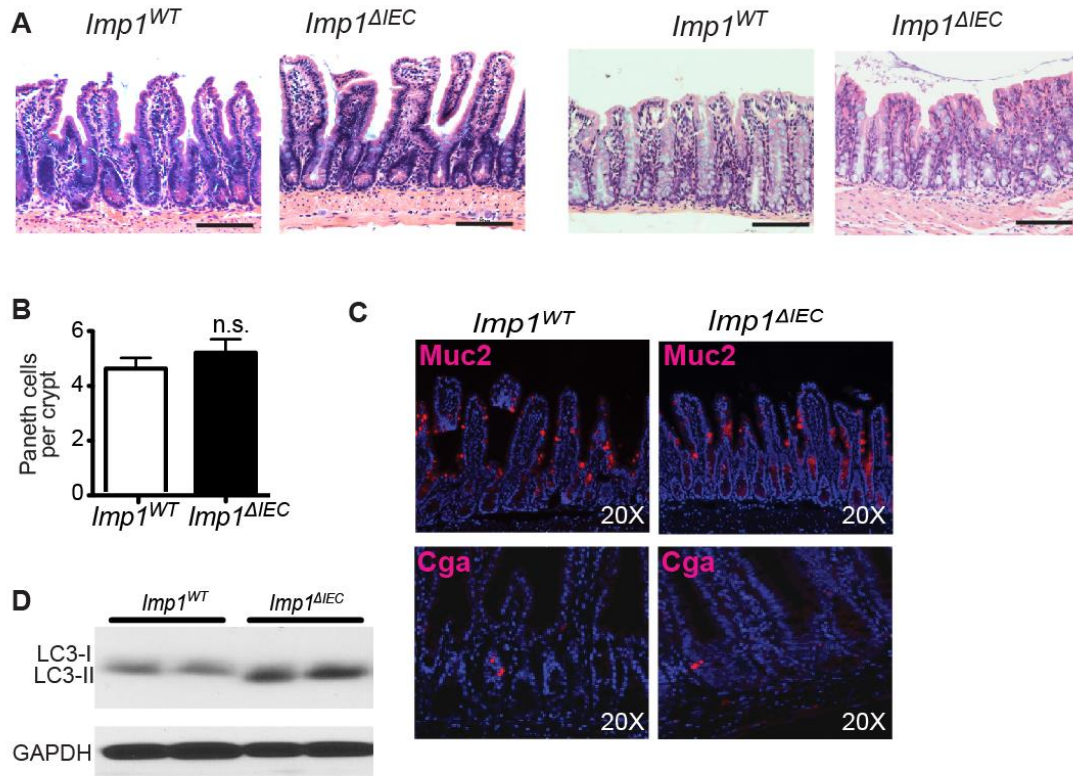
A. Representative H&E sections showing no overt morphological differences between the small intestine and colon in *Imp1^WT^* and *Imp1^ΔIEC^* mice. **B**. Quantification of Paneth cell number shows no differences between *Imp1^WT^* and *Imp1^ΔIEC^* mice. **C**. Representative immunofluorescence staining showing no differences in goblet cells (Muc2+) or enteroendocrine cells (Chromagranin+) between *Imp1^WT^* and *Imp1^ΔIEC^* mice. **D**. Western blot for LC3-I/LC3-II in isolated crypts from *Imp1^WT^* and *Imp1^ΔIEC^* mice revealed an increase in LC3 indicating increased autophagy flux. (n= 3 mice per genotype)

Supplementary Figure 10
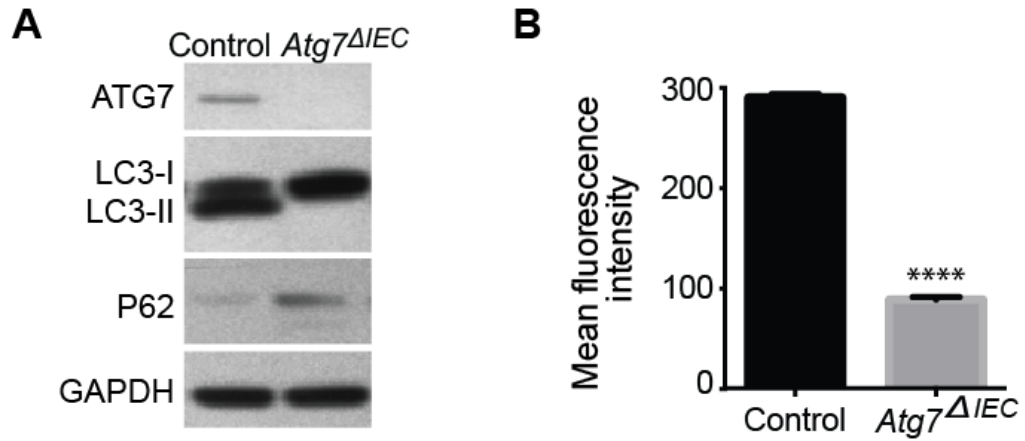
A. Representative western blot comparing $Atg7^{\Delta IEC}$ mice and controls. $Atg7^{\Delta IEC}$ mice show no ATG7 expression and decreased autophagic flux indicated by increased p62 and no LC3-II levels. **B**. Mean fluorescence intensity of CytoID is significantly reduced in epithelial cells from $Atg7^{\Delta IEC}$ mice indicating significantly decreased autophagy.

Supplementary Figure 11
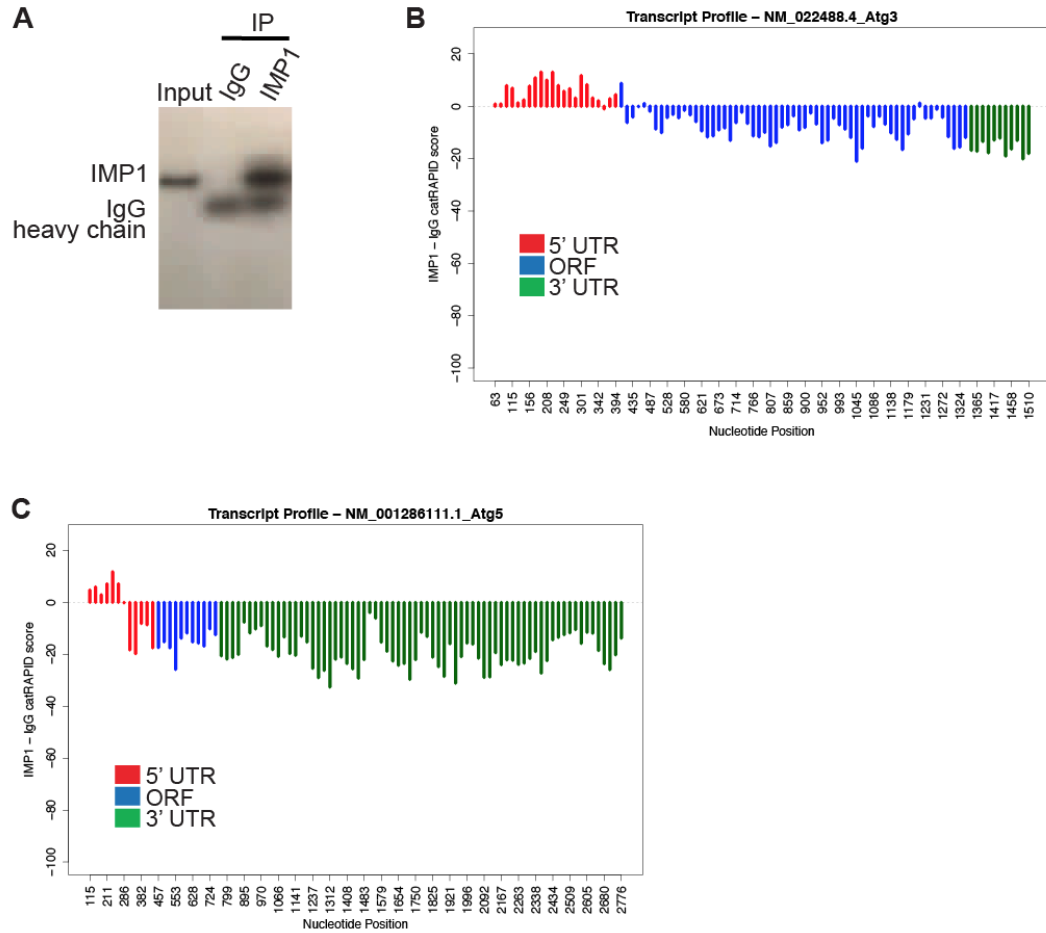
We evaluated binding of endogenous IMP1 to autophagy transcripts using RIP assays in Caco2 cells. **A.** Specific enrichment of IMP1 was confirmed by IP with either IMP1 or control IgG antibodies followed by Western blot for IMP1. Blot is representative of 3 independent experiments. **B, C.** CatRAPID plots show the binding propensity along the isoform sequence for *ATG3* and *ATG5.* Key: 5' UTRs in red, ORFs in blue and 3'UTRs in green.

Materials and methods

Human samples

Frozen colon tissue and FFPE samples from adult normal and Crohn's patients were obtained from the Cooperative Human Tissue Network (CHTN) via the University of Pennsylvania Center for Molecular Studies in Digestive and Liver Diseases Molecular Biology and Gene Expression Core. RNA was extracted from frozen tissue using Trizol (Thermo Fisher, Waltham, MA). Publicly available RNA-sequencing data from the RISK cohort of pediatric ileal Crohn's (Haberman et al. 2014) was evaluated for differential expression of IGF2BP1 (IMP1), IMP2, and IMP3. Sequenced reads were trimmed using Trim Galore! (version 0.4.4), and aligned to the GRCh37 reference genome using STAR, version 2.5.3a. Uniquely mapped reads were quantified by Ensembl gene IDs using featureCounts from Subread version 1.6.0. Lowly or unexpressed genes were removed from the analysis if they showed less than 2 counts per million in less than 5 samples across all conditions. Read counts were transformed with voom and evaluated for differential expression using limma.

Animals

Mice were cared for in accordance with University Laboratory Animal Resources requirements under an Institutional Animal Care and Use Committee-approved protocol. *VillinCre;Imp1-floxed* (*Imp1$^{\Delta IEC}$*) mice were generated previously (Hamilton et al. 2013) and maintained on a C57Bl/6 background. Control mice had floxed, intact alleles (*Imp1^{WT}*). Male and female mice were both used at 8-12 weeks. *Lgr5-EGFP-IRES-creERT2* mice were purchased from Jackson Laboratories. *Atg7-floxed* mice were kindly provided by RIKEN BRC through National Bio-Resource Project of MEXT, Japan (Komatsu et al. 2005). Mice were housed in specific pathogen-free conditions and fed standard, irradiated chow and water *ad libitum*.

Co-housed control and experimental genotypes were randomized at weaning across multiple cages. Mice were given 2.5% dextran sodium sulfate (40,000-50,000

kDa molecular weight; Affymetrix CAS 9011-18-1) in drinking water for chronic (Figure S1) or 5% DSS for acute colitis (Figure 5). For irradiation experiments, animals were given a single dose of 12Gy using Gammacell 40 Cesium 137 Irradiation Unit. Mouse jejunum was analyzed for irradiation experiments. During all experiments, body weights were recorded daily, and mice were euthanized before losing a maximum of 25% total body weight. Histological scoring was performed blinded by expert veterinary pathologist Enrico Radaelli according to published protocols (Washington et al. 2013). Sample sizes were determined based upon the investigators' prior experience with specific models (KEH, GDW).

Ribosome profiling

Ribosome profiling libraries from 3 pooled cell culture plates were prepared using a standard protocol (McGlincy and Ingolia 2017), with minor modifications. Separate 5' and 3' linkers were ligated to the RNA-fragment instead of 3' linker followed by circularization (Subtelny et al. 2014). 5' linkers contained 4 random nt unique molecular identifier (UMI) similar to a 5 nt UMI in 3' linkers. During size-selection, we restricted the footprint lengths to 18-34 nts. Matched RNA-seq libraries were prepared using RNA that was randomly fragmentation by incubating for 15 min at 95C with in 1 mM EDTA, 6 mM Na_2CO_3, 44 mM $NaHCO_3$, pH 9.3. RNA-seq fragments were restricted to 18-50 nts. Ribosomal rRNA were removed from pooled RNA-seq and footprinting samples using RiboZero (Epicenter MRZH116). cDNA for the pooled library were PCR amplified for 15 cycles. RNA-seq and footprinting reads were mapped to the human transcriptome using the riboviz pipeline (Oana Carja 2017b).

Autophagy analyses

CytoID Autophagy Detection Kit (Enzo Life Sciences) was used to stain single cell suspensions of crypt-enriched intestinal epithelium (1:100 in DPBS supplemented with 10% FBS at 37°C for 30 min) and co-stained with DAPI. Flow cytometry was performed using FACSCanto or LSR II cytometers (BD Biosciences) and FlowJo software (Tree Star). Unstained cells from each specimen were utilized to establish background fluorescence. The percent of CytoID-positive cells was determined in the live cell fraction (DAPI-negative). The geometric mean fluorescence intensity for live cells was determined for each specimen following subtraction of background fluorescence. Blinded scoring was utilized (KAW) [75, 76]. Enteroids were passaged 1 day prior to assays in order to obtain equivalent plating densities. Three hours prior to imaging, 2 μg/ml CytoID and 2 μg/ml Hoechst33342 (ENZO Life Science) were added in the medium and incubated at 37°C for 3 hours. 120 μM of chloroquine (ENZO Life Science) was used. Enteroids were immediately analyzed using confocal microscopy ECLIPSE Ti (Nikon). Six to ten enteroids per mouse were analyzed across three mice per genotype (blinded, RM).

catRAPID analyses

We used the *cat*RAPID *fragment* approach (Bellucci et al. 2011; Cirillo et al. 2013) to predict IMP1 binding to autophagy-related transcripts (i.e.: *MAP1LC3B, ATG3, BECN1, ATG5, ATG16L1* and *ATG7*). *ACTB* and *TNFRSF1B/ITGA7* were also included as positive and negative controls, respectively. In our analysis, we included different isoforms for each transcript, for a total of 25 different targets, including the positive and negative controls (http://s.tartaglialab.com/page/catrapid_group).

Transcript Score

Given a transcript isoform r_i, we used catRAPID *uniform fragmentation* to generate j overlapping fragments that cover the entire sequence. The fragments $r_{i,j}$ are then used to compute *cat*RAPID interacting propensies with IMP1 and IgG (negative control). We define the *interaction threshold* $q(r_i)$ as the highest interaction propensity score that IgG has with the j fragments generated from sequence r_i:

$$q(r_i) = \max_j [\rho(p = \text{IgG}, r = r_{i,j})]$$

(1)

For every IMP1 interaction with fragments, we computed the *normalized interaction* ρ' by subtracting the interaction threshold of the corresponding transcript to the *cat*RAPID interaction score.

$$\rho'(p = \text{IMP1}, r = r_{i,j}) = \rho(p = \text{IMP1}, r = r_{i,j}) - q(r_i))$$

(2)

Fragments with normalized interaction score $\rho' > 0$ are predicted to interact with IMP1. The *Isoform Score* of each isoform P_i (Fig. S4*A*) is computed as the average normalized interaction score of interacting fragments $\rho' > 0$ over the total number of fragments $n(i)$:

$$\Pi_i = \frac{1}{n(i)} \sum_j^{n(i)} \pi'(p = \text{IMP1}, r = r_{i,j}) \quad \forall \; j : \pi'(p = \text{IMP1}, r = r_{i,j}) > 0$$

(3)

We define the *Transcript Score* P_r (Fig. 5*A*) as a global interaction propensity of all isoforms belonging to a certain transcript. The *Transcript Score* is defined as the average of the Isoform Scores for all the isoforms analyzed for each transcript:

$$\Pi_r = \frac{1}{N(r)} \sum_i^{N(r)} \Pi_i$$

,

(4)

where $N(r)$ is the number of isoforms considered for each transcript.

Statistical analyses

Applying unpaired, two-tailed student's t-tests or 1-way ANOVA, with $P < 0.05$ as statistically significant, determined statistical significance of comparisons between control and experimental conditions unless otherwise noted in the figures legends. For all analyses, unless noted otherwise, data from a minimum of three experiments are presented as mean ± standard error. Sample sizes for individual experiments, including biological and technical replicates, are described in each figure legend, as well as number of experimental replicates.

Supplementary Methods

Cell lines

Human colon cancer cell line Caco2 (ATCC HTB-37) cells were obtained from ATCC, which provides STR authentication, within the past 18 months. Cells are tested for mycoplasma at least every 3 months. *IMP1* siRNA (h) (Santa Cruz, sc-40694) or Silencer® Select Negative Control No. 1 siRNA (Thermo Fisher Scientific, 4390843) was transfected in CaCo2 cells using Lipofectamine® RNAiMAX (Thermo Fisher Scientific,

13778075). *IMP1* was deleted in SW480 cells (ATCC® CCL-228™) by co-transfecting cells with IMP1 CRISPR/Cas9 KO Plasmid (h) (Santa Cruz; sc-401703) and IMP-1 HDR Plasmid (h) (Santa Cruz ; sc-401703 HDR) followed by sorting and clonal expansion of RFP+ve cells. Knockout was verified by western blotting for IMP1.

Histology

Small intestines were fixed in 10% formalin, processed and paraffin-embedded. Immunofluorescence (IF) staining was performed using heat antigen-retrieval in citric acid buffer (pH 6.0) and staining with antibodies. 5-ethynyl-2′-deoxyuridine (EdU) staining was performed using Click-iT® EdU Alexa Fluor® 488 Imaging Kit (C10337) as per manufacturer's protocol. For IMP1 IHC, blocking was performed using Animal-Free Blocker (Vector Laboratories). For all staining, no-primary and/or biological negative controls (*Imp1$^{\Delta IEC}$*) were used. Lysozyme scoring was performed according to published protocols (Cadwell et al. 2008; Adolph et al. 2013). Scoring of EdU-positive "microcolonies", where a microcolony is defined by a cluster of ≥5 EdU-positive cells from a single clone, were quantified, blinded, across at least 30 high-powered fields per animal for a total of 4 mice per genotype.

qRT-PCR

Small intestine crypt RNA was isolated using GeneJet RNA purification kit (ThermoFisher). Equal amounts of total RNA were reverse-transcribed using Taqman RT Reagents kit and resulting cDNA used with Power SYBR Green PCR Master Mix (Applied Biosystems/ThermoFisher) or Taqman Fast Universal PCR Master Mix (Applied Biosystems/ThermoFisher) and validated primer sets. Non-reverse transcribed samples were used as no RT controls. Gene expression was calculated using $R = 2^{(-\Delta\Delta C_t)}$ method, where changes in C_t values for the genes of interest were normalized to housekeeping

genes. All experiments were replicated in at least 3 independent experiments with technical replicates (duplicates).

Western blot

Caco2 cells or isolated mouse epithelial cells were harvested in western lysis buffer, resolved in reducing conditions on 4% to 12% gradient gels, and detected with ECL Prime western Blotting Detection Reagent (Amersham; RPN2232). Western blots were reproduced in at least three independent experiments.

Flow cytometry

For analysis of sorted *Lgr5-EGFP* and Paneth cells, single cell suspensions of crypt-enriched intestinal epithelium from the entire small intestine of *Lgr5-EGFP* mice were stained on ice for 30 minutes with cKit-PE-Cy7 (1:10; eBioscience) and CD24-PE (1:10, Biolegend) to label Paneth cells. DAPI was used to exclude dead cells. Sorting was performed using a FACS Aria II (BD Biosciences) with a 100μm nozzle. Gating and compensation were performed using a negative and single-color controls. Intestinal stem cells were isolated based on *Lgr5-EGFP* positivity. Paneth cells were isolated as *Lgr5-EGFP*-negative/cKit-PE-Cy7-positive/CD24-PE-positive/side-scatter high. RNA from *Lgr5*-ISC, Paneth cells, and non-sorted cells was isolated using the RNAqueous®-Micro Total RNA Isolation Kit (ThermoFisher).

Transmission electron microscopy

Mouse small intestine tissues were fixed in cacodylate-buffered 2.5% (w/v) glutaraldehyde, post-fixed in 2.0% osmium tetroxide, then embedded in epoxy resin and ultrathin sections post-stained in the University of Pennsylvania Electron Microscopy Resource Laboratory. Images were obtained using Jeol-1010 transmission electron

microscope fitted with a Hamamatsu digital camera and AMT Advantage imaging software. A total of 4 mice per genotype were evaluated by two investigators for Paneth cell granule morphology (KEH and BJW) (Klionsky et al. 2016). Image contrast was enhanced equally in all TEM photos.

Ribonucleoprotein particle (RNP)-immunoprecipitation

RNP-immunoprecipitations (RIPs) were performed in Caco2 cells using the RiboCluster Prolifer™ RIP-Assay Kit (Medical & Biological Laboratories) according to manufacturer's instructions. Anti-IMP1 (MBL RN007P, which targets 561-577aa) or control IgG (supplied in kit) were used. Quality control samples for total protein and RNA input as well as immunoprecipitated proteins were evaluated for each experiment. Isolated RNA was reverse-transcribed as noted above and qPCR performed using the oligonucleotides. Raw Ct values from IMP1- and IgG- immunoprecipitated samples were used to determine "percent input" for each target, followed by dividing IMP1-immunoprecipitated signal by the respective IgG signal. Data for each individual target were then expressed as fold-enrichment relative to negative control target *TNFRSF1B*. Positive controls were previously identified IMP1 targets *ACTB and PTGS2* (Ross et al. 1997; Manieri et al. 2012). Three independent RIP experiments were performed.

CHAPTER IV: SUMMARY

IMP1 is expressed in proliferating cells and is upregulated during injury and disease in the intestinal epithelium

Igf2 mRNA binding protein 1 (IMP1) is an mRNA binding protein identified originally as a translational modulator of c-Myc, β-actin, and Igf2 mRNAs. IMP1 is expressed ubiquitously during development in mice but has low expression in adult tissues. In our studies, we used the *Sox9-EGFP* mice and *Lgr5-EGFP* mice to show that *Imp1* is expressed in the proliferating stem cell compartment in the mouse intestinal epithelium. It is not expressed in differentiated cells. Furthermore, we have shown via qPCR and western blots that IMP1 is upregulated during radiation injury in mice. IMP1 is also upregulated in CRC patient tumors as well as in biopsy samples from Crohn's disease patients. TCGA analysis further corroborates these findings as *Imp1* is upregulated in more than 80% of colorectal tumors.

IMP1 loss shows global changes in gene expression at the translation and transcription levels

To understand completely the functional effects of RBP expression or deletion, evaluation of the protein landscape is required. In recent years, ribosome footprint profiling (RFP) has been developed as a powerful tool to obtain a global snapshot of actively translating transcripts within a cell. This ribosome-centric technique uses binding and density of ribosomes on a transcript as an indicator of active translation. Profiling is done by deep sequencing of ribosome bound transcripts as well as sequencing total RNA abundance. This technique can help distinguish between genes regulated at the transcriptome and translatome levels. The ratio of RFP to total mRNA abundance for each transcript reveals the translation efficiency for that gene that can be compared across genotypes or conditions.

Our studies showed that IMP1 loss (both alone and in the context of LIN28B overexpression) showed gene expression changes at the transcription and translation levels. IMP1 loss regulates expression of genes involved in key signaling pathways such as Wnt signaling, TNF signaling, autophagy, cell cycle, mTORC signaling, etc. Hence, IMP1 is a key regulator of gene expression in the intestinal epithelium.

IMP1 loss is protective during injury

We used three different independent models to study the role of IMP1 loss in response to injury in mice with intestinal epithelial cell-specific *Imp1* deletion using the *Villin* promoter. The *VillinCre;Imp1^{fl/fl}* mice were subjected to the following three injury models : 12 Gy whole body radiation, 2.5% chronic DSS colitis and 5% acute DSS colitis. In all three models, *VillinCre;Imp1^{fl/fl}* mice showed significantly lower weight loss as compared to *Imp1^{fl/fl}* mice controls. The quantification of regenerating Ki67+ microcolonies showed significantly increased regeneration in the *VillinCre;Imp1^{fl/fl}* mice. Hence, IMP1 loss was protective in these latter mice. This could be due to the upregulation of Wnt signaling and autophagy in these mice. This is further evidenced by the finding that knocking out ATG7 in these *VillinCre;Imp1^{fl/fl}* mice rescues the protective phenotype in radiation and acute colitis models.

IMP1 loss increases LIN28B-mediated intestinal tumorigenesis

Our lab developed mice with LIN28b overexpression in the intestinal epithelial cells (*Vil-Lin28b).* The *Vil-Lin28b* mice develop adenomas and adenocarcinomas between 9-12 months of age. These lesions are typically invasive unifocal or multifocal adenocarcinomas. No adenomas or adenocarcinomas were found in age-matched wild-type littermates. Thus, Lin28b is sufficient to serve as an oncogene in the small intestine,

the first report of this type. This study elucidated the role of IMP1 downstream of LIN28B overexpression. IMP1 is upregulated with LIN28B upregulation and IMP1 serves as a principle node of gene expression. This study showed that mice with LIN28B overexpression and IMP1 loss (*Vil-Lin28b; VillinCre;Imp1*^{fl/fl}) in the intestinal epithelium showed unexpectedly a significant increase in tumor number and higher grade of tumors. This is in part due to an increase in Wnt signaling and stem cell signature in the intestinal epithelium of these mice. The *Vil-Lin28b; VillinCre;Imp1*^{fl/fl} mice are also protected against radiation injury as compared to *Vil-Lin28b mice.*

IMP1 overexpression does not initiate tumorigenesis *in vivo*

We find that *VillinCre;Imp1*[OE] mice do not exhibit spontaneous tumor initiation, suggesting that IMP1 overexpression is itself insufficient to drive tumor initiation. Furthermore, *Villin-Lin28b*; *VillinCre;Imp1*[OE] mice show no tumors at 12 months of age. To that end, it is possible that IMP1 overexpression may serve as a "brake" or "checkpoint" to the oncogenic effects of LIN28B. The "checkpoint" regulation may be achieved through a variety of mechanisms ascribed to IMP1, such as sequestration of transcripts in IMP1 containing RNP granules (Weidensdorfer et al. 2009) (Jonson et al. 2007) (to avoid mRNA degradation and/or release the transcripts for translation at critical time points), reduction of miRNA mediated silencing of mRNA transcripts (Elcheva et al. 2009; Nishino et al. 2013; Busch et al. 2016; Degrauwe et al. 2016a) (for review see (van Kouwenhove et al. 2011)), or displacing miRNA containing RISCs (Elcheva et al. 2009). IMP1 may also enhance the expression of LIN28B by shielding *LIN28B* mRNA from regulation by let-7 *in vitro* (Busch et al. 2016).

Future directions

To completely understand the function of any RBP in a cell, we need to understand what target transcripts it binds to, the context-dependent binding, and downstream effect(s) on transcription and translation of the transcript(s). To that end, combining CLIP-seq with ribosome profiling or proteomics would provide an even more complete functional snapshot for a given RBP. Since IMP1 binds to and regulates hundreds of genes, it is difficult to focus on specific genes that regulate functions downstream of IMP1, notwithstanding the importance of IMP1 in modulating Wnt signaling.

LIN28B and IMP1 exhibit low expression in most adult tissues, suggesting that targeting them may have few deleterious effects. Inhibitors for LIN28B would prevent aberrant blockade of tumor suppressor let-7, whereas a specific IMP1 inhibitor would require targeting of tumor-promoting interactions while sparing tumor suppressor functions. Additionally, our studies evaluate direct binding of IMP1 to several autophagy mRNAs. This may help lay the foundation for development of new therapies for the selective modulation of autophagy (Kuo et al. 2015; Hooper et al. 2016). Indeed, it may be feasible to identify small molecule inhibitors to disrupt IMP1 interactions with specific mRNA targets, permitting specific modulation of a desired pathway without disrupting other important functional roles (Mahapatra et al. 2014). Thus, the future may hold opportunities to translate the mechanistic and *in vivo* findings of this thesis into translational therapeutics through the employment of 3D enteroids and mouse models. This may provide a platform for testing in human clinical trials for colorectal cancer.

References / Bibliography

.

Adolph TE, Tomczak MF, Niederreiter L, Ko HJ, Bock J, Martinez-Naves E, Glickman JN, Tschurtschenthaler M, Hartwig J, Hosomi S et al. 2013. Paneth cells as a site of origin for intestinal inflammation. *Nature* **503**: 272-276.

Ambros V, Horvitz HR. 1984. Heterochronic mutants of the nematode Caenorhabditis elegans. *Science* **226**: 409-416.

Anders S, Pyl PT, Huber W. 2015. HTSeq--a Python framework to work with high-throughput sequencing data. *Bioinformatics* **31**: 166-169.

Asano J, Sato T, Ichinose S, Kajita M, Onai N, Shimizu S, Ohteki T. 2017. Intrinsic Autophagy Is Required for the Maintenance of Intestinal Stem Cells and for Irradiation-Induced Intestinal Regeneration. *Cell Rep* **20**: 1050-1060.

Ascano M, Hafner M, Cekan P, Gerstberger S, Tuschl T. 2012. Identification of RNA-protein interaction networks using PAR-CLIP. *Wiley Interdiscip Rev RNA* **3**: 159-177.

Balzeau J, Menezes MR, Cao S, Hagan JP. 2017. The LIN28/let-7 Pathway in Cancer. *Front Genet* **8**: 31.

Barker N, van Es JH, Kuipers J, Kujala P, van den Born M, Cozijnsen M, Haegebarth A, Korving J, Begthel H, Peters PJ et al. 2007. Identification of stem cells in small intestine and colon by marker gene Lgr5. *Nature* **449**: 1003-1007.

Barriga FM, Montagni E, Mana M, Mendez-Lago M, Hernando-Momblona X, Sevillano M, Guillaumet-Adkins A, Rodriguez-Esteban G, Buczacki SJA, Gut M et al. 2017. Mex3a Marks a Slowly Dividing Subpopulation of Lgr5+ Intestinal Stem Cells. *Cell Stem Cell* **20**: 801-816 e807.

Bel S, Pendse M, Wang Y, Li Y, Ruhn KA, Hassell B, Leal T, Winter SE, Xavier RJ, Hooper LV. 2017. Paneth cells secrete lysozyme via secretory autophagy during bacterial infection of the intestine. *Science* **357**: 1047-1052.

Bell JL, Wachter K, Muhleck B, Pazaitis N, Kohn M, Lederer M, Huttelmaier S. 2013. Insulin-like growth factor 2 mRNA-binding proteins (IGF2BPs): post-transcriptional drivers of cancer progression? *Cell Mol Life Sci* **70**: 2657-2675.

Bellucci M, Agostini F, Masin M, Tartaglia GG. 2011. Predicting protein associations with long noncoding RNAs. *Nat Methods* **8**: 444-445.

Bennett CG, Riemondy K, Chapnick DA, Bunker E, Liu X, Kuersten S, Yi R. 2016. Genome-wide analysis of Musashi-2 targets reveals novel functions in governing epithelial cell migration. *Nucleic Acids Res* **44**: 3788-3800.

Bernstein PL, Herrick DJ, Prokipcak RD, Ross J. 1992. Control of c-myc mRNA half-life in vitro by a protein capable of binding to a coding region stability determinant. *Genes Dev* **6**: 642-654.

Blanco FF, Preet R, Aguado A, Vishwakarma V, Stevens LE, Vyas A, Padhye S, Xu L, Weir SJ, Anant S et al. 2016. Impact of HuR inhibition by the small molecule MS-444 on colorectal cancer cell tumorigenesis. *Oncotarget* **7**: 74043-74058.

Bley N, Lederer M, Pfalz B, Reinke C, Fuchs T, Glass M, Moller B, Huttelmaier S. 2015. Stress granules are dispensable for mRNA stabilization during cellular stress. *Nucleic Acids Res* **43**: e26.

Bohjanen PR, Moua ML, Guo L, Taye A, Vlasova-St Louis IA. 2015. Altered CELF1 binding to target transcripts in malignant T cells. *RNA* **21**: 1757-1769.

Boyerinas B, Park SM, Shomron N, Hedegaard MM, Vinther J, Andersen JS, Feig C, Xu J, Burge CB, Peter ME. 2008. Identification of let-7-regulated oncofetal genes. *Cancer Res* **68**: 2587-2591.

Brennan CM, Steitz JA. 2001. HuR and mRNA stability. *Cell Mol Life Sci* **58**: 266-277.

Brody JR, Dixon DA. 2018. Complex HuR function in pancreatic cancer cells. *Wiley Interdiscip Rev RNA*.

Brody JR, Gonye GE. 2011. HuR's role in gemcitabine efficacy: an exception or opportunity? *Wiley Interdiscip Rev RNA* **2**: 435-444.

Buchet-Poyau K, Courchet J, Le Hir H, Seraphin B, Scoazec JY, Duret L, Domon-Dell C, Freund JN, Billaud M. 2007. Identification and characterization of human Mex-3 proteins, a novel family of evolutionarily conserved RNA-binding proteins differentially localized to processing bodies. *Nucleic Acids Res* **35**: 1289-1300.

Burger E, Araujo A, Lopez-Yglesias A, Rajala MW, Geng L, Levine B, Hooper LV, Burstein E, Yarovinsky F. 2018. Loss of Paneth Cell Autophagy Causes Acute Susceptibility to Toxoplasma gondii-Mediated Inflammation. *Cell Host Microbe* **23**: 177-190 e174.

Busch B, Bley N, Muller S, Glass M, Misiak D, Lederer M, Vetter M, Strauss HG, Thomssen C, Huttelmaier S. 2016. The oncogenic triangle of HMGA2, LIN28B and IGF2BP1 antagonizes tumor-suppressive actions of the let-7 family. *Nucleic Acids Res* **44**: 3845-3864.

Cadwell K, Liu JY, Brown SL, Miyoshi H, Loh J, Lennerz JK, Kishi C, Kc W, Carrero JA, Hunt S et al. 2008. A key role for autophagy and the autophagy gene Atg16l1 in mouse and human intestinal Paneth cells. *Nature* **456**: 259-263.

Cadwell K, Patel KK, Komatsu M, Virgin HWt, Stappenbeck TS. 2009. A common role for Atg16L1, Atg5 and Atg7 in small intestinal Paneth cells and Crohn disease. *Autophagy* **5**: 250-252.

Cassola A, Noe G, Frasch AC. 2010. RNA recognition motifs involved in nuclear import of RNA-binding proteins. *RNA Biol* **7**: 339-344.

Castello A, Horos R, Strein C, Fischer B, Eichelbaum K, Steinmetz LM, Krijgsveld J, Hentze MW. 2013. System-wide identification of RNA-binding proteins by interactome capture. *Nat Protoc* **8**: 491-500.

Chandramouli K, Qian PY. 2009. Proteomics: challenges, techniques and possibilities to overcome biological sample complexity. *Hum Genomics Proteomics* **2009**.

Chang ET, Donahue JM, Xiao L, Cui Y, Rao JN, Turner DJ, Twaddell WS, Wang JY, Battafarano RJ. 2012. The RNA-binding protein CUG-BP1 increases survivin expression in oesophageal cancer cells through enhanced mRNA stability. *Biochem J* **446**: 113-123.

Chao JA, Patskovsky Y, Patel V, Levy M, Almo SC, Singer RH. 2010. ZBP1 recognition of beta-actin zipcode induces RNA looping. *Genes Dev* **24**: 148-158.

Chatterji P, Rustgi AK. 2018. RNA Binding Proteins in Intestinal Epithelial Biology and Colorectal Cancer. *Trends Mol Med* **24**: 490-506.

Chaudhury A, Cheema S, Fachini JM, Kongchan N, Lu G, Simon LM, Wang T, Mao S, Rosen DG, Ittmann MM et al. 2016. CELF1 is a central node in post-transcriptional regulatory programmes underlying EMT. *Nat Commun* **7**: 13362.

Chen J, Bardes EE, Aronow BJ, Jegga AG. 2009. ToppGene Suite for gene list enrichment analysis and candidate gene prioritization. *Nucleic Acids Res* **37**: W305-311.

Cifdaloz M, Osterloh L, Grana O, Riveiro-Falkenbach E, Ximenez-Embun P, Munoz J, Tejedo C, Calvo TG, Karras P, Olmeda D et al. 2017. Systems analysis identifies melanoma-enriched pro-oncogenic networks controlled by the RNA binding protein CELF1. *Nat Commun* **8**: 2249.

Cirillo D, Agostini F, Klus P, Marchese D, Rodriguez S, Bolognesi B, Tartaglia GG. 2013. Neurodegenerative diseases: quantitative predictions of protein-RNA interactions. *RNA* **19**: 129-140.

Cirillo D, Blanco M, Armaos A, Buness A, Avner P, Guttman M, Cerase A, Tartaglia GG. 2016. Quantitative predictions of protein interactions with long noncoding RNAs. *Nat Methods* **14**: 5-6.

Clevers HC, Bevins CL. 2013. Paneth cells: maestros of the small intestinal crypts. *Annu Rev Physiol* **75**: 289-311.

Cline MS, Craft B, Swatloski T, Goldman M, Ma S, Haussler D, Zhu J. 2013. Exploring TCGA Pan-Cancer data at the UCSC Cancer Genomics Browser. *Sci Rep* **3**: 2652.

Clingman CC, Deveau LM, Hay SA, Genga RM, Shandilya SM, Massi F, Ryder SP. 2014. Allosteric inhibition of a stem cell RNA-binding protein by an intermediary metabolite. *Elife* **3**.

Conway AE, Van Nostrand EL, Pratt GA, Aigner S, Wilbert ML, Sundararaman B, Freese P, Lambert NJ, Sathe S, Liang TY et al. 2016. Enhanced CLIP Uncovers IMP Protein-RNA Targets in Human Pluripotent Stem Cells Important for Cell Adhesion and Survival. *Cell Rep* **15**: 666-679.

Copetti T, Bertoli C, Dalla E, Demarchi F, Schneider C. 2009. p65/RelA modulates BECN1 transcription and autophagy. *Mol Cell Biol* **29**: 2594-2608.

Cui YH, Xiao L, Rao JN, Zou T, Liu L, Chen Y, Turner DJ, Gorospe M, Wang JY. 2012. miR-503 represses CUG-binding protein 1 translation by recruiting CUGBP1 mRNA to processing bodies. *Mol Biol Cell* **23**: 151-162.

Cunningham D, Atkin W, Lenz HJ, Lynch HT, Minsky B, Nordlinger B, Starling N. 2010. Colorectal cancer. *Lancet* **375**: 1030-1047.

Dai N, Ji F, Wright J, Minichiello L, Sadreyev R, Avruch J. 2017. IGF2 mRNA binding protein-2 is a tumor promoter that drives cancer proliferation through its client mRNAs IGF2 and HMGA1. *Elife* **6**.

Dai N, Rapley J, Angel M, Yanik MF, Blower MD, Avruch J. 2011. mTOR phosphorylates IMP2 to promote IGF2 mRNA translation by internal ribosomal entry. *Genes Dev* **25**: 1159-1172.

Dai N, Zhao L, Wrighting D, Kramer D, Majithia A, Wang Y, Cracan V, Borges-Rivera D, Mootha VK, Nahrendorf M et al. 2015. IGF2BP2/IMP2-Deficient mice resist

obesity through enhanced translation of Ucp1 mRNA and Other mRNAs encoding mitochondrial proteins. *Cell Metab* **21**: 609-621.

Daikuhara S, Uehara T, Higuchi K, Hosaka N, Iwaya M, Maruyama Y, Matsuda K, Arakura N, Tanaka E, Ota H. 2015. Insulin-Like Growth Factor II mRNA-Binding Protein 3 (IMP3) as a Useful Immunohistochemical Marker for the Diagnosis of Adenocarcinoma of Small Intestine. *Acta Histochem Cytochem* **48**: 193-204.

Darnell RB. 2010. HITS-CLIP: panoramic views of protein-RNA regulation in living cells. *Wiley Interdiscip Rev RNA* **1**: 266-286.

Dassi E, Re A, Leo S, Tebaldi T, Pasini L, Peroni D, Quattrone A. 2014. AURA 2: Empowering discovery of post-transcriptional networks. *Translation (Austin)* **2**: e27738.

de Araujo PR, Gorthi A, da Silva AE, Tonapi SS, Vo DT, Burns SC, Qiao M, Uren PJ, Yuan ZM, Bishop AJ et al. 2016. Musashi1 Impacts Radio-Resistance in Glioblastoma by Controlling DNA-Protein Kinase Catalytic Subunit. *Am J Pathol* **186**: 2271-2278.

de Sousa e Melo F, Kurtova AV, Harnoss JM, Kljavin N, Hoeck JD, Hung J, Anderson JE, Storm EE, Modrusan Z, Koeppen H et al. 2017. A distinct role for Lgr5+ stem cells in primary and metastatic colon cancer. *Nature* **543**: 676-680.

Degrauwe N, Schlumpf TB, Janiszewska M, Martin P, Cauderay A, Provero P, Riggi N, Suva ML, Paro R, Stamenkovic I. 2016a. The RNA Binding Protein IMP2 Preserves Glioblastoma Stem Cells by Preventing let-7 Target Gene Silencing. *Cell Rep* **15**: 1634-1647.

Degrauwe N, Suva ML, Janiszewska M, Riggi N, Stamenkovic I. 2016b. IMPs: an RNA-binding protein family that provides a link between stem cell maintenance in normal development and cancer. *Genes Dev* **30**: 2459-2474.

Denkert C, Koch I, von Keyserlingk N, Noske A, Niesporek S, Dietel M, Weichert W. 2006. Expression of the ELAV-like protein HuR in human colon cancer: association with tumor stage and cyclooxygenase-2. *Mod Pathol* **19**: 1261-1269.

Dimitriadis E, Trangas T, Milatos S, Foukas PG, Gioulbasanis I, Courtis N, Nielsen FC, Pandis N, Dafni U, Bardi G et al. 2007a. Expression of oncofetal RNA-binding protein CRD-BP/IMP1 predicts clinical outcome in colon cancer. *International journal of cancer Journal international du cancer* **121**: 486-494.

-. 2007b. Expression of oncofetal RNA-binding protein CRD-BP/IMP1 predicts clinical outcome in colon cancer. *Int J Cancer* **121**: 486-494.

Dobin A, Davis CA, Schlesinger F, Drenkow J, Zaleski C, Jha S, Batut P, Chaisson M, Gingeras TR. 2013. STAR: ultrafast universal RNA-seq aligner. *Bioinformatics* **29**: 15-21.

Dreyfuss G, Kim VN, Kataoka N. 2002. Messenger-RNA-binding proteins and the messages they carry. *Nat Rev Mol Cell Biol* **3**: 195-205.

Edge SB, Compton CC. 2010. The American Joint Committee on Cancer: the 7th edition of the AJCC cancer staging manual and the future of TNM. *Ann Surg Oncol* **17**: 1471-1474.

Edman P, Begg G. 1967. A protein sequenator. *Eur J Biochem* **1**: 80-91.

El-Salhy M, Gilja OH. 2017. Abnormalities in ileal stem, neurogenin 3, and enteroendocrine cells in patients with irritable bowel syndrome. *BMC Gastroenterol* **17**: 90.

Elcheva I, Goswami S, Noubissi FK, Spiegelman VS. 2009. CRD-BP protects the coding region of betaTrCP1 mRNA from miR-183-mediated degradation. *Mol Cell* **35**: 240-246.

Fabian MR, Sonenberg N, Filipowicz W. 2010. Regulation of mRNA translation and stability by microRNAs. *Annu Rev Biochem* **79**: 351-379.

Fakhraldeen SA, Clark RJ, Roopra A, Chin EN, Huang W, Castorino J, Wisinski KB, Kim T, Spiegelman VS, Alexander CM. 2015. Two Isoforms of the RNA Binding Protein, Coding Region Determinant-binding Protein (CRD-BP/IGF2BP1), are Expressed in Breast Epithelium, and Support Clonogenic Growth of Breast Tumor Cells. *J Biol Chem*.

Feng Y, Yao Z, Klionsky DJ. 2015. How to control self-digestion: transcriptional, post-transcriptional, and post-translational regulation of autophagy. *Trends in cell biology* **25**: 354-363.

Formeister EJ, Sionas AL, Lorance DK, Barkley CL, Lee GH, Magness ST. 2009. Distinct SOX9 levels differentially mark stem/progenitor populations and enteroendocrine cells of the small intestine epithelium. *American journal of physiology Gastrointestinal and liver physiology* **296**: G1108-1118.

Fuller MK, Faulk DM, Sundaram N, Shroyer NF, Henning SJ, Helmrath MA. 2012. Intestinal crypts reproducibly expand in culture. *J Surg Res* **178**: 48-54.

Gao C, Yu Z, Liu S, Xin H, Li X. 2015. Overexpression of CUGBP1 is associated with the progression of non-small cell lung cancer. *Tumour Biol* **36**: 4583-4589.

Gerstberger S, Hafner M, Tuschl T. 2014. A census of human RNA-binding proteins. *Nat Rev Genet* **15**: 829-845.

Giammanco A, Blanc V, Montenegro G, Klos C, Xie Y, Kennedy S, Luo J, Chang SH, Hla T, Nalbantoglu I et al. 2014. Intestinal epithelial HuR modulates distinct pathways of proliferation and apoptosis and attenuates small intestinal and colonic tumor development. *Cancer Res* **74**: 5322-5335.

Gracz AD, Ramalingam S, Magness ST. 2010. Sox9 expression marks a subset of CD24-expressing small intestine epithelial stem cells that form organoids in vitro. *American journal of physiology Gastrointestinal and liver physiology* **298**: G590-600.

Gregorich ZR, Ge Y. 2014. Top-down proteomics in health and disease: challenges and opportunities. *Proteomics* **14**: 1195-1210.

Gregorieff A, Clevers H. 2005. Wnt signaling in the intestinal epithelium: from endoderm to cancer. *Genes Dev* **19**: 877-890.

Gregorieff A, Liu Y, Inanlou MR, Khomchuk Y, Wrana JL. 2015. Yap-dependent reprogramming of Lgr5(+) stem cells drives intestinal regeneration and cancer. *Nature* **526**: 715-718.

Grencis RK, Worthington JJ. 2016. Tuft Cells: A New Flavor in Innate Epithelial Immunity. *Trends Parasitol* **32**: 583-585.

Grupp K, Wilking J, Prien K, Hube-Magg C, Sirma H, Simon R, Steurer S, Budaus L, Haese A, Izbicki J et al. 2014. High RNA-binding motif protein 3 expression is an independent prognostic marker in operated prostate cancer and tightly linked to ERG activation and PTEN deletions. *Eur J Cancer* **50**: 852-861.

Gu W, Katz Z, Wu B, Park HY, Li D, Lin S, Wells AL, Singer RH. 2012. Regulation of local expression of cell adhesion and motility-related mRNAs in breast cancer cells by IMP1/ZBP1. *Journal of cell science* **125**: 81-91.

Gu W, Pan F, Singer RH. 2009. Blocking beta-catenin binding to the ZBP1 promoter represses ZBP1 expression, leading to increased proliferation and migration of metastatic breast-cancer cells. *J Cell Sci* **122**: 1895-1905.

Gu W, Wells AL, Pan F, Singer RH. 2008. Feedback regulation between zipcode binding protein 1 and beta-catenin mRNAs in breast cancer cells. *Mol Cell Biol* **28**: 4963-4974.

Gutschner T, Hammerle M, Pazaitis N, Bley N, Fiskin E, Uckelmann H, Heim A, Grobeta M, Hofmann N, Geffers R et al. 2014. Insulin-like growth factor 2 mRNA-binding protein 1 (IGF2BP1) is an important protumorigenic factor in hepatocellular carcinoma. *Hepatology* **59**: 1900-1911.

Haber AL, Biton M, Rogel N, Herbst RH, Shekhar K, Smillie C, Burgin G, Delorey TM, Howitt MR, Katz Y et al. 2017. A single-cell survey of the small intestinal epithelium. *Nature* **551**: 333-339.

Haberman Y, Tickle TL, Dexheimer PJ, Kim MO, Tang D, Karns R, Baldassano RN, Noe JD, Rosh J, Markowitz J et al. 2014. Pediatric Crohn disease patients exhibit specific ileal transcriptome and microbiome signature. *J Clin Invest* **124**: 3617-3633.

Hafner M, Landthaler M, Burger L, Khorshid M, Hausser J, Berninger P, Rothballer A, Ascano M, Jr., Jungkamp AC, Munschauer M et al. 2010. Transcriptome-wide identification of RNA-binding protein and microRNA target sites by PAR-CLIP. *Cell* **141**: 129-141.

Hafner M, Max KE, Bandaru P, Morozov P, Gerstberger S, Brown M, Molina H, Tuschl T. 2013. Identification of mRNAs bound and regulated by human LIN28 proteins and molecular requirements for RNA recognition. *RNA* **19**: 613-626.

Hamilton KE, Chatterji P, Lundsmith ET, Andres SF, Giroux V, Hicks PD, Noubissi FK, Spiegelman VS, Rustgi AK. 2015. Loss of Stromal IMP1 Promotes a Tumorigenic Microenvironment in the Colon. *Mol Cancer Res* **13**: 1478-1486.

Hamilton KE, Noubissi FK, Katti PS, Hahn CM, Davey SR, Lundsmith ET, Klein-Szanto AJ, Rhim AD, Spiegelman VS, Rustgi AK. 2013. IMP1 promotes tumor growth, dissemination and a tumor-initiating cell phenotype in colorectal cancer cell xenografts. *Carcinogenesis* **34**: 2647-2654.

Han J, Lee Y, Yeom KH, Nam JW, Heo I, Rhee JK, Sohn SY, Cho Y, Zhang BT, Kim VN. 2006. Molecular basis for the recognition of primary microRNAs by the Drosha-DGCR8 complex. *Cell* **125**: 887-901.

Han Y, Ye A, Zhang Y, Cai Z, Wang W, Sun L, Jiang S, Wu J, Yu K, Zhang S. 2015. Musashi-2 Silencing Exerts Potent Activity against Acute Myeloid Leukemia and Enhances Chemosensitivity to Daunorubicin. *PLoS One* **10**: e0136484.

Hansen TV, Hammer NA, Nielsen J, Madsen M, Dalbaeck C, Wewer UM, Christiansen J, Nielsen FC. 2004. Dwarfism and impaired gut development in insulin-like growth factor II mRNA-binding protein 1-deficient mice. *Mol Cell Biol* **24**: 4448-4464.

Hentze MW, Castello A, Schwarzl T, Preiss T. 2018. A brave new world of RNA-binding proteins. *Nat Rev Mol Cell Biol*.

Hinman MN, Lou H. 2008. Diverse molecular functions of Hu proteins. *Cell Mol Life Sci* **65**: 3168-3181.

Ho TH, Bundman D, Armstrong DL, Cooper TA. 2005. Transgenic mice expressing CUG-BP1 reproduce splicing mis-regulation observed in myotonic dystrophy. *Hum Mol Genet* **14**: 1539-1547.

Hooper KM, Barlow PG, Stevens C, Henderson P. 2016. Inflammatory Bowel Disease Drugs: A Focus on Autophagy. *J Crohns Colitis*.

House RP, Talwar S, Hazard ES, Hill EG, Palanisamy V. 2015. RNA-binding protein CELF1 promotes tumor growth and alters gene expression in oral squamous cell carcinoma. *Oncotarget* **6**: 43620-43634.

Hu G, McQuiston T, Bernard A, Park YD, Qiu J, Vural A, Zhang N, Waterman SR, Blewett NH, Myers TG et al. 2015. A conserved mechanism of TOR-dependent RCK-mediated mRNA degradation regulates autophagy. *Nat Cell Biol* **17**: 930-942.

Huang da W, Sherman BT, Lempicki RA. 2009a. Bioinformatics enrichment tools: paths toward the comprehensive functional analysis of large gene lists. *Nucleic Acids Res* **37**: 1-13.

-. 2009b. Systematic and integrative analysis of large gene lists using DAVID bioinformatics resources. *Nat Protoc* **4**: 44-57.

Huttelmaier S, Zenklusen D, Lederer M, Dictenberg J, Lorenz M, Meng X, Bassell GJ, Condeelis J, Singer RH. 2005. Spatial regulation of beta-actin translation by Src-dependent phosphorylation of ZBP1. *Nature* **438**: 512-515.

Ingolia NT. 2016. Ribosome Footprint Profiling of Translation throughout the Genome. *Cell* **165**: 22-33.

Ingolia NT, Brar GA, Rouskin S, McGeachy AM, Weissman JS. 2013. Genome-wide annotation and quantitation of translation by ribosome profiling. *Curr Protoc Mol Biol* **Chapter 4**: Unit 4 18.

Ingolia NT, Brar GA, Stern-Ginossar N, Harris MS, Talhouarne GJ, Jackson SE, Wills MR, Weissman JS. 2014. Ribosome profiling reveals pervasive translation outside of annotated protein-coding genes. *Cell Rep* **8**: 1365-1379.

Ingolia NT, Lareau LF, Weissman JS. 2011. Ribosome profiling of mouse embryonic stem cells reveals the complexity and dynamics of mammalian proteomes. *Cell* **147**: 789-802.

Jang HH, Lee HN, Kim SY, Hong S, Lee WS. 2017. Expression of RNA-binding Motif Protein 3 (RBM3) and Cold-inducible RNA-binding protein (CIRP) Is Associated with Improved Clinical Outcome in Patients with Colon Cancer. *Anticancer Res* **37**: 1779-1785.

Jarvelin AI, Noerenberg M, Davis I, Castello A. 2016. The new (dis)order in RNA regulation. *Cell Commun Signal* **14**: 9.

Jiang H, Zhang X, Luo J, Dong C, Xue J, Wei W, Chen J, Zhou J, Gao Y, Yang C. 2012. Knockdown of hMex-3A by small RNA interference suppresses cell proliferation and migration in human gastric cancer cells. *Mol Med Rep* **6**: 575-580.

Jing Z, Han W, Sui X, Xie J, Pan H. 2015. Interaction of autophagy with microRNAs and their potential therapeutic implications in human cancers. *Cancer Lett* **356**: 332-338.

Jogi A, Brennan DJ, Ryden L, Magnusson K, Ferno M, Stal O, Borgquist S, Uhlen M, Landberg G, Pahlman S et al. 2009. Nuclear expression of the RNA-binding protein RBM3 is associated with an improved clinical outcome in breast cancer. *Mod Pathol* **22**: 1564-1574.

Jonson L, Vikesaa J, Krogh A, Nielsen LK, Hansen T, Borup R, Johnsen AH, Christiansen J, Nielsen FC. 2007. Molecular composition of IMP1 ribonucleoprotein granules. *Mol Cell Proteomics* **6**: 798-811.

Keene JD. 2007. RNA regulons: coordination of post-transcriptional events. *Nat Rev Genet* **8**: 533-543.

Kim D, Langmead B, Salzberg SL. 2015. HISAT: a fast spliced aligner with low memory requirements. *Nat Methods* **12**: 357-360.

Kim HH, Kuwano Y, Srikantan S, Lee EK, Martindale JL, Gorospe M. 2009. HuR recruits let-7/RISC to repress c-Myc expression. *Genes Dev* **23**: 1743-1748.

Kim HS, Lee C, Kim WH, Maeng YH, Jang BG. 2017a. Expression profile of intestinal stem cell markers in colitis-associated carcinogenesis. *Sci Rep* **7**: 6533.

Kim JH, Kwon HY, Ryu DH, Nam MH, Shim BS, Kim JH, Lee JY, Kim SH. 2017b. Inhibition of CUG-binding protein 1 and activation of caspases are critically involved in piperazine derivative BK10007S induced apoptosis in hepatocellular carcinoma cells. *PLoS One* **12**: e0186490.

King CE, Cuatrecasas M, Castells A, Sepulveda AR, Lee JS, Rustgi AK. 2011a. LIN28B promotes colon cancer progression and metastasis. *Cancer Res* **71**: 4260-4268.

King CE, Wang L, Winograd R, Madison BB, Mongroo PS, Johnstone CN, Rustgi AK. 2011b. LIN28B fosters colon cancer migration, invasion and transformation through let-7-dependent and -independent mechanisms. *Oncogene* **30**: 4185-4193.

Kishore S, Luber S, Zavolan M. 2010. Deciphering the role of RNA-binding proteins in the post-transcriptional control of gene expression. *Brief Funct Genomics* **9**: 391-404.

Klionsky DJ Abdelmohsen K Abe A Abedin MJ Abeliovich H Acevedo Arozena A Adachi H Adams CM Adams PD Adeli K et al. 2016. Guidelines for the use and interpretation of assays for monitoring autophagy (3rd edition). *Autophagy* **12**: 1-222.

Kobel M, Weidensdorfer D, Reinke C, Lederer M, Schmitt WD, Zeng K, Thomssen C, Hauptmann S, Huttelmaier S. 2007. Expression of the RNA-binding protein IMP1 correlates with poor prognosis in ovarian carcinoma. *Oncogene* **26**: 7584-7589.

Komatsu M, Waguri S, Ueno T, Iwata J, Murata S, Tanida I, Ezaki J, Mizushima N, Ohsumi Y, Uchiyama Y et al. 2005. Impairment of starvation-induced and constitutive autophagy in Atg7-deficient mice. *J Cell Biol* **169**: 425-434.

Konig J, Zarnack K, Rot G, Curk T, Kayikci M, Zupan B, Turner DJ, Luscombe NM, Ule J. 2010. iCLIP reveals the function of hnRNP particles in splicing at individual nucleotide resolution. *Nat Struct Mol Biol* **17**: 909-915.

Krause WJ, Yamada J, Cutts JH. 1985. Quantitative distribution of enteroendocrine cells in the gastrointestinal tract of the adult opossum, Didelphis virginiana. *J Anat* **140 (Pt 4)**: 591-605.

Kress C, Gautier-Courteille C, Osborne HB, Babinet C, Paillard L. 2007. Inactivation of CUG-BP1/CELF1 causes growth, viability, and spermatogenesis defects in mice. *Mol Cell Biol* **27**: 1146-1157.

Kuo SY, Castoreno AB, Aldrich LN, Lassen KG, Goel G, Dancik V, Kuballa P, Latorre I, Conway KL, Sarkar S et al. 2015. Small-molecule enhancers of autophagy modulate cellular disease phenotypes suggested by human genetics. *Proc Natl Acad Sci U S A* **112**: E4281-4287.

Lal S, Cheung EC, Zarei M, Preet R, Chand SN, Mambelli-Lisboa NC, Romeo C, Stout MC, Londin E, Goetz A et al. 2017. CRISPR Knockout of the HuR Gene Causes a Xenograft Lethal Phenotype. *Mol Cancer Res* **15**: 696-707.

Lan L, Appelman C, Smith AR, Yu J, Larsen S, Marquez RT, Liu H, Wu X, Gao P, Roy A et al. 2015. Natural product (-)-gossypol inhibits colon cancer cell growth by targeting RNA-binding protein Musashi-1. *Mol Oncol* **9**: 1406-1420.

Lang M, Berry D, Passecker K, Mesteri I, Bhuju S, Ebner F, Sedlyarov V, Evstatiev R, Dammann K, Loy A et al. 2017. HuR Small-Molecule Inhibitor Elicits Differential Effects in Adenomatosis Polyposis and Colorectal Carcinogenesis. *Cancer Res* **77**: 2424-2438.

Langmead B, Trapnell C, Pop M, Salzberg SL. 2009. Ultrafast and memory-efficient alignment of short DNA sequences to the human genome. *Genome Biol* **10**: R25.

Leandersson K, Riesbeck K, Andersson T. 2006. Wnt-5a mRNA translation is suppressed by the Elav-like protein HuR in human breast epithelial cells. *Nucleic Acids Res* **34**: 3988-3999.

Lee H, Palm J, Grimes SM, Ji HP. 2015. The Cancer Genome Atlas Clinical Explorer: a web and mobile interface for identifying clinical-genomic driver associations. *Genome Med* **7**: 112.

Lee J, An S, Choi YM, Lee J, Ahn KJ, Lee JH, Kim TJ, An IS, Bae S. 2016. Musashi-2 is a novel regulator of paclitaxel sensitivity in ovarian cancer cells. *Int J Oncol* **49**: 1945-1952.

Leeds P, Kren BT, Boylan JM, Betz NA, Steer CJ, Gruppuso PA, Ross J. 1997. Developmental regulation of CRD-BP, an RNA-binding protein that stabilizes c-myc mRNA in vitro. *Oncogene* **14**: 1279-1286.

Lemm I, Ross J. 2002. Regulation of c-myc mRNA decay by translational pausing in a coding region instability determinant. *Mol Cell Biol* **22**: 3959-3969.

Lewis K, Valanejad L, Cast A, Wright M, Wei C, Iakova P, Stock L, Karns R, Timchenko L, Timchenko N. 2017. RNA Binding Protein CUGBP1 Inhibits Liver Cancer in a Phosphorylation-Dependent Manner. *Mol Cell Biol* **37**.

Li D, Yan D, Tang H, Zhou C, Fan J, Li S, Wang X, Xia J, Huang F, Qiu G et al. 2009. IMP3 is a novel prognostic marker that correlates with colon cancer progression and pathogenesis. *Ann Surg Oncol* **16**: 3499-3506.

Li N, Yousefi M, Nakauka-Ddamba A, Jain R, Tobias J, Epstein JA, Jensen ST, Lengner CJ. 2014. Single-cell analysis of proxy reporter allele-marked epithelial cells establishes intestinal stem cell hierarchy. *Stem Cell Reports* **3**: 876-891.

Li N, Yousefi M, Nakauka-Ddamba A, Li F, Vandivier L, Parada K, Woo DH, Wang S, Naqvi AS, Rao S et al. 2015. The Msi Family of RNA-Binding Proteins Function Redundantly as Intestinal Oncoproteins. *Cell Rep* **13**: 2440-2455.

Lipinski MM, Hoffman G, Ng A, Zhou W, Py BF, Hsu E, Liu X, Eisenberg J, Liu J, Blenis J et al. 2010. A genome-wide siRNA screen reveals multiple mTORC1 independent signaling pathways regulating autophagy under normal nutritional conditions. *Developmental cell* **18**: 1041-1052.

Liu L, Christodoulou-Vafeiadou E, Rao JN, Zou T, Xiao L, Chung HK, Yang H, Gorospe M, Kontoyiannis D, Wang JY. 2014a. RNA-binding protein HuR promotes growth of small intestinal mucosa by activating the Wnt signaling pathway. *Mol Biol Cell* **25**: 3308-3318.

Liu L, Ouyang M, Rao JN, Zou T, Xiao L, Chung HK, Wu J, Donahue JM, Gorospe M, Wang JY. 2015. Competition between RNA-binding proteins CELF1 and HuR modulates MYC translation and intestinal epithelium renewal. *Mol Biol Cell* **26**: 1797-1810.

Liu TC, Gao F, McGovern DP, Stappenbeck TS. 2014b. Spatial and temporal stability of paneth cell phenotypes in Crohn's disease: implications for prognostic cellular biomarker development. *Inflamm Bowel Dis* **20**: 646-651.

Liu TC, Gurram B, Baldridge MT, Head R, Lam V, Luo C, Cao Y, Simpson P, Hayward M, Holtz ML et al. 2016. Paneth cell defects in Crohn's disease patients promote dysbiosis. *JCI Insight* **1**: e86907.

Liu TC, Naito T, Liu Z, VanDussen KL, Haritunians T, Li D, Endo K, Kawai Y, Nagasaki M, Kinouchi Y et al. 2017. LRRK2 but not ATG16L1 is associated with Paneth cell defect in Japanese Crohn's disease patients. *JCI Insight* **2**: e91917.

Love MI, Huber W, Anders S. 2014. Moderated estimation of fold change and dispersion for RNA-seq data with DESeq2. *Genome Biol* **15**: 550.

Lui J, Castelli LM, Pizzinga M, Simpson CE, Hoyle NP, Bailey KL, Campbell SG, Ashe MP. 2014. Granules harboring translationally active mRNAs provide a platform for P-body formation following stress. *Cell Rep* **9**: 944-954.

Lunde BM, Moore C, Varani G. 2007. RNA-binding proteins: modular design for efficient function. *Nat Rev Mol Cell Biol* **8**: 479-490.

Luo Y, Yu H, Ou W, Jia L, Huang Y. 2017. Characterization of rhodamine 123 low staining cells and their dynamic changes during the injured-repaired progress induced by 5-FU. *Pathol Res Pract* **213**: 742-748.

Madison BB, Jeganathan AN, Mizuno R, Winslow MM, Castells A, Cuatrecasas M, Rustgi AK. 2015. Let-7 Represses Carcinogenesis and a Stem Cell Phenotype in the Intestine via Regulation of Hmga2. *PLoS Genet* **11**: e1005408.

Madison BB, Liu Q, Zhong X, Hahn CM, Lin N, Emmett MJ, Stanger BZ, Lee JS, Rustgi AK. 2013a. LIN28B promotes growth and tumorigenesis of the intestinal epithelium via Let-7. *Genes Dev* **27**: 2233-2245.

-. 2013b. LIN28B promotes growth and tumorigenesis of the intestinal epithelium via Let-7. *Genes Dev* **27**: 2233-2245.

Mahapatra L, Andruska N, Mao C, Le J, Shapiro DJ. 2017. A Novel IMP1 Inhibitor, BTYNB, Targets c-Myc and Inhibits Melanoma and Ovarian Cancer Cell Proliferation. *Transl Oncol* **10**: 818-827.

Mahapatra L, Mao C, Andruska N, Zhang C, Shapiro DJ. 2014. High-throughput fluorescence anisotropy screen for inhibitors of the oncogenic mRNA binding protein, IMP-1. *J Biomol Screen* **19**: 427-436.

Manieri NA, Drylewicz MR, Miyoshi H, Stappenbeck TS. 2012. Igf2bp1 Is Required for Full Induction of Ptgs2 mRNA in Colonic Mesenchymal Stem Cells in Mice. *Gastroenterology*.

Martin M. 2011. Cutadapt removes adapter sequences from high-throughput sequencing reads. *EMBnetjournal* **17**: 10-12.

Massironi S, Del Gobbo A, Cavalcoli F, Fiori S, Conte D, Pellegrinelli A, Milione M, Ferrero S. 2017. IMP3 expression in small-intestine neuroendocrine neoplasms: a new predictor of recurrence. *Endocrine* **58**: 360-367.

Matsuda A, Ogawa M, Yanai H, Naka D, Goto A, Ao T, Tanno Y, Takeda K, Watanabe Y, Honda K et al. 2011. Generation of mice deficient in RNA-binding motif protein 3 (RBM3) and characterization of its role in innate immune responses and cell growth. *Biochem Biophys Res Commun* **411**: 7-13.

Matsuzawa-Ishimoto Y, Shono Y, Gomez LE, Hubbard-Lucey VM, Cammer M, Neil J, Dewan MZ, Lieberman SR, Lazrak A, Marinis JM et al. 2017. Autophagy protein ATG16L1 prevents necroptosis in the intestinal epithelium. *The Journal of experimental medicine* **214**: 3687-3705.

Mayr C, Bartel DP. 2009. Widespread shortening of 3'UTRs by alternative cleavage and polyadenylation activates oncogenes in cancer cells. *Cell* **138**: 673-684.

Mazan-Mamczarz K, Hagner PR, Corl S, Srikantan S, Wood WH, Becker KG, Gorospe M, Keene JD, Levenson AS, Gartenhaus RB. 2008. Post-transcriptional gene regulation by HuR promotes a more tumorigenic phenotype. *Oncogene* **27**: 6151-6163.

McGlincy NJ, Ingolia NT. 2017. Transcriptome-wide measurement of translation by ribosome profiling. *Methods* **126**: 112-129.

McManus CJ, May GE, Spealman P, Shteyman A. 2014. Ribosome profiling reveals post-transcriptional buffering of divergent gene expression in yeast. *Genome Res* **24**: 422-430.

Melling N, Simon R, Mirlacher M, Izbicki JR, Stahl P, Terracciano LM, Bokemeyer C, Sauter G, Marx AH. 2016. Loss of RNA-binding motif protein 3 expression is associated with right-sided localization and poor prognosis in colorectal cancer. *Histopathology* **68**: 191-198.

Michlewski G, Sanford JR, Caceres JF. 2008. The splicing factor SF2/ASF regulates translation initiation by enhancing phosphorylation of 4E-BP1. *Mol Cell* **30**: 179-189.

Mizuno R, Chatterji P, Andres SF, Hamilton KE, Simon L, Foley SW, Jeganathan AN, Gregory BD, Madison BB, Rustgi AK. 2018. Differential Regulation of LET-7 by LIN28B Isoform-specific Functions. *Mol Cancer Res*.

Mongroo PS, Noubissi FK, Cuatrecasas M, Kalabis J, King CE, Johnstone CN, Bowser MJ, Castells A, Spiegelman VS, Rustgi AK. 2011. IMP-1 displays cross-talk with K-Ras and modulates colon cancer cell survival through the novel proapoptotic protein CYFIP2. *Cancer Research* **71**: 2172-2182.

Moore S, Jarvelin AI, Davis I, Bond GL, Castello A. 2017. Expanding horizons: new roles for non-canonical RNA-binding proteins in cancer. *Curr Opin Genet Dev* **48**: 112-120.

Mori H, Sakakibara S, Imai T, Nakamura Y, Iijima T, Suzuki A, Yuasa Y, Takeda M, Okano H. 2001. Expression of mouse igf2 mRNA-binding protein 3 and its implications for the developing central nervous system. *J Neurosci Res* **64**: 132-143.

Morris AR, Mukherjee N, Keene JD. 2010. Systematic analysis of posttranscriptional gene expression. *Wiley Interdiscip Rev Syst Biol Med* **2**: 162-180.

Narbonne-Reveau K, Lanet E, Dillard C, Foppolo S, Chen CH, Parrinello H, Rialle S, Sokol NS, Maurange C. 2016. Neural stem cell-encoded temporal patterning delineates an early window of malignant susceptibility in Drosophila. *Elife* **5**.

Nielsen FC, Nielsen J, Christiansen J. 2001. A family of IGF-II mRNA binding proteins (IMP) involved in RNA trafficking. *Scand J Clin Lab Invest Suppl* **234**: 93-99.

Nielsen J, Christiansen J, Lykke-Andersen J, Johnsen AH, Wewer UM, Nielsen FC. 1999. A family of insulin-like growth factor II mRNA-binding proteins represses translation in late development. *Mol Cell Biol* **19**: 1262-1270.

Nielsen J, Kristensen MA, Willemoes M, Nielsen FC, Christiansen J. 2004. Sequential dimerization of human zipcode-binding protein IMP1 on RNA: a cooperative mechanism providing RNP stability. *Nucleic Acids Res* **32**: 4368-4376.

Nishikura K. 2010. Functions and regulation of RNA editing by ADAR deaminases. *Annu Rev Biochem* **79**: 321-349.

Nishino J, Kim S, Zhu Y, Zhu H, Morrison SJ. 2013. A network of heterochronic genes including Imp1 regulates temporal changes in stem cell properties. *Elife* **2**: e00924.

Noubissi FK, Elcheva I, Bhatia N, Shakoori A, Ougolkov A, Liu J, Minamoto T, Ross J, Fuchs SY, Spiegelman VS. 2006. CRD-BP mediates stabilization of betaTrCP1 and c-myc mRNA in response to beta-catenin signalling. *Nature* **441**: 898-901.

Noubissi FK, Goswami S, Sanek NA, Kawakami K, Minamoto T, Moser A, Grinblat Y, Spiegelman VS. 2009. Wnt signaling stimulates transcriptional outcome of the Hedgehog pathway by stabilizing GLI1 mRNA. *Cancer Research* **69**: 8572-8578.

Nwokafor CU, Sellers RS, Singer RH. 2016. IMP1, an mRNA binding protein that reduces the metastatic potential of breast cancer in a mouse model. *Oncotarget* **7**: 72662-72671.

Oana Carja JBP. 2017a. Evolutionary rescue through partly heritable phenotypic variability. *biorxiv*.

Oana Carja TX, Joshua B. Plotkin, Premal Shah. 2017b. riboviz: analysis and visualization of ribosome profiling datasets.

Oshima N, Yamada Y, Nagayama S, Kawada K, Hasegawa S, Okabe H, Sakai Y, Aoi T. 2014. Induction of cancer stem cell properties in colon cancer cells by defined factors. *PLoS One* **9**: e101735.

Parry L, Young M, El Marjou F, Clarke AR. 2013. Evidence for a crucial role of paneth cells in mediating the intestinal response to injury. *Stem Cells* **31**: 776-785.

Pereira B, Sousa S, Barros R, Carreto L, Oliveira P, Oliveira C, Chartier NT, Plateroti M, Rouault JP, Freund JN et al. 2013. CDX2 regulation by the RNA-binding protein MEX3A: impact on intestinal differentiation and stemness. *Nucleic Acids Res* **41**: 3986-3999.

Pinto M, Robineleon S, Appay MD, Kedinger M, Triadou N, Dussaulx E, Lacroix B, Simonassmann P, Haffen K, Fogh J et al. 1983. Enterocyte-Like Differentiation and Polarization of the Human-Colon Carcinoma Cell-Line Caco-2 in Culture. *Biol Cell* **47**: 323-330.

Piskounova E, Polytarchou C, Thornton JE, LaPierre RJ, Pothoulakis C, Hagan JP, Iliopoulos D, Gregory RI. 2011. Lin28A and Lin28B inhibit let-7 microRNA biogenesis by distinct mechanisms. *Cell* **147**: 1066-1079.

Pott J, Kabat AM, Maloy KJ. 2018. Intestinal Epithelial Cell Autophagy Is Required to Protect against TNF-Induced Apoptosis during Chronic Colitis in Mice. *Cell Host Microbe* **23**: 191-202 e194.

Potten CS. 2004. Radiation, the ideal cytotoxic agent for studying the cell biology of tissues such as the small intestine. *Radiat Res* **161**: 123-136.

Rahkonen N, Stubb A, Malonzo M, Edelman S, Emani MR, Narva E, Lahdesmaki H, Ruohola-Baker H, Lahesmaa R, Lund R. 2016. Mature Let-7 miRNAs fine tune expression of LIN28B in pluripotent human embryonic stem cells. *Stem Cell Res* **17**: 498-503.

Rezza A, Skah S, Roche C, Nadjar J, Samarut J, Plateroti M. 2010. The overexpression of the putative gut stem cell marker Musashi-1 induces tumorigenesis through Wnt and Notch activation. *J Cell Sci* **123**: 3256-3265.

Rioux JD, Xavier RJ, Taylor KD, Silverberg MS, Goyette P, Huett A, Green T, Kuballa P, Barmada MM, Datta LW et al. 2007. Genome-wide association study identifies new susceptibility loci for Crohn disease and implicates autophagy in disease pathogenesis. *Nature genetics* **39**: 596-604.

Roche KC, Gracz AD, Liu XF, Newton V, Akiyama H, Magness ST. 2015. SOX9 Maintains Reserve Stem Cells and Preserves Radioresistance in Mouse Small Intestine. *Gastroenterology*.

Rodriguez JM, Maietta P, Ezkurdia I, Pietrelli A, Wesselink JJ, Lopez G, Valencia A, Tress ML. 2013. APPRIS: annotation of principal and alternative splice isoforms. *Nucleic Acids Res* **41**: D110-117.

Rosenblum JS, Pemberton LF, Bonifaci N, Blobel G. 1998. Nuclear import and the evolution of a multifunctional RNA-binding protein. *J Cell Biol* **143**: 887-899.

Ross AF, Oleynikov Y, Kislauskis EH, Taneja KL, Singer RH. 1997. Characterization of a beta-actin mRNA zipcode-binding protein. *Mol Cell Biol* **17**: 2158-2165.

Ross J, Lemm I, Berberet B. 2001. Overexpression of an mRNA-binding protein in human colorectal cancer. *Oncogene* **20**: 6544-6550.

Runge S, Nielsen FC, Nielsen J, Lykke-Andersen J, Wewer UM, Christiansen J. 2000. H19 RNA binds four molecules of insulin-like growth factor II mRNA-binding protein. *J Biol Chem* **275**: 29562-29569.

Saitoh T, Fujita N, Jang MH, Uematsu S, Yang BG, Satoh T, Omori H, Noda T, Yamamoto N, Komatsu M et al. 2008. Loss of the autophagy protein Atg16L1 enhances endotoxin-induced IL-1beta production. *Nature* **456**: 264-268.

Sakurai T, Kashida H, Komeda Y, Nagai T, Hagiwara S, Watanabe T, Kitano M, Nishida N, Fujita J, Kudo M. 2017. Stress Response Protein RBM3 Promotes the Development of Colitis-associated Cancer. *Inflamm Bowel Dis* **23**: 66-74.

Sato T, Vries RG, Snippert HJ, van de Wetering M, Barker N, Stange DE, van Es JH, Abo A, Kujala P, Peters PJ et al. 2009. Single Lgr5 stem cells build crypt-villus structures in vitro without a mesenchymal niche. *Nature* **459**: 262-265.

Schafer S, Adami E, Heinig M, Rodrigues KE, Kreuchwig F, Silhavy J, van Heesch S, Simaite D, Rajewsky N, Cuppen E et al. 2015. Translational regulation shapes the molecular landscape of complex disease phenotypes. *Nat Commun* **6**: 7200.

Shinoda G, Shyh-Chang N, Soysa TY, Zhu H, Seligson MT, Shah SP, Abo-Sido N, Yabuuchi A, Hagan JP, Gregory RI et al. 2013. Fetal deficiency of lin28 programs life-long aberrations in growth and glucose metabolism. *Stem Cells* **31**: 1563-1573.

Smith CW, Valcarcel J. 2000. Alternative pre-mRNA splicing: the logic of combinatorial control. *Trends Biochem Sci* **25**: 381-388.

Specian RD, Oliver MG. 1991. Functional biology of intestinal goblet cells. *Am J Physiol* **260**: C183-193.

Stappenbeck TS, McGovern DPB. 2017. Paneth Cell Alterations in the Development and Phenotype of Crohn's Disease. *Gastroenterology* **152**: 322-326.

Stohr N, Kohn M, Lederer M, Glass M, Reinke C, Singer RH, Huttelmaier S. 2012. IGF2BP1 promotes cell migration by regulating MK5 and PTEN signaling. *Genes & development* **26**: 176-189.

Stohr N, Lederer M, Reinke C, Meyer S, Hatzfeld M, Singer RH, Huttelmaier S. 2006. ZBP1 regulates mRNA stability during cellular stress. *J Cell Biol* **175**: 527-534.

Subramanian A, Tamayo P, Mootha VK, Mukherjee S, Ebert BL, Gillette MA, Paulovich A, Pomeroy SL, Golub TR, Lander ES et al. 2005. Gene set enrichment analysis: A knowledge-based approach for interpreting genome-wide expression profiles. *Proceedings of the National Academy of Sciences* **102**: 15545-15550.

Subtelny AO, Eichhorn SW, Chen GR, Sive H, Bartel DP. 2014. Poly(A)-tail profiling reveals an embryonic switch in translational control. *Nature* **508**: 66-71.

Sureban SM, Murmu N, Rodriguez P, May R, Maheshwari R, Dieckgraefe BK, Houchen CW, Anant S. 2007. Functional antagonism between RNA binding proteins HuR and CUGBP2 determines the fate of COX-2 mRNA translation. *Gastroenterology* **132**: 1055-1065.

Sureban SM, Ramalingam S, Natarajan G, May R, Subramaniam D, Bishnupuri KS, Morrison AR, Dieckgraefe BK, Brackett DJ, Postier RG et al. 2008. Translation regulatory factor RBM3 is a proto-oncogene that prevents mitotic catastrophe. *Oncogene* **27**: 4544-4556.

Takeda N, Jain R, LeBoeuf MR, Wang Q, Lu MM, Epstein JA. 2011. Interconversion between intestinal stem cell populations in distinct niches. *Science* **334**: 1420-1424.

Tebaldi T, Dassi E, Kostoska G, Viero G, Quattrone A. 2014. tRanslatome: an R/Bioconductor package to portray translational control. *Bioinformatics* **30**: 289-291.

Tessier CR, Doyle GA, Clark BA, Pitot HC, Ross J. 2004. Mammary Tumor Induction in Transgenic Mice Expressing an RNA-Binding Protein. *Cancer Research* **64**: 209-214.

Tian H, Biehs B, Warming S, Leong KG, Rangell L, Klein OD, de Sauvage FJ. 2011. A reserve stem cell population in small intestine renders Lgr5-positive cells dispensable. *Nature* **478**: 255-259.

Tomczak K, Czerwinska P, Wiznerowicz M. 2015. The Cancer Genome Atlas (TCGA): an immeasurable source of knowledge. *Contemp Oncol (Pozn)* **19**: A68-77.

Tsanov KM, Pearson DS, Wu Z, Han A, Triboulet R, Seligson MT, Powers JT, Osborne JK, Kane S, Gygi SP et al. 2017. LIN28 phosphorylation by MAPK/ERK couples signalling to the post-transcriptional control of pluripotency. *Nat Cell Biol* **19**: 60-67.

Tsialikas J, Romer-Seibert J. 2015. LIN28: roles and regulation in development and beyond. *Development* **142**: 2397-2404.

Tsuboi K, Nishitani M, Takakura A, Imai Y, Komatsu M, Kawashima H. 2015. Autophagy Protects against Colitis by the Maintenance of Normal Gut Microflora and Secretion of Mucus. *J Biol Chem* **290**: 20511-20526.

Tu HC, Schwitalla S, Qian Z, LaPier GS, Yermalovich A, Ku YC, Chen SC, Viswanathan SR, Zhu H, Nishihara R et al. 2015. LIN28 cooperates with WNT signaling to drive invasive intestinal and colorectal adenocarcinoma in mice and humans. *Genes Dev* **29**: 1074-1086.

Ule J, Jensen KB, Ruggiu M, Mele A, Ule A, Darnell RB. 2003. CLIP identifies Nova-regulated RNA networks in the brain. *Science* **302**: 1212-1215.

van der Flier LG, Haegebarth A, Stange DE, van de Wetering M, Clevers H. 2009. OLFM4 is a robust marker for stem cells in human intestine and marks a subset of colorectal cancer cells. *Gastroenterology* **137**: 15-17.

van Kouwenhove M, Kedde M, Agami R. 2011. MicroRNA regulation by RNA-binding proteins and its implications for cancer. *Nat Rev Cancer* **11**: 644-656.

Van Landeghem L, Santoro MA, Krebs AE, Mah AT, Dehmer JJ, Gracz AD, Scull BP, McNaughton K, Magness ST, Lund PK. 2012. Activation of two distinct Sox9-EGFP-expressing intestinal stem cell populations during crypt regeneration after irradiation. *American journal of physiology Gastrointestinal and liver physiology* **302**: G1111-1132.

Van Nostrand EL, Pratt GA, Shishkin AA, Gelboin-Burkhart C, Fang MY, Sundararaman B, Blue SM, Nguyen TB, Surka C, Elkins K et al. 2016. Robust transcriptome-wide discovery of RNA-binding protein binding sites with enhanced CLIP (eCLIP). *Nat Methods* **13**: 508-514.

VanDussen KL, Liu TC, Li D, Towfic F, Modiano N, Winter R, Haritunians T, Taylor KD, Dhall D, Targan SR et al. 2014. Genetic variants synthesize to produce paneth cell phenotypes that define subtypes of Crohn's disease. *Gastroenterology* **146**: 200-209.

Venugopal A, Subramaniam D, Balmaceda J, Roy B, Dixon DA, Umar S, Weir SJ, Anant S. 2016. RNA binding protein RBM3 increases beta-catenin signaling to increase stem cell characteristics in colorectal cancer cells. *Mol Carcinog* **55**: 1503-1516.

Vikesaa J, Hansen TV, Jonson L, Borup R, Wewer UM, Christiansen J, Nielsen FC. 2006. RNA-binding IMPs promote cell adhesion and invadopodia formation. *EMBO J* **25**: 1456-1468.

Viswanathan SR, Daley GQ. 2010. Lin28: A microRNA regulator with a macro role. *Cell* **140**: 445-449.

Viswanathan SR, Powers JT, Einhorn W, Hoshida Y, Ng TL, Toffanin S, O'Sullivan M, Lu J, Phillips LA, Lockhart VL et al. 2009. Lin28 promotes transformation and is associated with advanced human malignancies. *Nat Genet* **41**: 843-848.

Vlasova-St Louis I, Bohjanen PR. 2011. Coordinate regulation of mRNA decay networks by GU-rich elements and CELF1. *Curr Opin Genet Dev* **21**: 444-451.

Wachter K, Kohn M, Stohr N, Huttelmaier S. 2013. Subcellular localization and RNP formation of IGF2BPs (IGF2 mRNA-binding proteins) is modulated by distinct RNA-binding domains. *Biol Chem* **394**: 1077-1090.

Wang G, Huang Z, Liu X, Huang W, Chen S, Zhou Y, Li D, Singer RH, Gu W. 2016a. IMP1 suppresses breast tumor growth and metastasis through the regulation of its target mRNAs. *Oncotarget* **7**: 15690-15702.

Wang L, Feng Z, Wang X, Wang X, Zhang X. 2010. DEGseq: an R package for identifying differentially expressed genes from RNA-seq data. *Bioinformatics* **26**: 136-138.

Wang S, Li N, Yousefi M, Nakauka-Ddamba A, Li F, Parada K, Rao S, Minuesa G, Katz Y, Gregory BD et al. 2015a. Transformation of the intestinal epithelium by the MSI2 RNA-binding protein. *Nat Commun* **6**: 6517.

Wang T, Han P, He Y, Zhao C, Wang G, Yang W, Shan M, Zhu Y, Yang C, Weng M et al. 2016b. Lin28A enhances chemosensitivity of colon cancer cells to 5-FU by promoting apoptosis in a let-7 independent manner. *Tumour Biol* **37**: 7657-7665.

Wang T, He Y, Zhu Y, Chen M, Weng M, Yang C, Zhang Y, Ning N, Zhao R, Yang W et al. 2016c. Comparison of the expression and function of Lin28A and Lin28B in colon cancer. *Oncotarget* **7**: 79605-79616.

Wang T, Xiao G, Chu Y, Zhang MQ, Corey DR, Xie Y. 2015b. Design and bioinformatics analysis of genome-wide CLIP experiments. *Nucleic Acids Res* **43**: 5263-5274.

Wang Y, Jiang CQ, Fan LF. 2015c. Correlation of Musashi-1, Lgr5, and pEGFR expressions in human small intestinal adenocarcinomas. *Tumour Biol* **36**: 6075-6082.

Wang Z, Gerstein M, Snyder M. 2009. RNA-Seq: a revolutionary tool for transcriptomics. *Nat Rev Genet* **10**: 57-63.

Wang ZL, Li B, Luo YX, Lin Q, Liu SR, Zhang XQ, Zhou H, Yang JH, Qu LH. 2018. Comprehensive Genomic Characterization of RNA-Binding Proteins across Human Cancers. *Cell Rep* **22**: 286-298.

Washabau RJ. 2013. Chapter 57 Small Intestine. *Canine and Feline Gastroenterology*: 651-728.

Washington MK, Powell AE, Sullivan R, Sundberg JP, Wright N, Coffey RJ, Dove WF. 2013. Pathology of rodent models of intestinal cancer: progress report and recommendations. *Gastroenterology* **144**: 705-717.

Weidensdorfer D, Stohr N, Baude A, Lederer M, Kohn M, Schierhorn A, Buchmeier S, Wahle E, Huttelmaier S. 2009. Control of c-myc mRNA stability by IGF2BP1-associated cytoplasmic RNPs. *RNA* **15**: 104-115.

Whitelegge JP, le Coutre J, Lee JC, Engel CK, Prive GG, Faull KF, Kaback HR. 1999. Toward the bilayer proteome, electrospray ionization-mass spectrometry of large, intact transmembrane proteins. *Proc Natl Acad Sci U S A* **96**: 10695-10698.

Xia L, Sun C, Li Q, Feng F, Qiao E, Jiang L, Wu B, Ge M. 2015. CELF1 is Up-Regulated in Glioma and Promotes Glioma Cell Proliferation by Suppression of CDKN1B. *Int J Biol Sci* **11**: 1314-1324.

Yang H, Rao JN, Wang JY. 2014. Posttranscriptional Regulation of Intestinal Epithelial Tight Junction Barrier by RNA-binding Proteins and microRNAs. *Tissue Barriers* **2**: e28320.

Yaniv K, Yisraeli JK. 2002. The involvement of a conserved family of RNA binding proteins in embryonic development and carcinogenesis. *Gene* **287**: 49-54.

Ye F, Jin P, Cai X, Cai P, Cai H. 2017. High RNA-Binding Motif Protein 3 (RBM3) Expression is Independently Associated with Prolonged Overall Survival in Intestinal-Type Gastric Cancer. *Med Sci Monit* **23**: 6033-6041.

Yee KS, Wilkinson S, James J, Ryan KM, Vousden KH. 2009. PUMA- and Bax-induced autophagy contributes to apoptosis. *Cell death and differentiation* **16**: 1135-1145.

Yiakouvaki A, Dimitriou M, Karakasiliotis I, Eftychi C, Theocharis S, Kontoyiannis DL. 2012. Myeloid cell expression of the RNA-binding protein HuR protects mice from pathologic inflammation and colorectal carcinogenesis. *J Clin Invest* **122**: 48-61.

Young LE, Sanduja S, Bemis-Standoli K, Pena EA, Price RL, Dixon DA. 2009. The mRNA binding proteins HuR and tristetraprolin regulate cyclooxygenase 2 expression during colon carcinogenesis. *Gastroenterology* **136**: 1669-1679.

Yousefi M, Li N, Nakauka-Ddamba A, Wang S, Davidow K, Schoenberger J, Yu Z, Jensen ST, Kharas MG, Lengner CJ. 2016. Msi RNA-binding proteins control reserve intestinal stem cell quiescence. *J Cell Biol* **215**: 401-413.

Zhang H, Zong Y, Qiu G, Jia R, Xu X, Wang F, Wu D. 2018. Silencing Lin28 promotes apoptosis in colorectal cancer cells by upregulating let7c targeting of antiapoptotic BCL2L1. *Mol Med Rep*.

Zhang J, Ratanasirintrawoot S, Chandrasekaran S, Wu Z, Ficarro SB, Yu C, Ross CA, Cacchiarelli D, Xia Q, Seligson M et al. 2016. LIN28 Regulates Stem Cell Metabolism and Conversion to Primed Pluripotency. *Cell Stem Cell* **19**: 66-80.

Zhang L, Lee JE, Wilusz J, Wilusz CJ. 2008. The RNA-binding protein CUGBP1 regulates stability of tumor necrosis factor mRNA in muscle cells: implications for myotonic dystrophy. *J Biol Chem* **283**: 22457-22463.

Zhong Y, Karaletsos T, Drewe P, Sreedharan VT, Kuo D, Singh K, Wendel HG, Ratsch G. 2017. RiboDiff: detecting changes of mRNA translation efficiency from ribosome footprints. *Bioinformatics* **33**: 139-141.

Zhou P, Zhang Y, Ma Q, Gu F, Day DS, He A, Zhou B, Li J, Stevens SM, Romo D et al. 2013a. Interrogating translational efficiency and lineage-specific transcriptomes using ribosome affinity purification. *Proc Natl Acad Sci U S A* **110**: 15395-15400.

Zhou WJ, Geng ZH, Spence JR, Geng JG. 2013b. Induction of intestinal stem cells by R-spondin 1 and Slit2 augments chemoradioprotection. *Nature* **501**: 107-111.

Zhou X, Ma X, Wang Z, Sun C, Wang Y, He Y, Zhang H. 2015. Radiation-induced hyperproliferation of intestinal crypts results in elevated genome instability with inactive p53-related genomic surveillance. *Life Sci* **143**: 80-88.

Zhu L, Gibson P, Currle DS, Tong Y, Richardson RJ, Bayazitov IT, Poppleton H, Zakharenko S, Ellison DW, Gilbertson RJ. 2009. Prominin 1 marks intestinal stem cells that are susceptible to neoplastic transformation. *Nature* **457**: 603-607.